LIBRARY Michigan State University

PLACE IN RETURN BOX to remove this checkout from your record. TO AVOID FINES return on or before date due.

DATE DUE	DATE DUE	DATE DUE

MSU Is An Affirmative Action/Equal Opportunity Institution c:circ/datedus.pm3-p.:

THE DEPENDENCE OF THE EFFECTIVE YOUNG'S MODULUS OF GLASS/EPOXY AND GLASS/GLUE LAMINATES ON ADHESION AREA AND GLUE BOND THICKNESS

By

KIYONG LEE

A THESIS

Submitted to

MICHIGAN STATE UNIVERSITY

in partial fulfillment of the requirements

for the degree of

MASTER OF SCIENCE

Department of Materials Science and Mechanics

ABSTRACT

THE DEPENDENCE OF THE EFFECTIVE YOUNG'S MODULUS OF GLASS/EPOXY AND GLASS/GLUE LAMINATES ON ADHESION AREA AND GLUE BOND THICKNESS

By

KIYONG LEE

The effects of adhesives on the effective elastic modulus of adhered soda-lime-silica microscope glass slides were investigated using three different kinds of adhesives: super glue, epoxy cement and epoxy resin. The specimens were thus three-layer composites, with a bond layer sandwiched between two glass slides.

A sonic resonance technique was used to determine the elastic moduli of single slides, glass slide/glue composite specimens and epoxy resin specimens. The prismatic bar-shaped specimens were suspended horizontally from a driver and a pick-up transducers. The fundamental flexural frequencies of specimens were used to calculate the elastic modulus.

The change of Young's modulus of adhered soda-lime-silica microscope slides was observed as a function of adhesion area percent. Young's moduli decreased continuously with decreasing the adhesion area. For an area percent adhesion less than 30 to 35 percent the Young's moduli decreased relatively rapidly with a decrease in the adhesion area. The effective Young's modulus of the laminates changed from about 70 GPa for 100 percent area coverage of adhesive down to about 15 GPa for an area coverage of about 1 percent for a single glue spot. For specimens having a 100 percent area coverage of adhesive, the effective Young's modulus of the laminates changed by about 4 GPa as the glue bond thickness ranged from 0.025 mm to 0.275 mm.

TABLE OF CONTENTS

			Page
LIST	OF 1	Pables	
LIST	OF P	IGURES	
1.	INTRO	DUCTION AND REVIEW OF LITERATURE	1
1.1.		External Crack' model	3
1.2.	•	Rule of Mixtures (ROM)' Model	8
1.3.		Dynamic Beam Vibration' Model	12
1.4.		Description of Current study and Outline of Remaining Text	17
2. 1	EXPE	IMENTAL PROCEDURE	18
2.1.		Materials	19
2.1.	1.	Microscope Slides	19
2.1.		Adhesives	19
2.2.		The Measurement Of Mass	23
2.3.		The Measurement Of Thickness	24
2.4.		Applying Adhesives And Preparing Glass Slide/Glue Composite Specimens	26
2.4.	1.	Applying 'Super Glue'	26
2.4.		Applying 'Epoxy Cement'	27
2.4.		Applying 'Epoxy Resin'	31
2.5.		The Measurement Of Area Fraction Of Glue	32
2.5.	1.	Template Method For Small Circle-Shaped Glue Spots	32
2.5.		Grid Counting Method For Irregularly-Shaped Glue Spots	34
2.6.		The Measurement Of Elastic Modulus	37
2.7.		Making Epoxy Resin Specimens	43
3. R	ESULI	S AND DISCUSSION	47
3.1.		Effects of Adhesion Area, Number of Glue Spots, and	48
		Glue Bond Thickness	
3.1.	1.	The Effects of Super Glue Adhesion on Elastic Modulus	48
3.1.	2.	The Effects of Epoxy Cement Adhesion on Elastic	62
		Modulus	
3.2.		The Effects of Epoxy Resin Adhesion on Elastic Modulus	62
3.2.	1.	The Effect of Adhesion Area on Elastic Modulus	62
3.2.	2.	The Effect of Glue Bond Thickness on Elastic Modulus	62
3.2.	2.1.	Glass Slide/Epoxy Resin Composite Specimens having a	66
		Fixed Glue Composition but Different Adhesion Areas	
3.2.	2.2.	Glass Slide/Epoxy Resin Composite Specimens of	70
		Differing Glue Composition and Fixed Adhesion Areas	
3.2.	3.	The Effect of Epoxy Resin Composition on Elastic Modulus	76
3.2.	4.	Experimentally obtained Elastic Moduli, Densities and	77
		Poisson's Ratios of Epoxy Resin Specimens	
3.2.	5.	Comparison of Rule of Mixtures and Dynamic Beam	77
		Vibration models	
3.2.	6.	Change of Effective Young's Modulus of Glass Slide/	86
		Glue Specimen with respect to Glue-Bond Thickness	
		Ranges at Fixed Adhesion Areas	

3.2.7.	Possible Physical Mechanisms for the Difference between the Measured Modulus of the Glass Slide/Glue Composite Specimens and the Predictions of the ROM and	91
3.2.8.	Dynamic Modulus Models Possible Changes in Effective Young's Modulus of a Bond Layer for the Difference between the Experimentally Determined Modulus and the Moduli Predicted from the ROM Model	93
3.2.9.	Dependence of the ROM and the Dynamic Modulus Models on the Relative Glue Bond Thickness and Comparison with Experimental Results	95
3.2.10.	Possible Changes in Effective Young's Modulus of a Glass Slide/Glue Specimen for the Difference between the Measured Moduli and the Moduli Predicted from the Dynamic Modulus Model	98
3.2.11.	Consideration of Insufficient Bonding as a Possible Factor for Deviation of Measured Elastic Moduli from the Moduli predicted by ROM Model	106
3.3.	General Trends in Effective Young's Modulus on Adhesion	109
4. SUNO	ARY AND CONCLUSIONS	120
4.1.	The Effect of Adhesion Area on Elastic Modulus	120
4.2.	The Effect of Number of Glue Spots on Elastic Modulus	121
4.3.	The Effect of Glue Bond Thickness on Elastic Modulus	122
4.4.		123
	The Effect of Epoxy Resin Composition on Elastic Modulus	
4.5.	The Comparison of the ROM model and the Dynamic Beam Vibration model	124
4.6.	Future Work and Practical Applications of This Study	124
Appendix	A. Calculation of Adhesion Area by a Template Method	126
Appendix		126
FF	and the corresponding Young's Modulus of each	
	glass slide/glue composite specimen	
D.	-1. The experimental data for the glass slide/super	128
ъ.	glue composite specimens having one glue spot	120
_		120
В	-2. The experimental data for the glass slide/super	130
	glue composite specimens having two glue spot	
В	-3. The experimental data for the glass slide/super	131
	glue composite specimens having three glue spot	
В	-4. The experimental data for the glass slide/super	133
	glue composite specimens having five glue spots	
В	-5. The experimental data for the glass slide/epoxy	134
	cement composite specimens having one glue spot	
R	-6. The experimental data for the glass slide/epoxy	135
_	cement composite specimens having three glue spots	100
Ð	-7. The experimental data for the glass slide/epoxy	136
5		130
	resin composite specimen having three glue spots	
_	of 50% resin and 50 % hardener	
В	-8. The experimental data for the glass slide/epoxy	139
	resin composite specimens adhered by the epoxy	
	resin of 35% resin and 65% hardener	
В	-9. The experimental data for the glass slide/epoxy	140
	resin composite specimens adhered by the epoxy	
	resin of 65% resin and 35% hardener	
В	-10. The experimental data for the glass slide/epoxy	141
_	resin composite specimens adhered by the epoxy	
	resin of 80% resin and 20% hardener	
TIRL OL	references	142

LIST OF TABLES

Table	Numbe	er e	Page
Table	1.	Classification of the glass slide/super glue composite specimens according to the number of glue spots and the range of glue thickness.	28
Table	2.	Classification of the glass slide/epoxy cement composite specimens according to the number of glue spots.	30
Table	3.	Classification of the glass slide/epoxy resin composite specimens according to the composition of the glue and the range of glue thickness.	33
Table	4.	Classification of the glass slide/epoxy resin composite specimens with 100 % adhesion area. These specimens were included in the experimental comparison of the ROM and the Dynamic Beam Vibration models (Section 3.3.5).	33
Table	5.	For the sonic resonance method, the relative position of nodes according to the vibrational mode.	41
Table	6.	Comparison of experimentally obtained elastic moduli, densities and Poisson's ratios with reference values.	74
Table	7.	Young's moduli (GPa) of glass slide/epoxy resin composite specimens obtained from the regression curves in Figure 33. The table shows representative Young's moduli of glass slide/epoxy resin composite specimens having a given adhesion areas and a glue bond thickness within a given range of glue bond thickness.	87
Table	8.	Elastic modulus of quenched polymer glass as a function of the quench medium temperature [19].	92
Table	9.	Pressure derivatives of elastic constants of MgO at 23°C, NaCl, KCl at 22°C, and Quartz at 25°C [20-22].	94
Table	10.	Young's modulus of epoxy resin layer in a glass slide/epoxy resin composite specimen to compensate for the ROM model.	96
Table	11.	Comparison of measured Young's moduli of a glass slide layer with Young's moduli of the glass slide layer calculated from the Dynamic modulus model required to obtain the measured effective Young's moduli.	104

Table	Numbe	er	Page
Table	12.	Comparison of measured Young's moduli of a glue bond layer with Young's moduli of the glue bond layer calculated from the Dynamic modulus model required to obtain the measured effective Young's moduli.	105
Table	13.	Measured Young's moduli and moduli predicted from the ROM and the Dynamic Modulus models as a function of relative thickness obtained from the corresponding regression curves in Figure 38.	107
Table	14.	Young's moduli obtained from a regression curve in Figure 28 and the difference between the Young's moduli, E_{100} , for adhesion area of 100% and the Young's moduli, E, for adhesion area ranging from 0% to 100%.	108
Table	15.	Effective Young's modulus calculated from the ROM model and comparison with the experimental modulus values based on Figure 49.	114
Table	16.	Differences between the data of the super glue, the epoxy cement and the epoxy resin shown in Table 15.	115

LIST OF FIGURES

Figure	Number	age
Figure	 Elliptical Internal Cracks (a), External Cracks (b) under uniaxial loading [1]. 	4
Figure	 Composite specimen composed of layers 1, 2 and a bond layer for Rule of Mixtures model [5], where uniaxial tension is assumed for the elastic modulus determination. 	9
Figure	3. Composite specimen composed of layer 1, 2 and a bond layer for Dynamic Beam Vibration model [5], where the specimen is driven at flexural resonance to determine the elastic modulus.	13
Figure	4. Photograph of glass slide/epoxy resin composite specimen which shows three glue spots and points marked for the measurement of glue bond thickness.	20
Figure	5. Change of normalized mass of various glues (0, ● Elmer's School Glue; □, ■ Cement For Plastic Models; △, △ Epoxy Cement; ◊, ♦ Super Glue) as a function of time in hours after gluing.	22
Figure	 Relative position(s) of glue spot(s): (a) one glue spot, (b) two glue spots, (c) three glue spots, (d) five glue spots, where L=length of specimen and W=width of specimen. 	25
Figure	7. Photograph of epoxy resin (i.e. "Quick Setting Epoxy Adhesive"), a 7.65 cm x 7.65 cm piece of standard notepad paper and a stick for mixing and applying.	29
Figure	8. Template used for measurement of the area fraction of the smaller circular glue spots on the composite specimens.	35
Figure	 Grid paper used for measurement of the area fraction of irregularly shaped larger glue spots on the composite specimens. 	36
Figure	 Photograph of the sonic resonance apparatus. (A glass slide/glue specimen is suspended in the air) 	38
Figure	11. A block diagram of the sonic resonance apparatus [15].	39

Figur e	Numbe	er	Page
Figure	12.	Photograph of epoxy resin specimens. The ratios of resin and hardener used for each specimen are 50%:50%, 65%:35% and 80%:20%, respectively.	46
Figur e	13.	For a super glue bond layer, the effect of the number of super glue spots on Young's modulus as a function of adhesion area(%). The curves represent a least-squares best fit to equation 31.	49
Figure	14.	For a super glue bond layer, the effect of the number of super glue spots on Young's modulus as a function of adhesion area(%). The curves represent a least-squares best fit to equation 32.	50
Figur e	15.	For a super glue bond layer, the effect of the number of super glue spots on Young's modulus as a function of adhesion area(%). The curves represent a least-squares best fit to equation 33.	51
Figure	16.	For a super glue bond layer, the effect of the super glue on Young's modulus as a function of adhesion area(%) with the data for specimens having 2, 3 and 5 glue spots lumped together. The curve represents a least-squares best fit to equation 31.	53
Figure	17.	For a super glue bond layer, the effect of the super glue on Young's modulus as a function of adhesion area(%) with the data for specimens having 2, 3 and 5 glue spots lumped together. The curve represents a least-squares best fit to equation 32.	54
Figur e	18.	For a super glue bond layer, the effect of the super glue on Young's modulus as a function of adhesion area(%) with the data for specimens having 2, 3, 5 glue spots lumped together. The curve represents a least-squares best fit to equation 33.	55
Figur e	19.	For a super glue bond layer, the effect of glue bond thickness of super glue on Young's modulus as a function of adhesion area(%) for specimens having one super glue spot. The curves represent a least -squares best fit to equation 31.	56
Figur e	20.	For a super glue bond layer, the effect of glue bond thickness of super glue on Young's modulus as a function of adhesion area(%) for specimens having one super glue spot. The curves represent a least—squares best fit to equation 32.	57
Figur e	21.	For a super glue bond layer, the effect of glue bond thickness of super glue on Young's modulus as a function of adhesion area(%) for specimens having one super glue spot. The curves represent a least—squares best fit to equation 33.	58
Figur e	22.	For a super glue bond layer, the effect of glue bond thickness of super glue on Young's modulus as a function of adhesion area(%) for specimens having two and three super glue spots. The curves represent a least-squares best fit to equation 31.	59

Figure	Numbe	er	Page
Figure	23.	For a super glue bond layer, the effect of glue bond thickness of super glue on Young's modulus as a function of adhesion area(%) for specimens having two and three super glue spots. The curves represent a least-squares best fit to equation 32.	60
Figur e	24.	For a super glue bond layer, the effect of glue bond thickness of super glue on Young's modulus as a function of adhesion area(%) for specimens having two and three super glue spots. The curves represent a least-squares best fit to equation 33.	61
Figur e	25.	For an epoxy cement bond layer, the effect of epoxy cement on Young's modulus as a function of adhesion area(%) for specimens having one and three glue spots. The curves represent a least-squares best fit to equation 31.	63
Figur e	26.	For an epoxy cement bond layer, the effect of epoxy cement on Young's modulus as a function of adhesion area(%) for specimens having one and three glue spots. The curves represent a least-squares best fit to equation 32.	64
Figure	27.	For an epoxy cement bond layer, the effect of epoxy cement on Young's modulus as a function of adhesion area(%) for specimens having one and three glue spots. The curves represent a least-squares best fit to equation 33.	65
Figure	28.	For an epoxy resin bond layer, the effect of epoxy resin on Young's modulus as a function of adhesion area(%). The curve represents a least-squares best fit to equation 31.	67
Figur e	29.	For an epoxy resin bond layer, the effect of epoxy resin on Young's modulus as a function of adhesion area(%). The curve represents a least-squares best fit to equation 32.	68
Figur e	30.	For an epoxy resin bond layer, the effect of epoxy resin on Young's modulus as a function of adhesion area(%). The curve represents a least-squares best fit to equation 33.	69
Figure	31.	For an epoxy resin bond layer, the effect of glue bond thickness of epoxy resin on Young's modulus as a function of adhesion area(%). The curves represent a least-squares best fit to equation 31.	71
Figur e	32.	For an epoxy resin bond layer, the effect of glue bond thickness of epoxy resin on Young's modulus as a function of adhesion area(%). The curves represent a least-squares best fit to equation 32.	72
Figure	33.	For an epoxy resin bond layer, the effect of glue bond thickness of epoxy resin on Young's modulus as a function of adhesion area(%). The curves	73

Figure	Numbe	er	Page
Figure	34.	For an epoxy resin bond layer, the effect of composition of epoxy resin on Young's modulus as a function of relative glue bond thickness. The curves represent a least-squares best fit to equation 34.	75
Figur e	35.	Comparison of ROM and Dynamic Beam Vibration models for epoxy bonds made from an initial composition of 50% resin and 50% hardener. The curves represent a least-squares best fit to equation 36.	79
Figur e	36.	Comparison of ROM and Dynamic Beam Vibration models for epoxy bonds made from an initial composition of 65% resin and 35% hardener. The curves represent a least-squares best fit to equation 36.	80
Figure	37.	Comparison of ROM and Dynamic Beam Vibration models for epoxy bonds made from an initial composition of 80% resin and 20% hardener. The curves represent a least-squares best fit to equation 36.	81
Figure	38.	Comparison of experimentally determined moduli with the moduli predicted from the Rule of Mixtures and Dynamic Beam Vibration models as a function of relative glue bond thickness for 50% resin and 50% hardener. The curves represent a least-squares best fit to equation 37.	82
Figure	39.	Comparison of experimentally determined moduli with the moduli predicted from the Rule of Mixtures and Dynamic Beam Vibration models as a function of relative glue bond thickness for 65% resin and 35% hardener. The curves represent a least-squares best fit to equation 37.	83
Figure	40.	Comparison of experimentally determined moduli with the moduli predicted from the Rule of Mixtures and Dynamic Beam Vibration models as a function of relative glue bond thickness for 80% resin and 20% hardener. The curves represent a least-squares best fit to equation 37.	84
Figure	41.	Change of Young's modulus with respect to glue-bond thickness ranges ($R_1:0.025-0.075$ mm, $R_2:0.125-0.175$ mm, $R_3:0.225-0.275$ mm) at adhesion area percent, A, ranging from 0% to 40%. The data were obtained from the three regression curves using equation 33 in Figure 33.	88
Figur e	42.	Change of Young's modulus with respect to glue-bond thickness ranges ($R_1:0.025-0.075~mm$, $R_2:0.125-0.175~mm$, $R_3:0.225-0.275~mm$) at adhesion area percent, A, ranging from 50% to 100%. The data were obtained from the three regression curves using equation 33 in Figure 33.	89

Figure	Numbe	er	Page
Figure	43.	Change of the measured and the calculated Young's modulus with respect to glue-bond thickness ranges ($R_1:0.025-0.075~mm$, $R_2:0.125-0.175~mm$, $R_3:0.225-0.275~mm$) at 100% adhesion area. The calculated data were obtained from the three regression curves using equation 33 in Figure 33.	90
Figur e	44.	Calculated Young's moduli of epoxy resin bond layer to compensate for the Rule of Mixtures model.	97
Figure	45.	Comparison of experimentally determined Young's modulus (.) and calculated Young's modulus from the Dynamic Modulus model () and the ROM model () for 50% resin and 50% hardener.	99
Figur e	46.	Comparison of experimentally determined Young's modulus (*) and calculated Young's modulus from the Dynamic Modulus model () and the ROM model () for 65% resin and 35% hardener.	100
Figure	47.	Comparison of experimentally determined Young's modulus (.) and calculated Young's modulus from the Dynamic Modulus model () and the ROM model () for 80% resin and 20% hardener.	101
Figure	48.	The general trend in Young's modulus between super glue adhered specimens and epoxy cement adhered specimens for one glue spot as a function of adhesion area(%).	110
Figure	49.	The general trend in Young's modulus of glass slide /super glue, epoxy cement, and epoxy resin composite specimens having two or more glue spots as a function of adhesion area(%).	111
Figure	50.	The effect of the glue bond thickness on Young's modulus between the super glue and the epoxy resin adhered composite specimens as a function of adhesion area(%).	112
Figure	51.	Change in elastic modulus of a glass slide for the super glue and the epoxy cement adhered composite specimens.	118
Figur e	52.	Change in elastic modulus of a glass slide for the super glue and the epoxy resin adhered composite specimens.	119

1. INTRODUCTION AND REVIEW OF LITERATURE

The primary motivation for this research was to explore the feasibility of using sonic resonance elasticity measurements to nondestructively assess the integrity of adhesive bonds in laminate composites. For example, one could envision using sonic resonance measurements to monitor (in-situ) the time-evolution of the degradation of a bond layer in a laminate composite heated to temperatures at which the adhesive degrades. Alternatively, one could use elasticity measurements as a quality-control tool to evaluate bond-layer defects (such as incomplete bonding) that might occur during processing of laminate composites. However, before elasticity measurements can be employed to assess bond integrity, one must first understand how the experimentally-determined elasticity values change as a function of variables such as the relative bond adhesion area and the bond thickness. This study seeks to help establish the basic understanding needed to realize the potential of elastic modulus measurements of laminate composites (especially in the arena of the analysis of bondphase defects or bond degradation).

As a model laminate composite specimen, we chose to use two glass microscope slides bonded by a variety of adhesives. Glass microscope slides were appropriate for this study because glass microscope slides are: (1) readily available, (2) relatively inexpensive, in part due to the fact that microscope slides may be employed in the as-received state, without dimensioning, grinding, or polishing, (3) comparatively uniform (in the as-received state) in terms of external slide dimensions and elastic moduli, (3) brittle (which is important since the primary area of interest for the author is ceramics and ceramic composites).

In addition to the relation of this research to damage assessment in brittle laminate composites, this study has application to the subject of external cracks in materials (Figure 1). An external crack

may be defined loosely as a crack which penetrates a solid, leaving only a single, unbroken internal ligament surrounded by a continuous, surface-breaking cracks (often considered in fracture mechanics) in which the cracked area is (typically) small compared to the specimen cross-section. Composite specimens in this study which were adhered only by a single glue spot centered on a long-transverse specimen face might model such an external crack (Figure 1). Specimens adhered by two or more glue spots might model delamination cracks. However, it must be emphasized that the specimens used in this study would only be appropriate to model planar cracks located at the midplane of a prismatic bar. The specimen would not be appropriate to model other crack geometries, crack face orientations, or spatial distributions of cracks.

In this paper, the effects of adhesives on the effective elastic modulus of adhered soda-lime-silica microscope glass slides were investigated using three different kinds of adhesives. The area fraction, thickness, and composition of adhesives affected the measured elastic modulus for glass slide/glue composite specimens. Also a 'Rule of Mixtures' model and a 'Dynamic Beam Vibration' model were compared with experimental results of the glass slide/glue composite specimens containing a layer of 100 percent adhesion area sandwiched between two glass slide layers.

Before discussing the experimental procedure and results of this study, we shall briefly review the 'Rule of Mixtures' model, the 'Dynamic Beam Vibration' model and an 'External Crack' model in order to compare differences and similarities between our study and such models. The following reviews shall show the assumptions and results of each model. The glass slide/glue composite specimens used in this study can be considered as a three-layer composite composed of two slide glasses and adhesive. Therefore the models considered shall be confined to those models which deal with three-layer composites.

1.1. 'External Crack' model

Kemeny and Cook introduced an 'external crack' model to estimate the effect of strongly interacting cracks which is very common in rocks with a high crack density [1]. In this section, Kemeny and Cook's assumptions for the external crack model and the stress intensity factor calculation shall be reviewed for two dimensional internal cracks and external cracks (Figure 1).

Kemeny and Cook [1] considered a random distribution of flat, internal cracks or external cracks in a linear elastic, isotropic and homogeneous medium. Narrow elliptical internal cracks and external cracks were considered [1], the surfaces of which were assumed to be friction-free.

Assuming plane strain, the intrinsic Young's modulus, E, can be related to the effective Young's modulus, \bar{E} , for a solid containing cracks under a uniaxial stress σ [1, 2].

$$-\frac{\sigma^2 V}{2\overline{E}} = -\frac{\sigma^2 V}{2E} + \Delta \Psi \tag{1}$$

where V = volume of the body containing the cracks

AT = increase in strain energy due to the presence of the cracks.

For a two dimensional elastic body, U_e , the additional strain energy due to the existence of a single internal crack of length 2c is given by $\{1, 3\}$

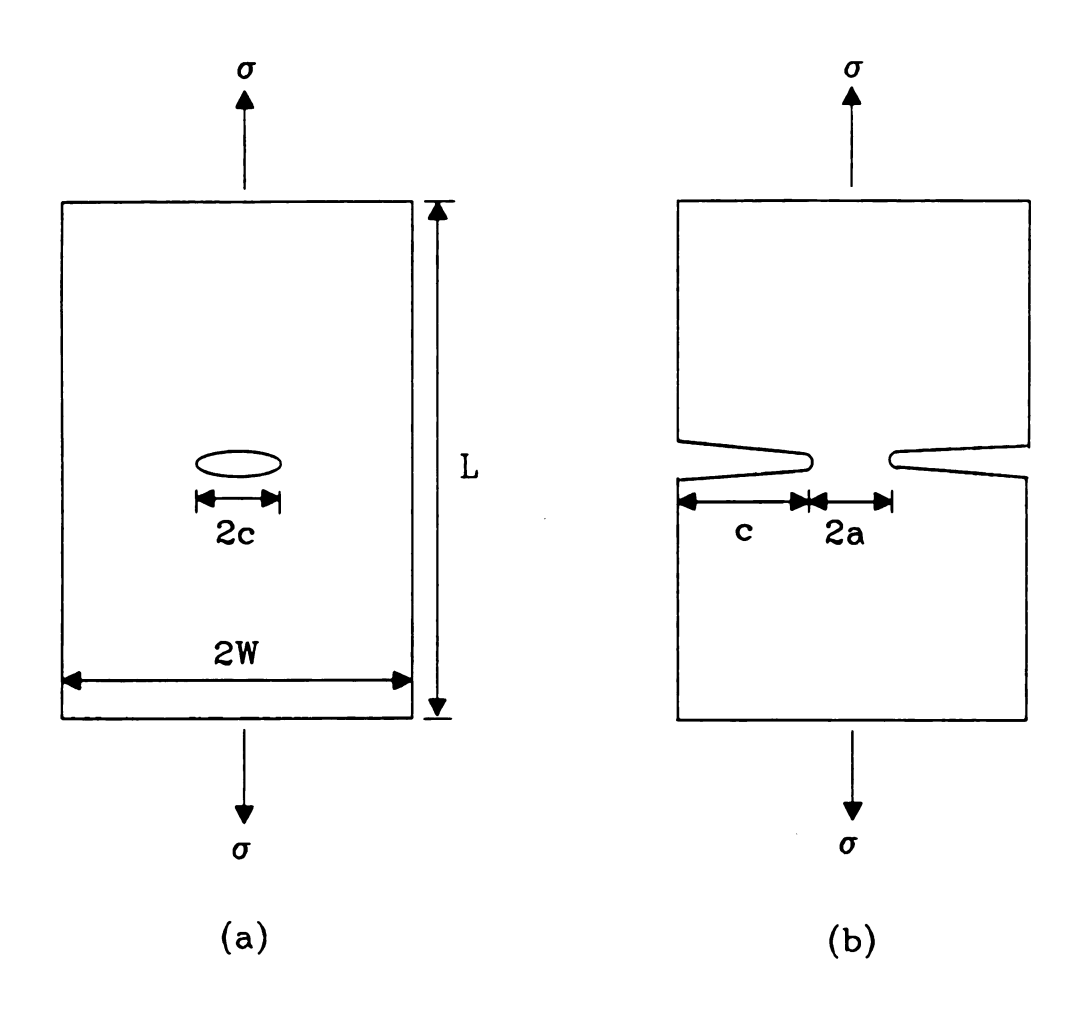


Figure 1. Elliptical Internal Cracks (a), External Cracks (b) under uniaxial loading [1].

$$U_{c} = \frac{2(1-v^{2})}{E} \int_{0}^{c} \left[K_{i}^{2} + K_{ii}^{2} + \frac{K_{ii}^{2}}{(1-v)} \right] dc$$
 (2)

where E = intrinsic Young's modulus

v = Poisson's ratio

 K_i = crack tip stress intensity factor for opening mode

 $K_{I\!I}$ = crack tip stress intensity factor for shearing mode

 K_{III} = crack tip stress intensity factor for tearing mode of deformation.

For a single external crack, the lower and upper limits of integration in equation 2 are replaced by a and a+c, where a is the contact length for the external crack, and c is the length of the external crack surrounding the contact area [1].

A plate of width 2W, height h, and unit thickness containing either an internal crack of length 2c or an external crack of contact length 2a gives the following crack tip stress intensity factors under the uniaxial tension σ at an angle θ to the sides of height h [1, 4].

For an internal crack [1, 4]

$$K_I = \sigma \sqrt{\pi c} \sin^2 \theta \tag{3a}$$

$$K_{II} = \sigma \sqrt{\pi c} \sin \theta \cos \theta \qquad c \ll W$$
 (3b)

$$K_{m}=0. (3c)$$

For an external crack [1, 4]

$$K_{l} = \frac{\sigma 2W}{\sqrt{\pi a}} \sin^{2}\theta \tag{4a}$$

$$K_{II} = \frac{\sigma 2W}{\sqrt{\pi a}} \sin \theta \cos \theta \qquad a << W$$
 (4b)

$$K_{m}=0. (4c)$$

Substituting equations 3a-3c and 4a-4c into equation 2 and integrating gives the additional strain energies due to a single internal crack or single external crack under uniform stress, respectively, as [1]

$$U_{\epsilon}(\theta) = \pi c^2 \sigma^2 \sin^2 \theta \frac{(1-v^2)}{E}$$
 (5)

$$U_{\epsilon}(\theta) = 8W^{2}\sigma^{2} \sin^{2}\theta \ln \left[\left(\frac{a+c}{a} \right) \frac{(1-v^{2})}{E\pi} \right]. \tag{6}$$

Kemeny and Cook [1] assumed that N internal cracks or external cracks are randomly distributed in the body with a mean internal crack length squared $\langle c^2 \rangle$ or a mean external crack contact length squared $\langle a^2 \rangle$. Taking a cylindrical average from zero to 2π , the average of $\sin^2\theta$, denoted as $\langle \sin^2\theta \rangle = 1/2$. Also making the approximation that W=c for a<<W, the total strain energy due to a random distribution of either internal cracks or external cracks , respectively, is given by [1]

$$U_{\epsilon} = N\sigma^{2}\pi \overline{C}^{2} \frac{(1-v^{2})}{2E} \tag{7}$$

$$U_{c} = N\sigma^{2}\pi\overline{c}^{2} \ln \left[\left(\frac{\overline{a} + \overline{c}}{\overline{a}} \right) \frac{(1-v^{2})}{\pi E} \right]$$
 (8)

where \bar{c} = effective internal crack length (\bar{c}^2 = < c^2 >/N) \bar{a} = effective external crack contact length (\bar{a}^2 = < a^2 >/N).

Substituting equations 7 and 8 into equation 1 gives the effective Young's modulus for a body containing a random distribution of either internal cracks or external cracks, respectively, as [1]

$$\frac{\overline{E}}{E} = \frac{1}{1 + \pi m (1 - v^2)} \tag{9}$$

$$\frac{\overline{E}}{E} = \frac{1}{1 + \frac{8}{\pi} m \ln \left[\left(1 + \frac{1}{n} \right) (1 - v^2) \right]}$$
 (10)

where $m = N\bar{c}^2/V$

= crack density parameter

 $n = \bar{a}/\bar{c}$

= external crack shape parameter which characterizes
the relative amount of contact per unit area.

The effects of varying the two parameters m and n can be predicted from equations 9 and 10. For both internal cracks and external cracks,

as the crack density approaches infinity, the effective Young's modulus approaches zero. For the external cracks, while the crack density m is held constant, the effective Young's modulus decreases with the decrease of the relative crack contact area n [1].

A key assumption for the Kemeny and Cook model [1] is that material undergoing a plane strain under a uniaxial stress is linear elastic, isotropic and homogeneous. Also, Kemeny and Cook considered the flat, friction free, elliptical internal cracks or external cracks to be randomly distributed within the body. In our study, Young's modulus of glass slide/glue composite specimens was calculated from free vibration. However, the area surrounding the glue spots can be considered as external cracks, so has relevance to the current study for the determination of the effective modulus of the glue layer.

1.2. 'Rule of Mixtures (ROM)' Model

In this study the glass slide/glue composite specimens contained a glue layer between two glass slides. Thus, the glass slide/glue composite specimen configuration can be considered as a three layered composite. Therefore, this review shall concentrate on the ROM model for estimation of effective elastic modulus of a three layer composite [5]. The main assumptions for the ROM model shall be noted and compared with the physical reality of the glass slide/glue composite specimens included in our study.

When a load is unidirectionally applied to a three layer composite (Figure 2), the strain of each layer is equal to the effective strain, $\epsilon_{\rm eff}$, of the composite [5, 6]:

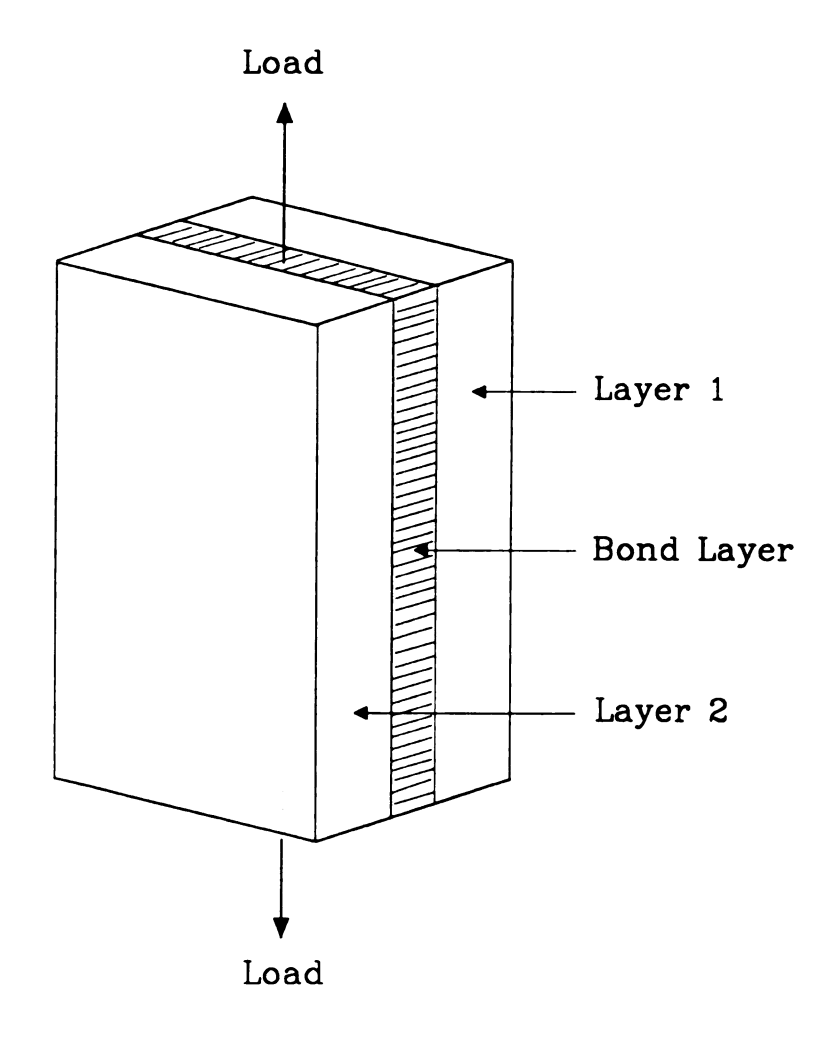


Figure 2. Composite specimen composed of layers 1, 2 and a bond layer for Rule of Mixtures model [1], where uniaxial tension is assumed for the elastic modulus determination. For this study, layers 1 and 2 were glass microscope slides.

$$\varepsilon_{ii} = \varepsilon_{ii} = \varepsilon_b = \varepsilon_{df} \tag{11}$$

where subscripts '11', '12' and 'b' refer to layers 1, 2 and bond layer sandwiched between the layers 1 and 2, respectively.

Equation 11 is based on the assumption of perfect interfacial bonding between layer 1, layer 2 and bond layer, such that there is no sliding of a layer on an adjacent layer [6].

Assuming elastic behavior of each layer, the stresses are given by [5, 6]

$$\sigma_{ii} = E_{ii} \epsilon_{ii} \tag{12a}$$

$$\sigma_n = E_n \, \varepsilon_n \tag{12b}$$

$$\sigma_b = E_b \ \varepsilon_b \tag{12c}$$

Accordingly, the load on each layer can be given by [5]

$$P_{II} = \sigma_{II} A_{II} = E_{II} \varepsilon_{II} A_{II} \tag{13a}$$

$$P_{ii} = \sigma_{ii} A_{ii} = E_{ii} \epsilon_{ii} A_{ii} \tag{13b}$$

$$P_b = \sigma_b A_b = E_b \varepsilon_b A_b \tag{13c}$$

where A_{II} , A_{II} and A_{b} are the cross-sectional areas of the layers 1, 2 and bond layer, respectively.

The effective load applied to the composite, $P_{df} = P_{II} + P_{I2} + P_b$ and effective cross sectional area of the composite, $A_{df} = A_{II} + A_{I2} + A_b$, such that [5, 6]

$$P_{eff} = \sigma_{eff} A_{eff} = \sigma_{ll} A_{ll} + \sigma_{l2} A_{l2} + \sigma_{b} A_{b} . \tag{14}$$

Therefore, [5, 6]

$$\sigma_{eff} = \sigma_{II} \frac{A_{II}}{A_{eff}} + \sigma_{I2} \frac{A_{I2}}{A_{eff}} + \sigma_b \frac{A_b}{A_{eff}}$$

$$= \sigma_{II} V_{II} + \sigma_{I2} V_{I2} + \sigma_b V_b$$
(15)

where V_{ii} , V_{ii} and V_{b} are the volume fractions of the layers 1, 2 and the bond layer.

Differentiating equation 15 with respect to strain yields

$$\frac{d\sigma_{eff}}{d\varepsilon} = \frac{d\sigma_{u}}{d\varepsilon} V_{u} + \frac{d\sigma_{u}}{d\varepsilon} V_{u} + \frac{d\sigma_{b}}{d\varepsilon} V_{b} . \tag{16}$$

With the assumption of elastic behavior in each layer, $d\sigma_{ll}/d\varepsilon$, $d\sigma_{ll}/d\varepsilon$ and $d\sigma_{b}/d\varepsilon$ can be represented by the corresponding elastic moduli. As a result, \bar{E}_{3ROM} , the effective elastic modulus of the three layer composite [5, 6]

$$\overline{E}_{SROM} = E_{II}V_{II} + E_{II}V_{II} + E_{b}V_{b} . \tag{17}$$

The principal assumptions of the ROM model are perfect interfacial bonding between layers and the linear elastic behavior of each layer. Linear elastic behavior means that the slope of stress-strain curve of each layer, $d\sigma/ds$, is linear. This linearity is typically applicable for glass or ceramic composites [6].

1.3. 'Dynamic Beam Vibration' model

In the dynamic beam vibration model, beam vibrations can be described approximately by the Bernoulli-Euller beam equation [7, 8]. For the free, undamped vibration of a monolithic bar, the Bernoulli-Euler beam equation is given by [5, 7-9]

$$EI \frac{\partial^4 W(x,t)}{\partial x^4} + \frac{A\rho}{G} \frac{\partial^2 W(x,t)}{\partial t^2} = 0$$
 (18)

where E = Young's modulus

I = the second moment of inertia of the cross section of
 the bar with respect to the neutral axis

W = transverse deflection of the bar, which is a function
 of position x along longitudinal axis and time t

A = cross sectional area of the bar

 ρ = density of the bar

G = acceleration due to gravity.

For a three-layer composite in which a bond layer is sandwiched between layers 1 and 2 (Figure 3) and assuming perfect interfacial bonding

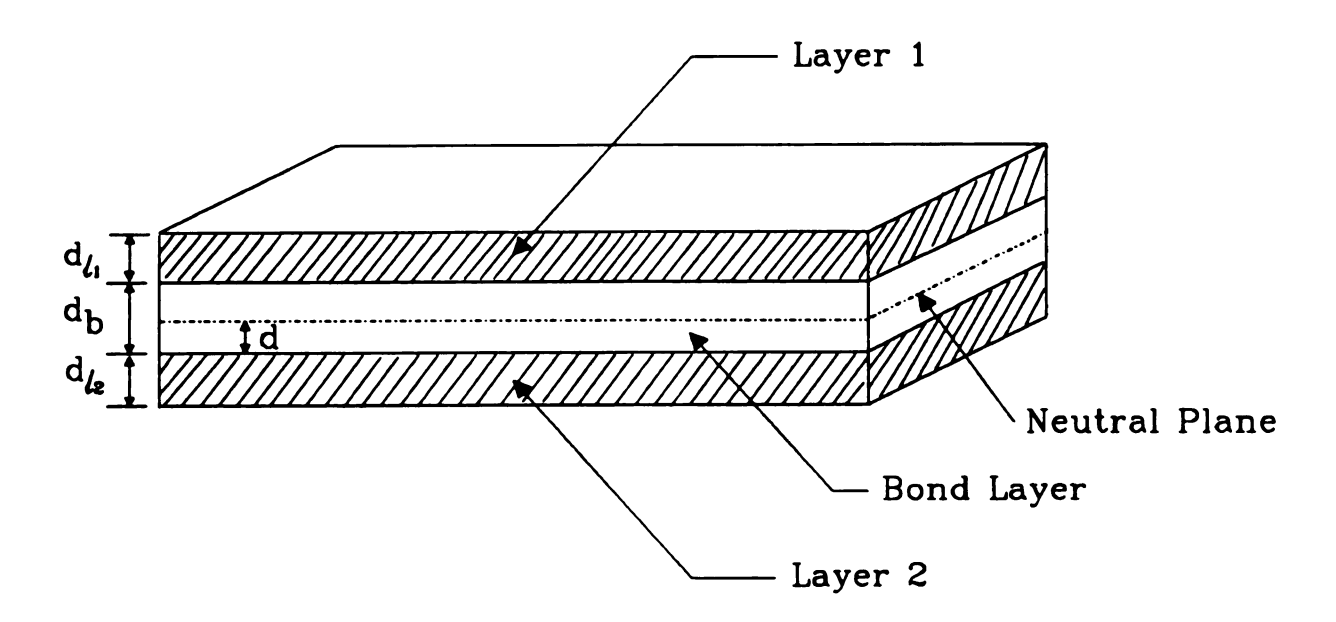


Figure 3. Composite specimen composed of layer 1, 2 and a bond layer for Dynamic Beam Vibration model [5], where the specimen is driven at flexural resonance to determine the elastic modulus. As in figure 1, layers 1 and 2 were glass microscope slides for this study.

between the layer 1 or 2 and the bond layer, equation 18 becomes [5, 9]

$$(E_{ii}I_{ii} + E_{i2}I_{i2} + E_{b}I_{b}) \frac{\partial^{4}W(x,t)}{\partial x^{4}} + \frac{(A_{ii}\rho_{ii} + A_{i2}\rho_{i2} + A_{b}\rho_{b})}{G} \frac{\partial^{2}W(x,t)}{\partial t^{2}} = 0$$
(19)

where subscripts '11', '12' and 'b' refer to layers 1, 2 and bond layer, respectively.

In equation 19, the $(A_{il}\rho_{il}+A_{i2}\rho_{i2}+A_{b}\rho_{b})$ term can be expressed as $A_{C}\rho_{C}$, where A_{C} is cross sectional area of the composite $(A_{c}=A_{il}+A_{i2}+A_{b})$ and ρ_{C} is the average density of the composite $\rho_{c}=(A_{il}\rho_{il}+A_{i2}\rho_{i2}+A_{b}\rho_{b})/(A_{il}+A_{i2}+A_{b})$ [5, 9].

For free-free suspension of a bar, the bending moments and the shearing forces must be zero at both ends of the bar, such that the boundary conditions for the transverse vibration can be given by [5, 7-9]:

bending moments

$$(EI)_c \frac{\partial^2 W(0,t)}{\partial x^2} = 0 , \quad (EI)_c \frac{\partial^2 W(L,t)}{\partial x^2} = 0 \quad \text{for } t \ge 0$$
 (20a)

shearing forces

$$(EI)_c \frac{\partial^3 W(0,t)}{\partial x^3} = 0 , \quad (EI)_c \frac{\partial^3 W(L,t)}{\partial x^3} = 0 \qquad \text{for } t \ge 0$$
 (20b)

where L = length of the bar.

Applying the above boundary conditions to equation 19 gives the fundamental flexural resonance frequency of the three-layer composite [5, 7-9]

$$F = \frac{11.1528}{L^2} \left[\frac{(E_{II} I_{II} + E_{I2} I_{I2} + E_b I_b)G}{A_c \rho_c} \right]^{\frac{1}{2}}$$
 (21)

$$I_{II} = \int_{d_b-d}^{d_b+d_0-d} y^2 dA = \left[(d_b-d)^2 d_{II} + (d_b-d) d_{II}^2 + \frac{d_{II}^2}{3} \right] W$$
 (22a)

$$I_{12} = \int_{-d_{-}}^{-d_{-}} y^2 dA = \left[\frac{d_{12}^3}{3} + d_{12}^2 d + d_{12} d^2 \right] W$$
 (22b)

$$I_b = \int_{a}^{d_b - d} y^2 dA = \left[\frac{d_b^3}{3} - d_b^2 d + d_b d^2 \right] W$$
 (22c)

where d_{11} , d_{12} = thickness of layers 1 and 2, respectively

d_b = thickness of bond layer

y = position along transverse axis

W = width of the bar.

From the equilibrium of the axial forces,

$$\int_{A_{-d}}^{A_{+}} \sigma_{ii} dA + \int_{-d_{-i}}^{-d} \sigma_{i2} dA + \int_{-d}^{-d} \sigma_{b} dA = 0$$
 (23)

where σ_{ii} = normal stress of layer 1 (σ_{ii} = $E_{ii}y/r$)

 $\sigma_{\rm p}$ = normal stress of layer 2 ($\sigma_{\rm p}$ = E_py/r)

 $\sigma_{\rm b}$ = normal stress of bond layer ($\sigma_{\rm b}$ = $E_{\rm b}y/r$)

y = position along transverse axis

r = radius of curvature of the neutral axis.

From the equilibrium condition given in equation 23, the distance, d, from the neutral axis to the interface between the layer 1 or 2 and the bond layer is calculated in terms of known values [5, 10],

$$d = \frac{(E_{II} d_{II}^2 + 2E_{II} d_{II} d_b + E_b d_b^2 - E_{II} d_{II}^2)}{(2E_{II} d_{II} + 2E_b d_b + 2E_{II} d_{II})}.$$
 (24)

Substituting equation 24 into 22, in turn, 22 into 21, the fundamental flexural resonance frequency can be calculated.

The effective elastic modulus, \bar{E}_{3DYN} , of a three-layer composite is given by [5]

$$\overline{E}_{3DIN} = \frac{(E_{II} I_{II} + E_{I2} I_{I2} + E_{b} I_{b})}{(I_{II} + I_{II} + I_{b})} . \tag{25}$$

In the dynamic modulus model, perfect interfacial bonding between two layers and bond layer is a key assumption.

1.4. Description of Current Study and Outline of Remaining Text

The current study investigates the effects of adhesion on the effective Young's modulus, glass slide/glue composite specimens. The effective Young's modulus of each specimen was determined by the experimental procedure which shall be discussed in section 2 'Experimental Procedure'. In section 2, the materials and the procedures used to fabricate the specimens and the technique to determine the effective Young's moduli shall be discussed in detail.

Section 3 'Results and Discussion' includes an analysis of the experimental results in terms of several empirical equations. The effects of adhesion area, the number of glue spots, and the glue bond thickness on the effective Young's modulus of the glass slide/glue specimens shall be discussed in detail. Also, the experimental modulus values shall be compared with the values predicted from the ROM and the Dynamic modulus models discussed in sections 1.2 and 1.3.

2. EXPERIMENTAL PROCEDURE

In this study microscope glass slides were glued to make glass slide/glue composite specimens using three types of adhesives. The adhesives were 'Sure Shot Super Glue (Devcon Corp., Wood Dale, IL, made in Japan)', 'Elmer's Epoxy Cement (Borden Inc., HPPG, Columbus, Ohio, 43215)' and 'Quick Setting Epoxy Adhesive (Super Glue Corporation, Hollis, N.Y., 11423)'. As will be discussed in the following sections each type of adhesive was applied on glass slides and the thickness and mass of glass slides, adhesives and final glass slide/glue composite specimens were measured.

The area fraction of adhesive applied on each glass slide/glue composite specimen was determined using two different methods, template method and grid counting method. For epoxy resin (i.e. 'Quick Setting Epoxy Adhesive'), glass slide/epoxy resin composite specimens were prepared with 100 percent adhesion area but differing compositions of resin and hardener in order to investigate the effect of the composition on the effective Young's modulus of the three layer composite.

Also, five epoxy resin specimens were made of epoxy resin itself. Different compositions of resin and hardener were incorporated in the epoxy resin specimens in order to measure the epoxies' intrinsic Young's modulus and investigate the effect of composition on the epoxy resin specimens. For all the epoxy resin specimens included in this study, the sonic resonance technique was used to determine Young's modulus through free-free suspension of specimen.

2.1. Materials

2.1.1. Microscope Slides

Soda-lime-silica glass microscope slides made by 'Erie Scientific Company' (Model No. 2954-F, Division of Sybron Corp., Portsmouth Industrial Park, Portsmouth, N.H. 03801) were used for this study (Figure 4). The approximate mass of individual slides was 5.7 grams and the dimension was 7.62 cm x 2.54 cm (3 inches by 1 inch) with an approximate thickness of 1.2 mm. Individual glass slides had square edges (Beveled edge glass slides are available but were not included in this study).

2.1.2. Adhesives

Before performing the experimental portion of this study, four different kinds of adhesives were considered. The four adhesives were (1) 'Sure Shot Super Glue', (2) 'Elmer's Epoxy Cement', (3) 'Cement For Plastic Models (No. 3501, The Testor Corporation, Rockford, IL 61108)', and (4) 'Elmer's School Glue (Borden Inc., Dept CP, Columbus, Ohio 43215)'. The large change of mass of adhesives with the lapse of time for experimental period make the exact mass measurements of specimens difficult and may result in some errors in measuring the elastic modulus.

To select the most appropriate adhesives, the mass change of each adhesive was measured as a function of time. A total of eight glass slide/glue composite specimens was made by adhering two glass slides

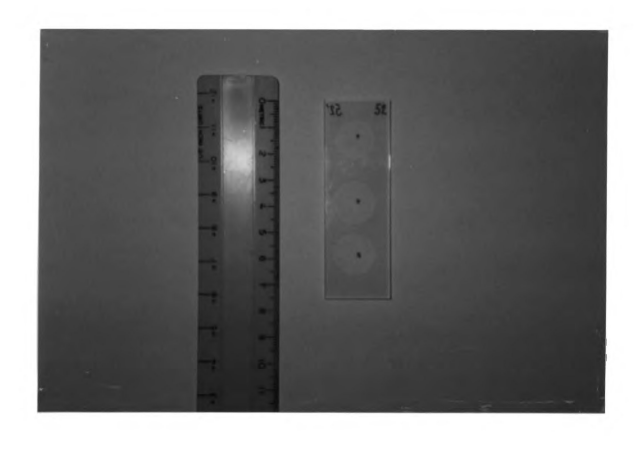


Figure 4. Photograph of glass slide/epoxy resin composite specimen which shows three glue spots and points marked for the measurement of glue bond thickness.

using each adhesive. One hour after gluing the mass of each glass slide/glue composite specimen was measured. During a ninety two hour period the mass of each glass slide/glue composite specimen was remeasured a total of fifteen times. The mass measurements were then normalized with respect to the initial mass. Figure 5 shows the mass as a function of time. The data was fit by a least-squares procedure to an equation of the form

$$m_N = 1 - K_1 \ln(K_2 T) \tag{26}$$

where $m_N = normalized mass of glue$

= mass of glue at one hour after gluing/mass of glue at time T
 (hours) after gluing

 K_1 and K_2 = constants

The mass of glass slide/glue composite specimens adhered by super glue (i.e. 'Sure Shot Super Glue') and epoxy cement (i.e. 'Elmer's Epoxy Cement') changed by 0.0003 g in four days (Figure 5). The mass of 'Elmer's School Glue' and 'Cement For Plastic Models' adhesives changed by up to 0.0125 g in four days because of volatile components in the adhesive (Figure 5). As a result of their mass stability with respect to time, super glue and epoxy cement were selected as adhesives to be included in our study. After selecting the adhesives, epoxy resin (i.e. 'Quick Setting Epoxy Adhesive') was added as a desired adhesive for further experiment.

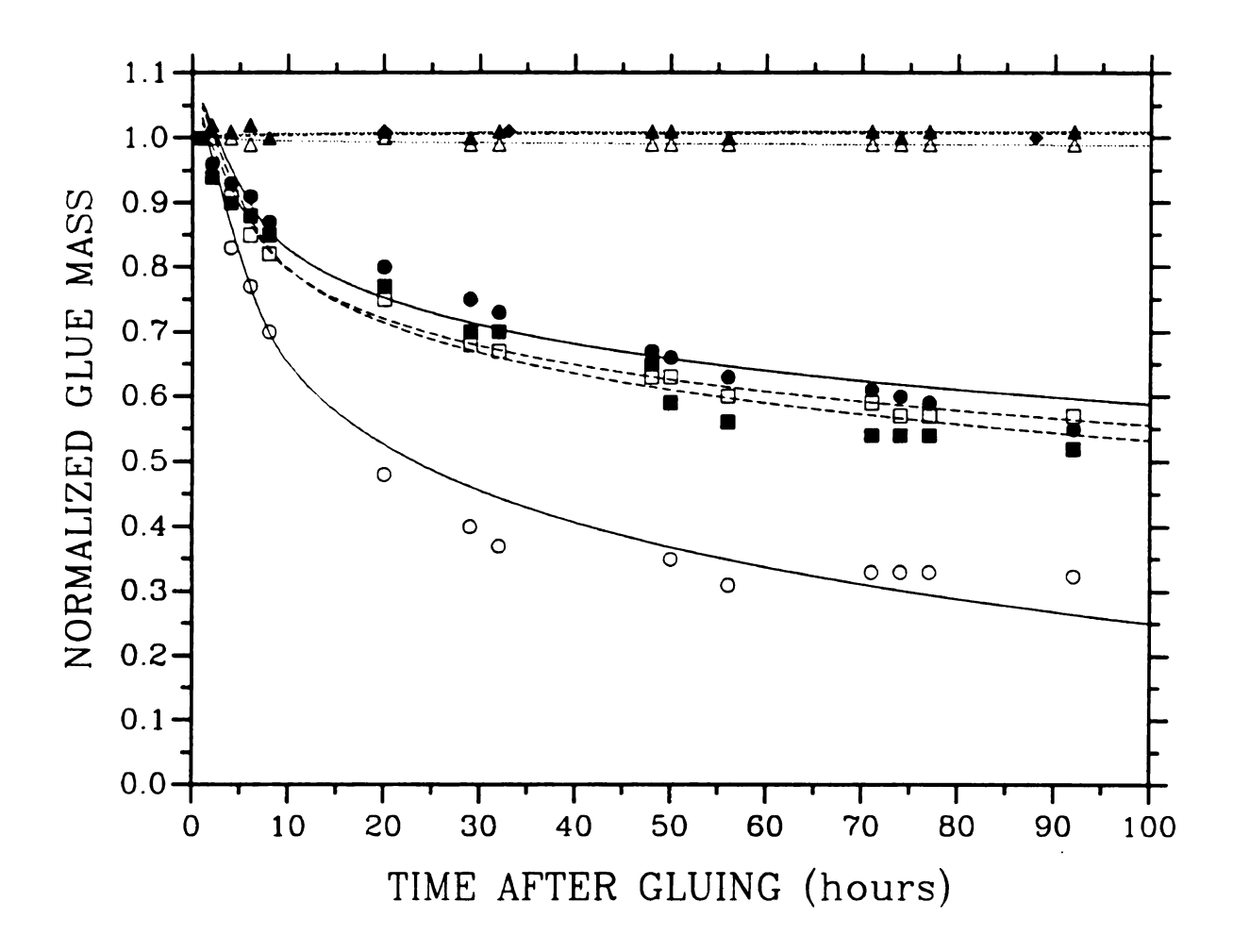


Figure 5. Change of normalized mass of various glues (0, • Elmer's School Glue; \Box , = Cement For Plastic Models; Δ , Δ Epoxy Cement; \Diamond , \Diamond Super Glue) as a function of time in hours after gluing. In this figure, normalized glue mass refers to the ratio of the initial mass of the glue to the glue mass at a later time. The curves represent a least-squares best fit to equation 26. (— K_1 =0.1696, K_2 =0.8292, r=0.9720 and K_1 =0.1014, K_2 =0.5818, r=0.9720; --- K_1 =0.1017, K_2 =0.7908, r=0.9896 and r=0.1120, r=0.6509, r=0.9565; ····· r=0.0027, r=0.6144, r=0.6281 and r=0.0014, r=14.8621, r=0.0834; --- r=1.00012, r=4.0128, r=0.2358 and r=0.0012, r=4.0128, r=0.2358

2.2. The Measurement Of Mass

Before gluing, the mass of individual glass slides was measured using an electronic balance (Model No. A 210 P, Sartorius Corp., 140 Wilbur Pl., Bohemia, N.Y.). This balance is accurate to within ±0.0001 gram.

Super glue, epoxy cement and epoxy resin adhesives had different setting times. Two criteria were used to determine the setting time for the adhesives. First, a shear force was applied to a glass slide/glue composite specimen. If the slides did not move with respect to one another due to the shear couple (which was applied by hand), then the lack of shear was taken as one indication that the adhesive had set. Secondly, when the glue extruded from the edge of a glass slide/glue composite specimen was no longer sticky, then this was taken as another indication that the glue had set. If both criteria (lack of shearing and lack of stickiness) were satisfied, then the adhesive was considered to be set. For adhesion area less than about sixty five percent (in glass slide/glue composite specimens having three glue spots), there was typically no extruded glue from the glass slide/glue composite specimen edges. In these cases, then the shearing criterion was the single criterion used to determine setting time. The setting time of each adhesive determined in this manner was about one hour for the super glue and twenty four hours for the epoxy cement. Thus, the mass of the glass slide/super glue and the glass slide/epoxy cement composite specimens was measured in at least one hour and twenty four hours after gluing, respectively. On the other hand, the setting time of the epoxy resin was variable depending on the ratio of resin and hardener in the epoxy. For an epoxy composition of 50 percent resin and 50 percent hardener the setting time was four hours and for other epoxy compositions of resin and hardener (20%:80%, 35%:65%, 65%:35%, and 80%:20%) the setting time was one to two days. Therefore, the mass was measured in at least four hours for the glass slide/glue composite specimens made by epoxy resin of 50 percent resin and 50 percent hardener and in at least two days for the glass slide/glue composite specimens made by epoxy resin of the other compositions.

2.3. The Measurement Of Thickness

A micrometer (Model No. M115-25, MITUTOYO, made in Japan) was used to measure the thickness of individual glass slides, adhesives and glass slide/glue composite specimens. The micrometer can measure lengths to within ±0.001 mm. First, the position(s) of a point(s) where a glue spot(s) was to be made was determined by eye and marked on a pair of glass slides using a dark-colored permanent marker having a fine point (Figure 4). Schema of the glue spot (marked points) are shown in Figure 6.

After marking the point(s), the thickness of individual slides was measured at the marked point(s). For glass slide/glue composite specimens measured at two or more points, the thickness was averaged. Within one hour after measuring the mass of glass slide/glue composite specimens (Section 2.2.) the thickness of glass slide/glue composite specimens was measured at the marked points and averaged. As a result, the precise thickness of glue could be determined from the difference between the thickness of glass slide/glue composite specimen and the summed thickness of two glass slides.

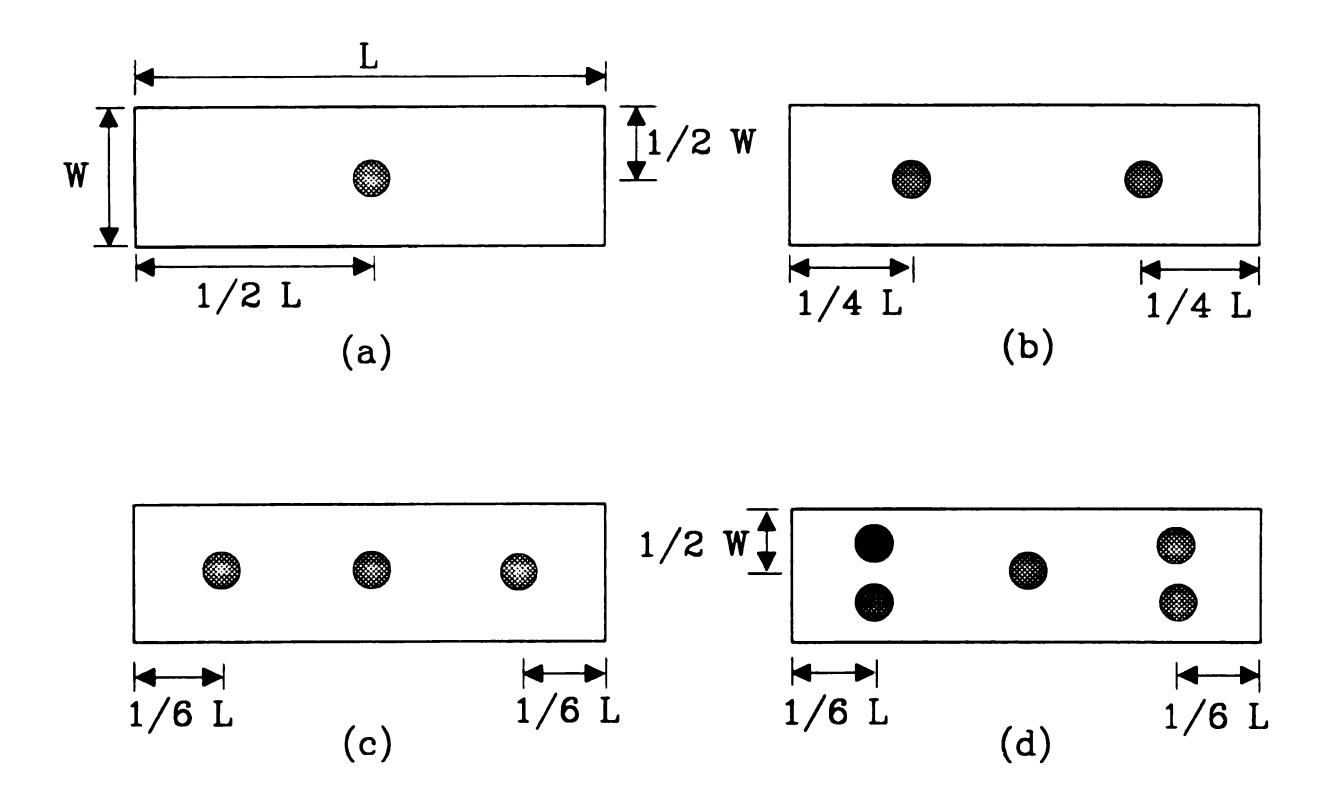


Figure 6. Relative position(s) of glue spot(s): (a) one glue spot, (b) two glue spots, (c) three glue spots, (d) five glue spots, where L=length of specimen and W=width of specimen.

2.4. Applying Adhesives and Preparing Glass Slide/Glue Composite Specimens

2.4.1. Applying 'Super Glue'

Effects of the glue area fraction, the number of glue spots and the thickness of glue on the Young's modulus were investigated using super glue. For the investigation, glass slide/super glue composite specimens with different glue area fraction, number of glue spots and thickness of glue were made by applying one, two, three or five glue spots on one slide (Figure 6).

Within a few seconds after glue spots were made, the second slide was placed upon the first slide where the super glue had been applied, resulting in a glass slide/super glue composite specimen (Figure 4). Within a few seconds after gluing, some pressure (about 20 Newtons to 118 Newtons) was applied on the glass slide/super glue composite specimen using the investigator's two thumbs. As the mass of glue and the pressure applied to the slide increased, the larger the area fraction of glue was and the thinner the glue was after bonding. Therefore, with each glue application, different mass of glue and pressure were used to obtain glass slide/super glue composite specimens with various area fraction of glue between 0 percent and 100 percent and with glue bond thicknesses within one of the three following thickness ranges, 0.010 mm - 0.012 mm, 0.019 mm - 0.021 mm and 0.028 mm - 0.030mm. One hundred and forty six glass slide/super glue composite specimens were made by this procedure but only sixty seven glass slide/super glue composite specimens had a glue thickness that was within one of the above thickness ranges. An additional twenty one

glass slide/super glue composite specimens with the desired area fraction of glue were selected to investigate the effect of adhesion area even though the thicknesses of the glass slide/super glue composite specimens were not in the above three thickness ranges. The total of eighty eight glass slide/super glue composite specimens used in this study are listed in Table 1.

2.4.2. Applying 'Epoxy Cement'

The epoxy cement was composed of two components, resin and hardener, which were contained in two separate tubes. To mix the epoxy, ribbons of the resin and the hardener of approximately the same length were squeezed onto a 7.65 cm x 7.65 cm piece of standard notepad paper (Figure 7). The resin and hardener were mixed using a small rod. Epoxy glue with the composition of approximately 50 percent resin and 50 percent hardener was made. In order to investigate only the effects of area fraction and number of glue spots, one or three glue spots were applied on one slide. Within a few seconds the second slide was put on the slide where the glue was applied. Pressure was applied to the glass slide/epoxy cement composite specimen in the same manner as for the super glue. The twenty glass slide/epoxy cement composite specimens made by this technique are listed in Table 2.

Table 1. Classification of the glass slide/super glue composite specimens according to the number of glue spots and the range of glue thickness.

NUMBER OF GLUE SPOTS	RANGE OF GLUE THICKNESS (mm)	NUMBER OF SPECIMENS (TOTAL 88)
One glue spot	0.010 - 0.012	7
	0.019 - 0.021	11
	0.028 - 0.031	6
	others	4
Two glue spots	0.010 - 0.012	3
	0.019 - 0.021	8
	0.028 - 0.030	0
	others	2
Three glue spots	0.010 - 0.012	12
	0.019 - 0.021	6
	0.028 - 0.030	0
	others	6
Five glue spots	0.010 - 0.012	1
	0.019 - 0.021	0
	0.028 - 0.030	0
	others	4
*	0.010 - 0.012	1
	0.019 - 0.021	2
	0.028 - 0.030	0
	others	5

^{*} Specimens having adhesion area greater than 90% which could not be classified according to the number of glue spots.



Figure 7. Photograph of epoxy resin (i.e. "Quick Setting Epoxy Adhesive"), a 7.65 cm piece of standard notepad paper and a stick for mixing and applying.

Table 2. Classification of the glass slide/epoxy cement composite specimens according to the number of glue spots.

NUMBER OF GLUE SPOTS	NUMBER OF SPECIMENS
One glue spot	10
Three glue spots	10

2.4.3. Applying 'Epoxy Resin'

In order to investigate the effect of adhesive composition as well as the effects of the area fraction and the thickness of the adhesive, adhesives of various compositions of resin and hardener were made. First, using a balance (Serial No. 2155, E.H. Sargent & Co., Mettler instrument corp., Hightstown N.J.) with the accuracy of 0.0001 gram, the mass was measured for the small piece of paper onto which the resin and the hardener was to be squeezed for mixing. Then, the resin was squeezed onto the paper and the mass was remeasured. In order to obtain five different compositions of resin and hardener (20%:80%, 35%:65%, 50%:50%, 65%:35% and 80%:20%), the mass of the hardener was calculated and the required mass was squeezed on the same piece of paper using the balance. The resin and hardener was mixed on the paper using a small stick so that the desired compositions of adhesive was obtained. The resin, hardener, the notepad paper and stick used for mixing in this study are shown in Figure 7. Within ten minutes after mixing the resin and the hardener, three glue spots were made on one slide using a stick. The positions of the glue spots were selected in the same manner as in super glue. Then, the second slide was put on the slide where the glue was applied, resulting in a glass slide/epoxy resin composite specimen (Figure 4). The selected thickness ranges of the epoxy adhesive were 0.025 - 0.075 mm, 0.125 - 0.175 mm and 0.225 - 0.275 mm. Pressure applied by the investigator's thumbs was used to obtain desired thickness and the various area fractions of adhesive. One hundred and ten glass slide/epoxy resin composite specimens were made with three glue spots or 100 percent coverage of glue. However, four glass slide/epoxy resin composite specimens resulted in misalignments between

the two slides after gluing (That is, the "top" and "bottom" slides were not coincident). The misaligned glass slide/epoxy resin composite specimens were excluded from the investigation. In addition, ten glass slide/epoxy resin composite specimens glued with the adhesive composition of 20 percent resin and 80 percent hardener were excluded because the fundamental flexural frequencies had amplitudes that were too low and peaks that were so broad that accurate modulus measurements could not be made. Data for a total of ninety six glass slide/epoxy resin composite specimens was included in this investigation (Tables 3 and 4).

2.5. The Measurement Of Area Fraction Of Glue

Two techniques were used for the measurement of the glass slide/glue composite specimen's glue area fraction. The selection of the measurement technique depended on the shape of glued area in each glass slide/glue composite specimen.

2.5.1. Template Method For Small Circle-Shaped Glue Spots

When small amounts of glue were applied and two glass slides were glued together for smaller than about sixty five percent area of glue (in glass slide/glue composite specimens having three glue spots), the glue spots tended to spread in circle, regardless of what type of glue was used. For the circular glue spots a template (Kum Sung, No 001, pencil allowance 0.5 mm, made in Korea) having forty one circles of

Table 3. Classification of the glass slide/epoxy resin composite specimens according to the composition of the glue and the range of glue thickness.

COMPOSITION OF GLUE (RESIN : HARDENER)	RANGE OF GLUE THICKNESS (mm)	NUMBER OF SPECIMENS (Total 70)
50% : 50%	0.025 - 0.075	16
50% : 50%	0.125 - 0.175	13
50% : 50%	0.225 - 0.275	14
50% : 50%	others	27

Table 4. Classification of the glass slide/epoxy resin composite specimens with 100 % adhesion area. These specimens were included in the experimental comparison of the ROM and the Dynamic Beam Vibration models (Section 3.3.5).

COMPOSITION OF GLUE (RESIN : HARDENER)	AREA FRACTION OF GLUE (%)	NUMBER OF SPECIMENS (TOTAL 39)
20% : 80%	100	0
35% : 65%	100	8
50% : 50%	100	13
65% : 35%	100	10
80% : 20%	100	8

various sizes from 1.5 mm to 35 mm was used to measure the glue area fraction. The size increment between adjacent circles on the template was either 0.5 mm or 1 mm (Figure 8).

The template was placed over each of the glass slide/glue composite specimen's glue spots. The size of each glue spot was determined from the template circle that most closely matched the glue spot diameter.

As a result, a somewhat accurate glue area fraction could be calculated over the area of glass slide/glue composite specimen (See Appendix A).

2.5.2. Grid Counting Method For Irregularly-Shaped Glue Spots

For heavier glue masses and larger glue area fractions, the glued area tended to be irregular which meant that the template method mentioned in section 2.5.1. could no longer be applied. Therefore, a grid counting method which employed translucent grid paper ruled into 1/8" squares was used to measure glue area fractions (Figure 9).

First, a line was traced along the edge of glued area on a glass slide/glue composite specimen itself with dark-colored pen. Then, the glass slide/glue composite specimen was put under the paper mentioned above. The traced line was re-drawn on the translucent grid paper in order to count the number of squares within the glued area. In counting the number of squares, the squares that the trace line intersected were counted as half-squares. As a result, the glue area fraction could be calculated from the ratio of the number of grid squares within glued area to total number of grid squares covered by the glass slide/glue composite specimen surface. The surface area of a glass slide/glue composite specimen 7.62 cm x 2.54 cm (3 inches by 1 inch) is equivalent

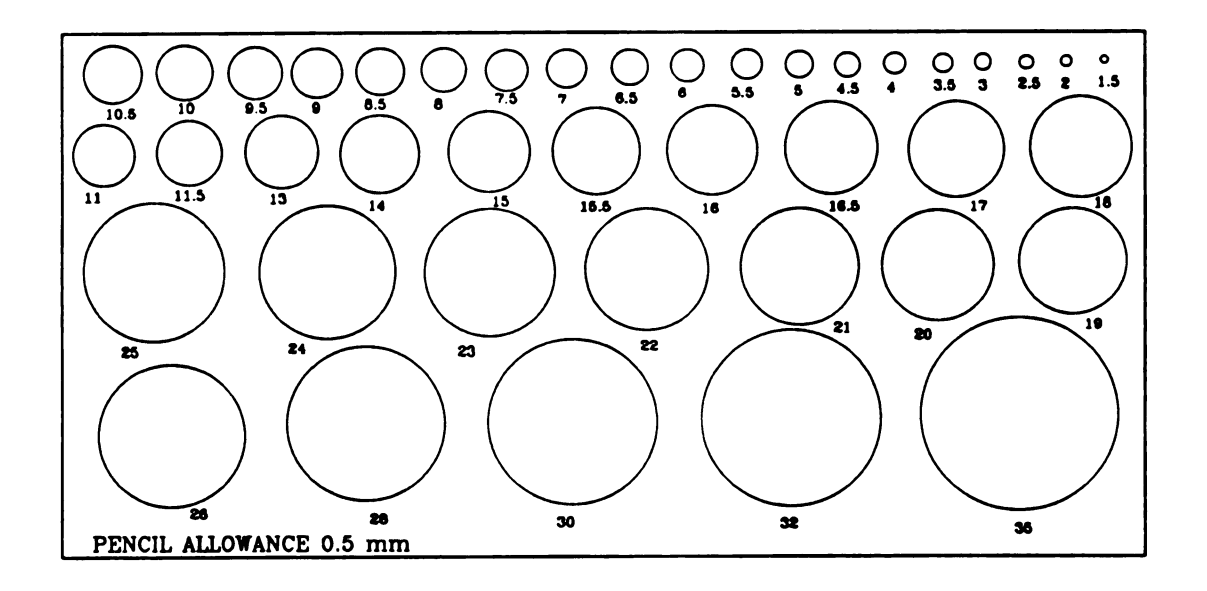


Figure 8. Template used for measurement of the area fraction of the smaller circular glue spots on the composite specimens. The diameter in millimeters is marked below each circle. (The measuring unit of each circle is millimeter.)

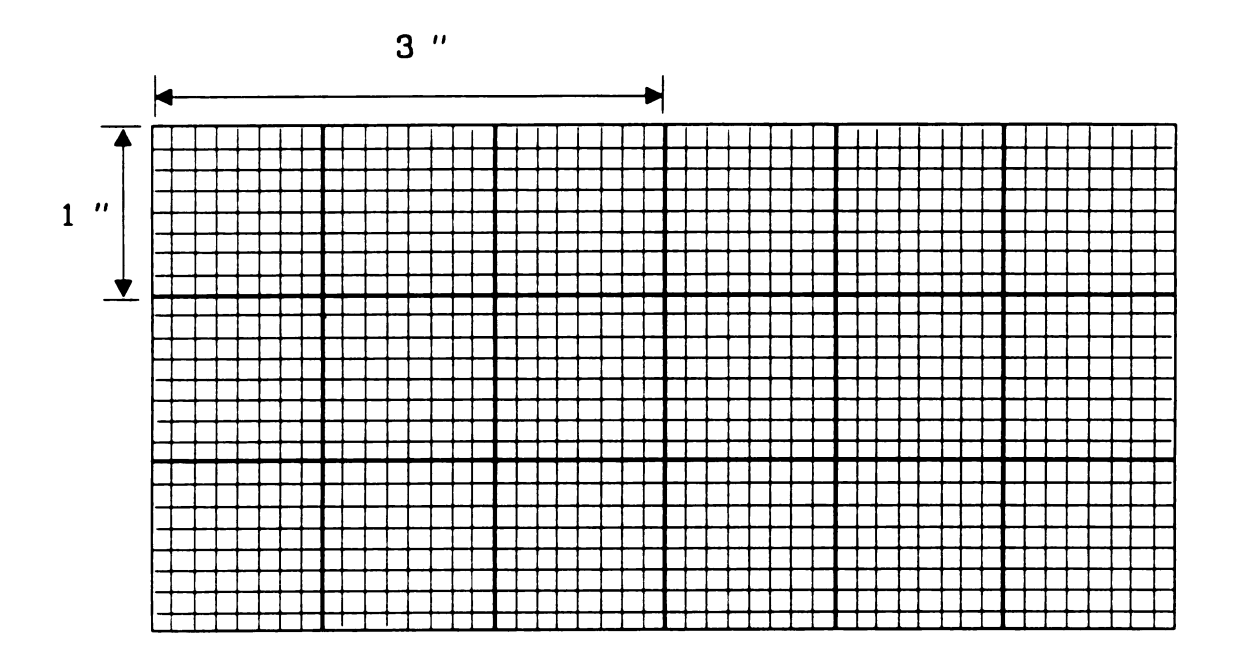


Figure 9. Grid paper used for measurement of the area fraction of irregularly shaped larger glue spots on the composite specimens.

to 192 grid squares.

2.6. The Measurement Of Elastic Modulus

In this study, the sonic resonance technique was used to determine the elastic moduli of single slides, glass slide/glue composite specimens and epoxy resin specimens [11]. The apparatus included a rectangular specimen suspended horizontally from a driver and a pick-up transducers by cotton threads (shown in Fig 10 and schematically in Figure 11).

An electrical signal was generated by the frequency synthesizer (3325A Synthesizer/Function Generator, Hewlett-Packard). The signal was transmitted to a piezoelectric driver transducer (Model No. 62-1, Astatic Corp., Conneaut, Ohio) and converted to mechanical movement. The specimen then vibrated the suspending cotton thread. The resulting mechanical movement generated in the specimen was transmitted to the pick-up transducer through the cotton threads. The pick-up transducer converted the mechanical movement to an electrical signal. The electrical signal was then filtered and amplified (4302 Dual 24DB/Octave Filter-Amplifier made by Ithaco, Ithaca, N.Y.). The filtered and amplified signal was then fed into an oscilloscope (V-1100A, 100MHz Oscilloscope made by Hitachi, Japan), a voltmeter (8050A Digital Multimeter made by Fluke, Everett, WA.) and a counter (5314A, Universal Counter made by Hewlett-Packard).

Mechanical resonant frequencies can be found by monitoring the digital voltmeter and oscilloscope while changing the frequency of an electrical signal. In order to determine the elastic modulus of

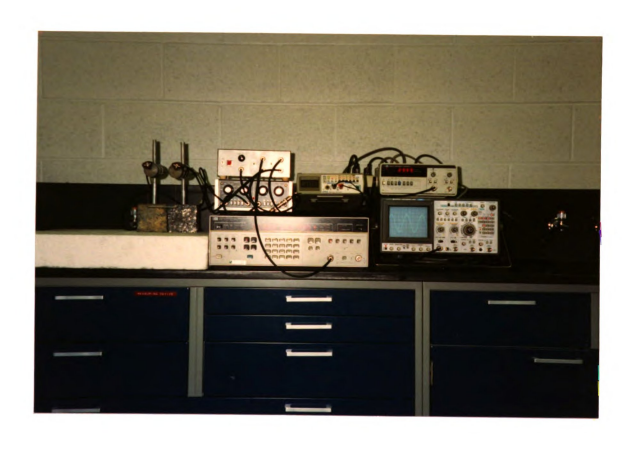


Figure 10. Photograph of the sonic resonance apparatus.

(A glass slide/glue specimen is suspended in the air)

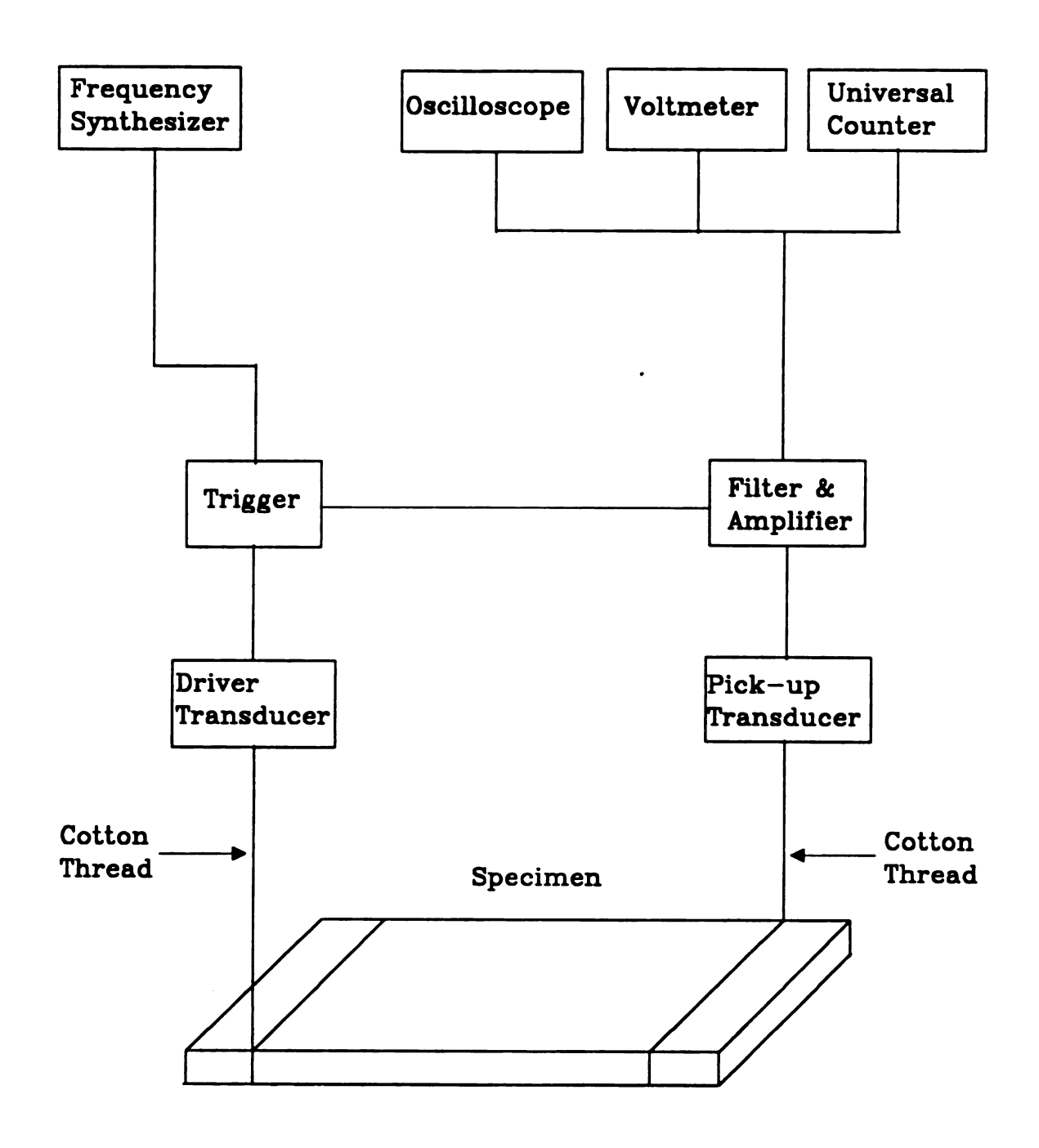


Figure 11. A block diagram of the sonic resonance apparatus [15].

specimen, one must identify the vibrational modes of the specimen [12, 13]. The resonant mode identification was performed using a steel wire to probe for the locations of nodes and antinodes. Nodes have no vertical displacement and antinodes have a maximum displacement. The location of nodes and antinodes are unique to a specific vibrational mode (Table 5 [12]), thus once the position of the nodes and antinodes are known, then the vibrational mode has been uniquely identified.

When a steel wire is placed upon a nodal position, the amplitude of the resonant frequency changes little since there is no vertical displacement at the node. When the wire is placed away from the nodal position, the amplitude decreases because the wire suppresses the mechanical vibration. In this study, the amplitude of a vibrational frequency was measured while the damping wire was moved in 2 mm increments from the left edge of specimen to the right edge. The locations of nodes and antinodes at selected resonant frequencies were determined by plotting amplitude versus relative position of wire. Comparing the node and antinode location information (found via the steel probe wire) with Table 5, the vibrational mode of each resonant frequency was identified.

The fundamental flexural frequencies and torsional frequencies of specimens thus were determined at room temperature in air. The elastic moduli and shear moduli could be calculated from these resonance frequencies by using the following equations [14-16]. Elastic modulus, E, of a rectangular specimen is given by [14-16]

Table 5. For the sonic resonance method, the relative position of nodes according to the vibrational mode.
L is the length of the rectangular specimen.

MODES OF VIBRATION	FLEXURAL MODES	TORSIONAL MODES
Fundamental	0.224 L 0.776 L	0.500 L
First Overtone or	0.132 L	0.250 L
Harmonic*	0.500 L	0.750 L
	0.868 L	

^{*} First overtone refers to the flexural vibration, while the first harmonic refers to the torsional vibration.

$$E = \frac{0.94642 L^4 \rho S_{flex} F_{flex}^2}{D^2}$$

$$= \frac{0.94642 L^4 m S_{flex} F_{flex}^2}{D^3 W}$$
(27)

where L = length of the specimen

 ρ = mass density of the material

 S_{flex} = the shape factor for flexural vibration of prismatic bars

 \mathbf{F}_{flex} = fundamental flexural resonant frequency

D = cross sectional dimension in the direction of vibration

m = mass of the specimen

W =width of the specimen.

The shape factor, S_{flex} , for the rectangular specimen is the function of the specimen dimensions and Poisson's ratio given by [14-16]

$$S_{flex} = 1 + 6.585(1 + 0.0752v + 0.8109v^{2})(\frac{D}{L})^{2} - 0.868(\frac{D}{L})^{4}$$

$$- \frac{8.34(1 + 0.2023v + 2.173v^{2})(\frac{D}{L})^{4}}{1 + 6.338(1 + 0.14081v + 1.53v^{2})(\frac{D}{L})^{2}}$$
(28)

where v = Poisson's ratio.

The shear modulus, G, of a rectangular specimen is given by [14-16]

$$G = 4L^2 \rho S_{tors} \left(\frac{F_{tors}}{N} \right)^2 \tag{29}$$

where L = length of the specimen

 ρ = mass density of the material

 \mathbf{S}_{tors} = the shape factor for torsional vibration of prismatic bars

F_{ton} = torsional resonant frequency

N = an integer (which is unity for the fundamental mode).

The shape factor, S_{ton} , for the rectangular specimen is given by [14-16]

$$S_{lors} = \frac{\left[1 + \left(\frac{W}{t}\right)^{2}\right]\left[1 + 0.0085N^{2}\left(\frac{W}{L}\right)^{2}\right]}{4 - 2.521\left(\frac{t}{W}\right)\left(1 - \frac{1.991}{\exp\left(\frac{\pi W}{t}\right) + 1}\right)} - 0.06\left(\frac{NW}{L}\right)^{1.5}\left(\frac{W}{t} - 1\right)^{2}$$
(30)

where W = width of the specimen

t = thickness of the specimen.

2.7. Making Epoxy Resin Specimens

To investigate the effect of glue composition on the measured elastic moduli and to compare the modulus results to the Rule of Mixtures and to the Dynamic Beam Vibration models, epoxy resin specimens were fabricated using five different epoxy glue compositions including the ratios of resin and hardener of 20%:80%, 35%:65%, 50%:50%, 65%:35% and 80%:20%.

A rectangular plastic box of dimension 94.5 mm x 27.4 mm, height 13.5 mm, and wall thickness 1.8 mm was used as a mold for the epoxy resin specimens. The mass of the plastic-box mold was measured, then the desired quantity of resin was squeezed into the mold and the total mass was measured. From the net mass of resin, the required mass of hardener for the desired composition was calculated and squeezed into the same mold. Then, the resin and hardener were mixed to a homogeneous state in the box, using a small stick.

Within 3 minutes after mixing, the mold was placed in a vacuum chamber pumped by a roughing pump (Welch Duo-Seal Vacuum Pump, Model No. 1402, Serial No. 121054, Sargent-Welch Scientific Co., 7300 North Linder Avenue, Skokie, IL, 60076). The vacuum helped to remove pores which appeared during the mixing of the resin and the hardener. After pumping for about twenty seconds, the mold was removed of the vacuum chamber to check the existence of large pores. In case of there were still many large pores in the epoxy, the mold was placed in the chamber again. The vacuum chamber was then pumped down one or two more times until the large pores were removed.

The setting time was different from specimen to specimen. The molds were removed from the five epoxy resin specimens when the glue was no longer sticky. After about three weeks the molds of three out of the five epoxy resin specimens having epoxy resin composition of the ratios of resin and hardener of 50%:50%, 65%:35%, and 80%:20% were removed by grinding. Two epoxy resin specimens with the epoxy resin compositions of 20%:80% and 35%:65% still were not set even after two months. Thus only three epoxy resin specimens having the ratios of resin and hardener of 50%:50%, 65%:35%, 80%:20% were used as a part of the comparison of ROM and Dynamic Beam Vibration models.

The three final epoxy resin specimens are shown in Figure 12. The epoxy resin resulted from mixing of white resin and yellow hardener, so that we can see from Figure 12 that the more content of the resin was included in a epoxy resin specimen, the whiter the color of the epoxy resin specimen was.



Figure 12. Photograph of epoxy resin specimens. The ratios of resin and hardener used for each specimen are 50%:50%, 65%:35% and 80%:20%, respectively.

3. RESULTS AND DISCUSSION

For the effect of glue area fraction or glue bond thickness on elastic modulus, three candidate equations were used,

$$E = E_{100} [1 - C_1 X^{C_1}]$$
 (31)

$$E = E_{100} [1 - C_3 Exp(C_4X)]$$
 (32)

$$E = C_5 \left[1 - C_6 X^3 \right] \tag{33}$$

where E = Elastic modulus of glass slide/glue composite specimen E_{100} = average elastic modulus of glass slide/glue composite specimen of 100 percent adhesion area (Appendix B) C_1 , C_2 , C_3 , C_4 , C_5 and C_6 = constants

X = 1 - Area fraction of glue.

For the super glue and the epoxy cement, the glass slide/glue composite specimens having 100 percent adhesion area could not be fabricated because three to eight irregularly-shaped pores with sizes of about 0.5 mm up to 8 mm were always included within the glue bond layer. Thus, the elastic moduli of the glass slide/glue composite specimens having greater adhesion area than 90% were averaged to obtain E_{100} (Appendix B).

The three equations 31-33 were used to analyze our experimental results. As will be discussed in the following sections, equations 31

and 32 gave the best descriptions of the effect of adhesion area on the observed Young's modulus. Equation 33 gave the best description of the effect of glue bond thickness on the effective Young's modulus. The success of equation 33 in describing the glue bond thickness effect may be related to the fact that the modulus at x=0 (where x is 1-A and A=glue bond area) is given by C₅, where C₅ is a fitted parameter. In contrast, the value of modulus for x=0 in equation 31 and 32 was E₁₀₀, which was average elastic modulus of glass slide/glue composite specimen of 100 percent adhesion area based on the experimentally obtained elastic modulus at 100% adhesion area (Appendix B).

3.1. Effects of Adhesion Area, Number of Glue Spots, and Glue Bond Thickness

3.1.1. The Effects of Super Glue Adhesion on Elastic Modulus

The effects of adhesion area, number of glue spots and glue bond thickness on the Young's modulus of glass slide/super glue composites were studied using super glue. Figures 13-15 illustrate the Young's modulus as a function of adhesion area according to the number of glue spots. Without regard to the number of glue spots, Young's modulus of adhered glass slides decreased continuously with decreasing the adhesion area.

The Young's modulus for glass slide/super glue composite specimens having one glue spot changed as a function of total adhered area in a different manner from that for glass slide/super glue composite specimens having two, three and five glue spots. For two or more glue

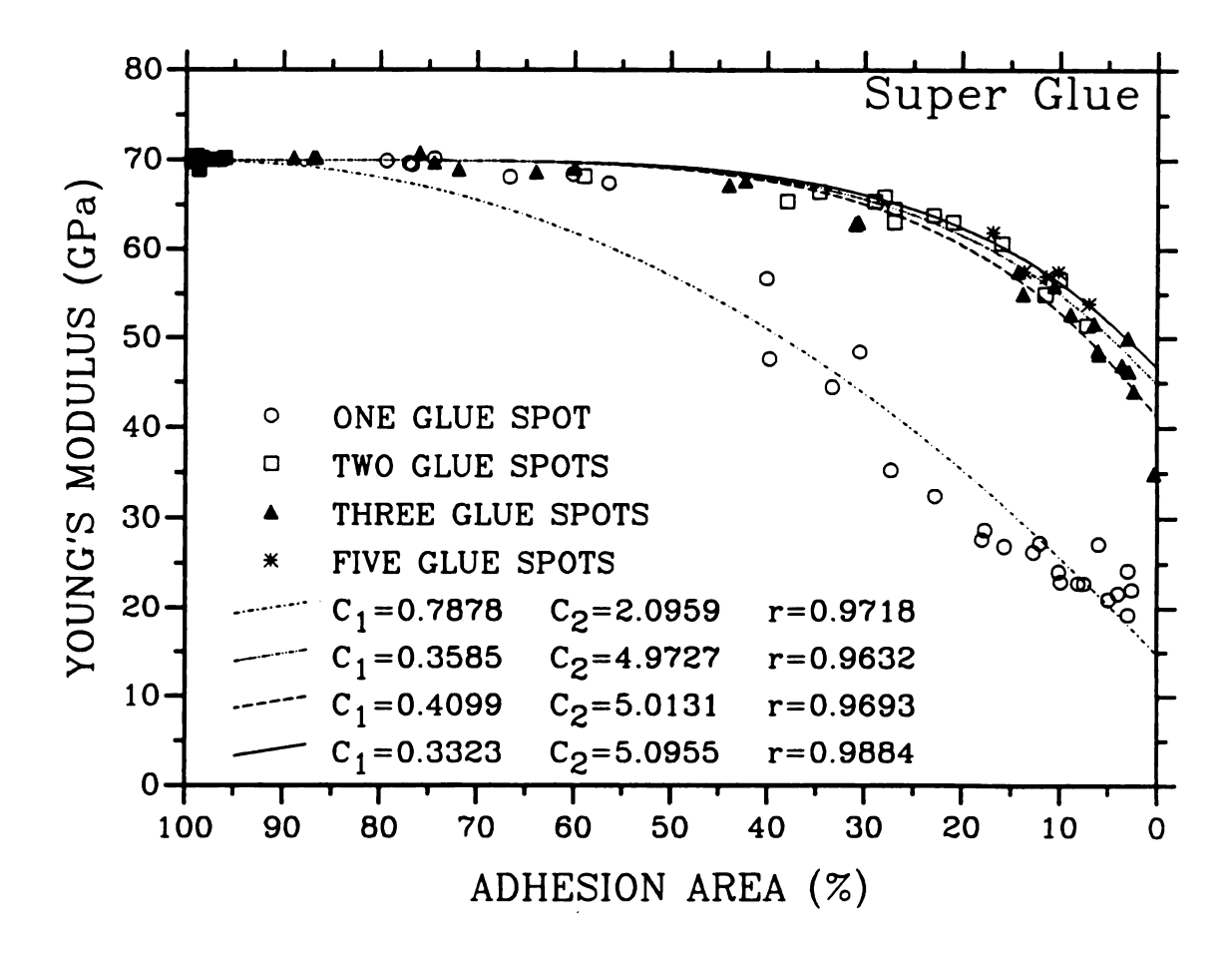


Figure 13. For a super glue bond layer, the effect of the number of super glue spots on Young's modulus as a function of adhesion area(%). The curves represent a least-squares best fit to equation 31.

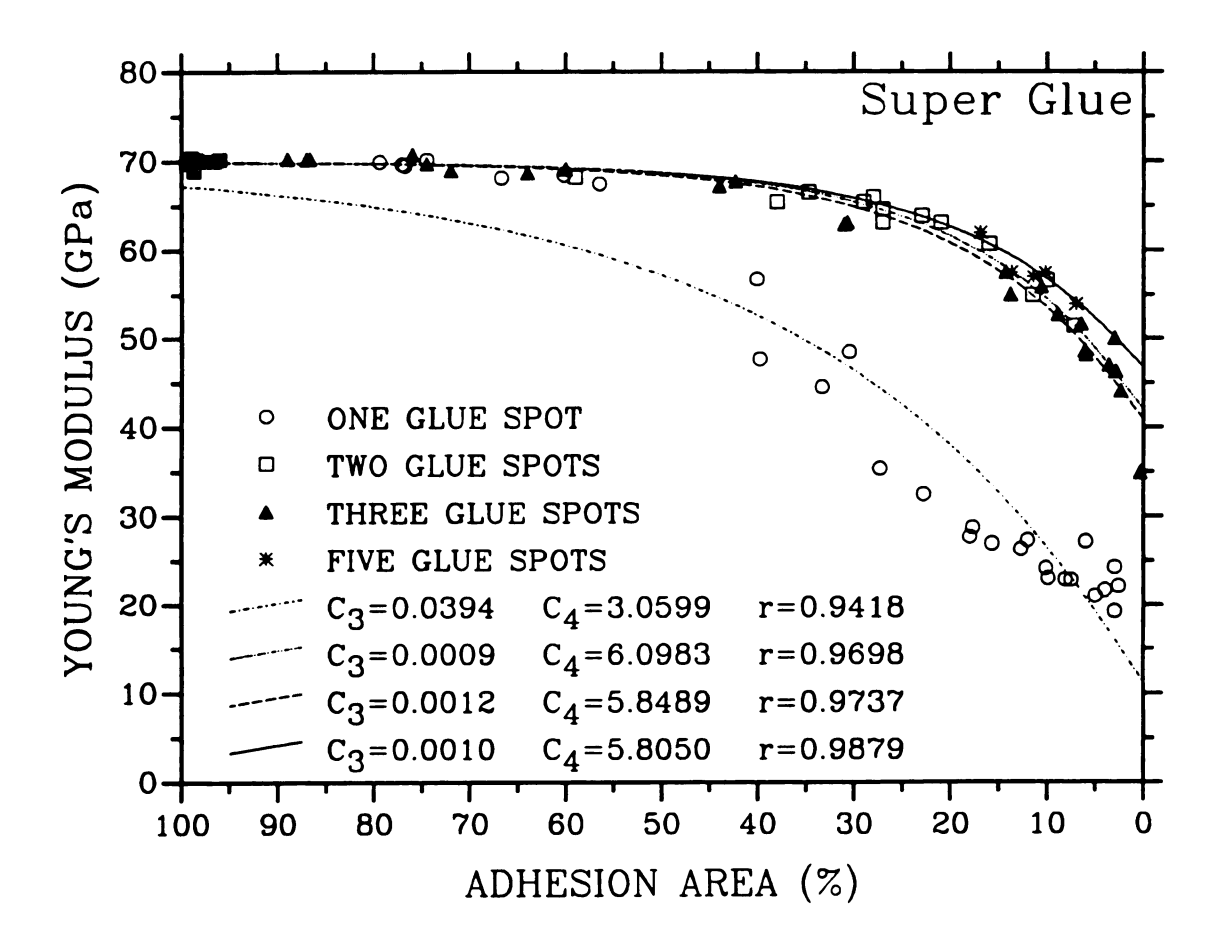


Figure 14. For a super glue bond layer, the effect of the number of super glue spots on Young's modulus as a function of adhesion area(%). The curves represent a least-squares best fit to equation 32.

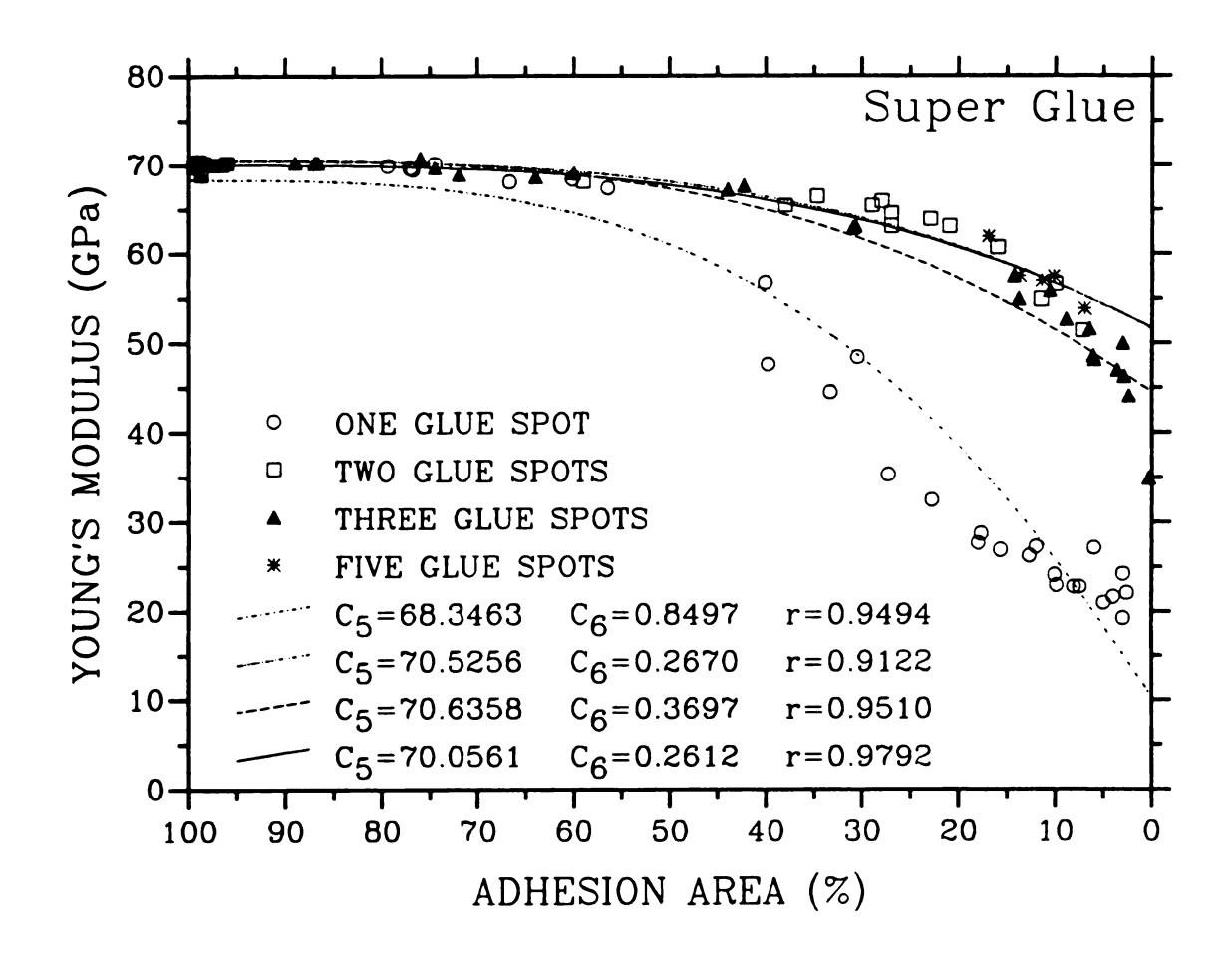


Figure 15. For a super glue bond layer, the effect of the number of super glue spots on Young's modulus as a function of adhesion area(%). The curves represent a least-squares best fit to equation 33.

spots, the three curves nearly superimpose (Figures 13-15). For the glass slide/super glue composite specimens having two, three, and five glue spots, the Young's modulus versus area fraction of three curves decreased relatively rapidly for area fractions less than about 30 to 35 percent (Figures 13-15). Due to similar trends for the Young's modulus data for the glass slide/super glue composite specimens having two, three and five glue spots were plotted using the same symbol and analyzed using a least squares best fit program (Figures 16-18).

To investigate the effect of glue bond thickness, the data for glass slide/super glue composite specimens having one glue spot were plotted separately according to a pre-selected range of glue bond thickness (Figures 19-21).

The analysis and plotting of the data for the glass slide/super glue composite specimens having two and three glue spots were performed in the same manner as for the data of the glass slide/super glue composite specimens having one glue spot (Figures 22-24). However, the effect of the super glue bond thickness on the measured elastic modulus of the glass slide/super glue composite specimens is not pronounced. The weak dependence of Young's modulus upon the thickness of the super glue bond may result from the relative thinness of the super glue bonds compared to the glass slide thickness (See Table 1 for the thickness of the super glue bonds and Table 3 for the thickness of the epoxy bonds).

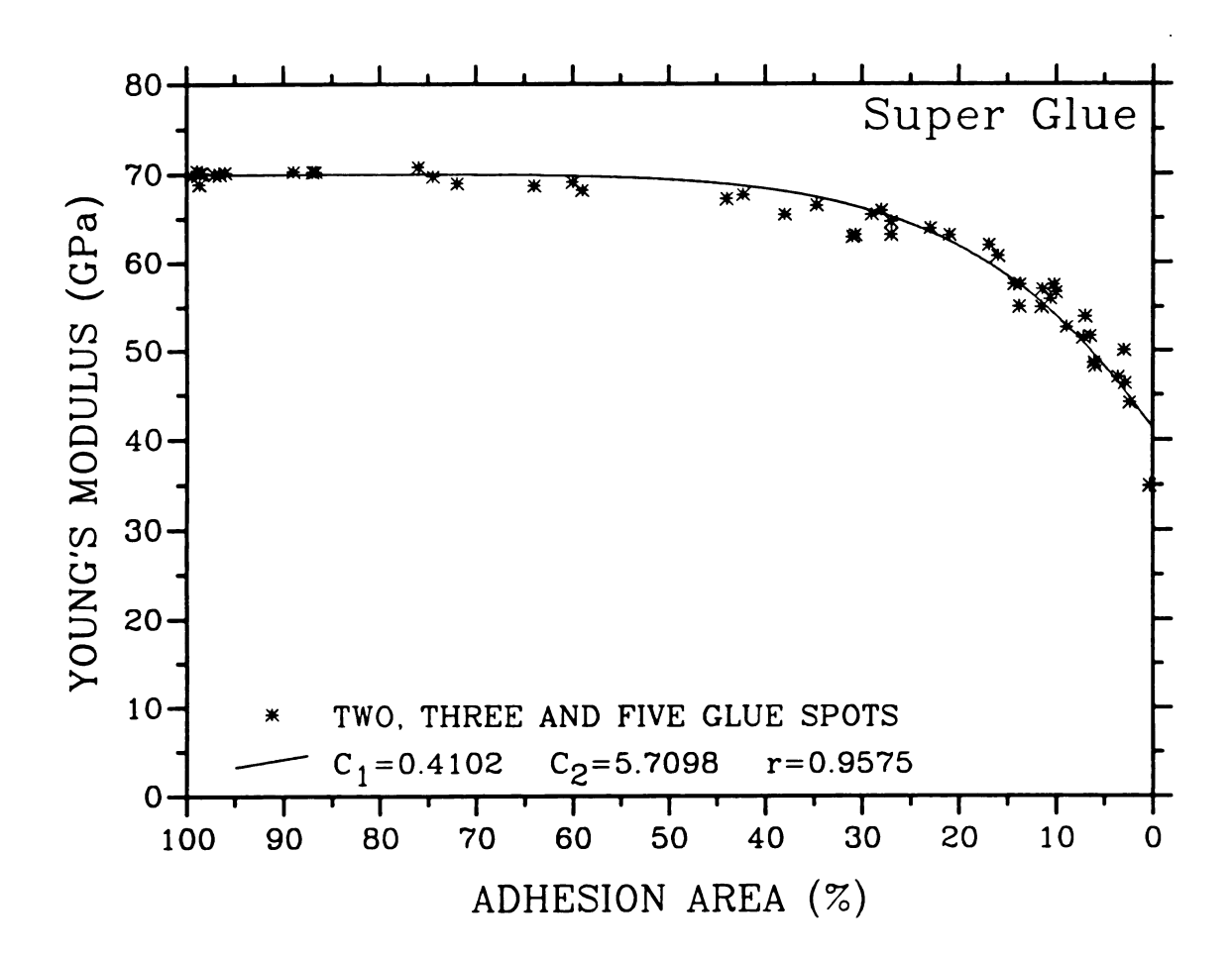


Figure 16. For a super glue bond layer, the effect of the super glue on Young's modulus as a function of adhesion area(%) with the data for specimens having 2, 3 and 5 glue spots lumped together. The curve represents a least-squares best fit to equation 31.

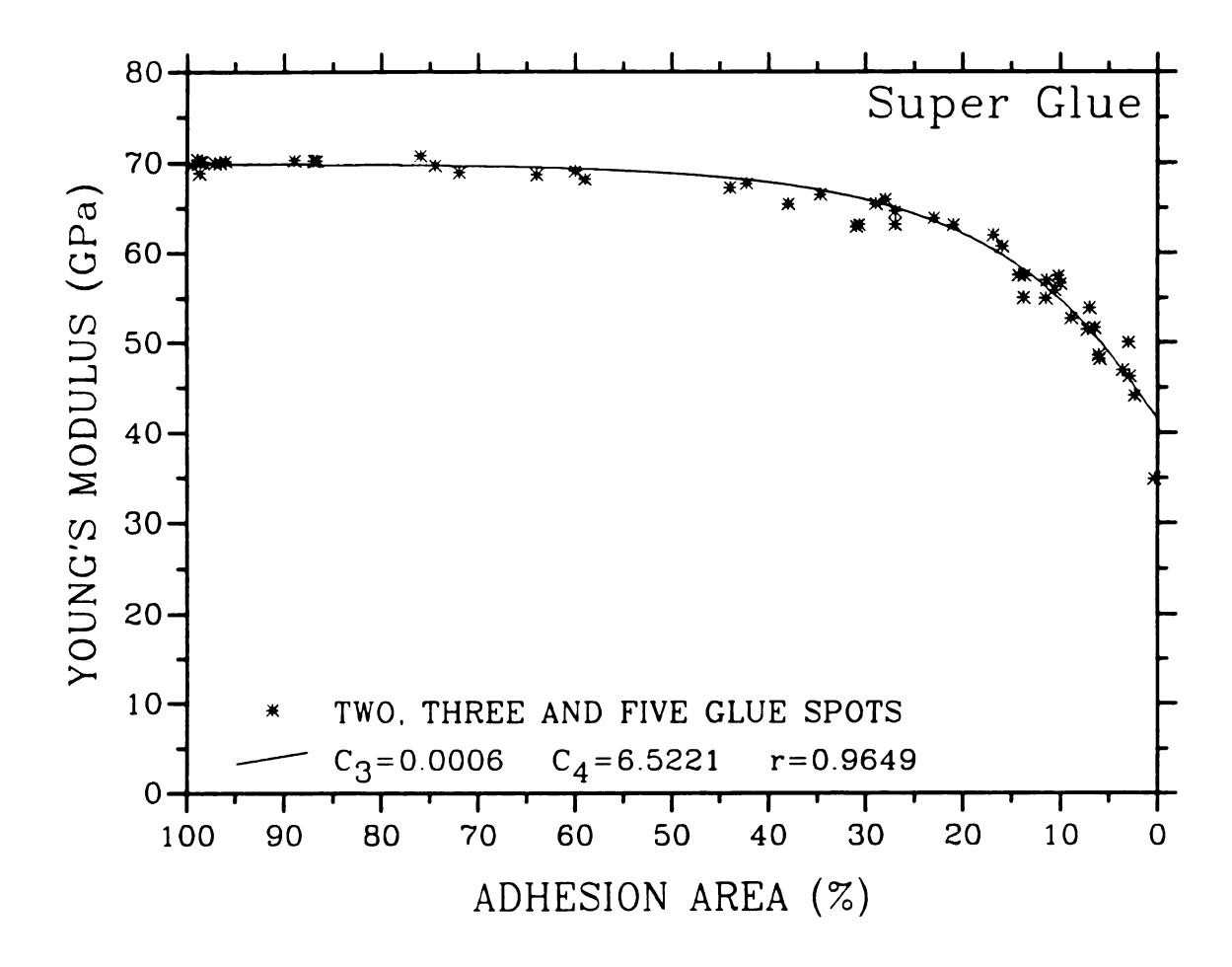


Figure 17. For a super glue bond layer, the effect of the super glue on Young's modulus as a function of adhesion area(%) with the data for specimens having 2, 3 and 5 glue spots lumped together. The curve represents a least-squares best fit to equation 32.

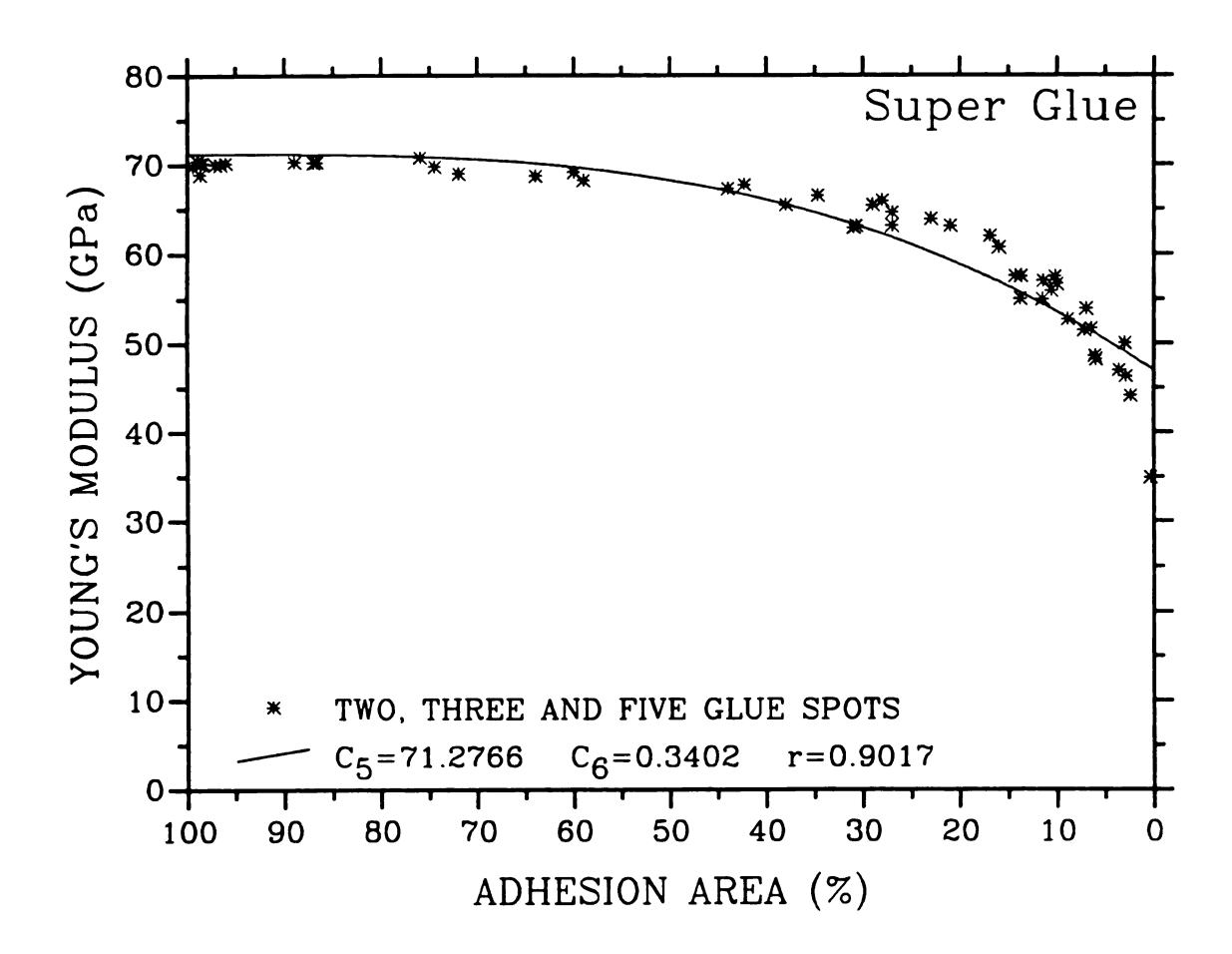


Figure 18. For a super glue bond layer, the effect of the super glue on Young's modulus as a function of adhesion area(%) with the data for specimens having 2, 3, 5 glue spots lumped together. The curve represents a least-squares best fit to equation 33.

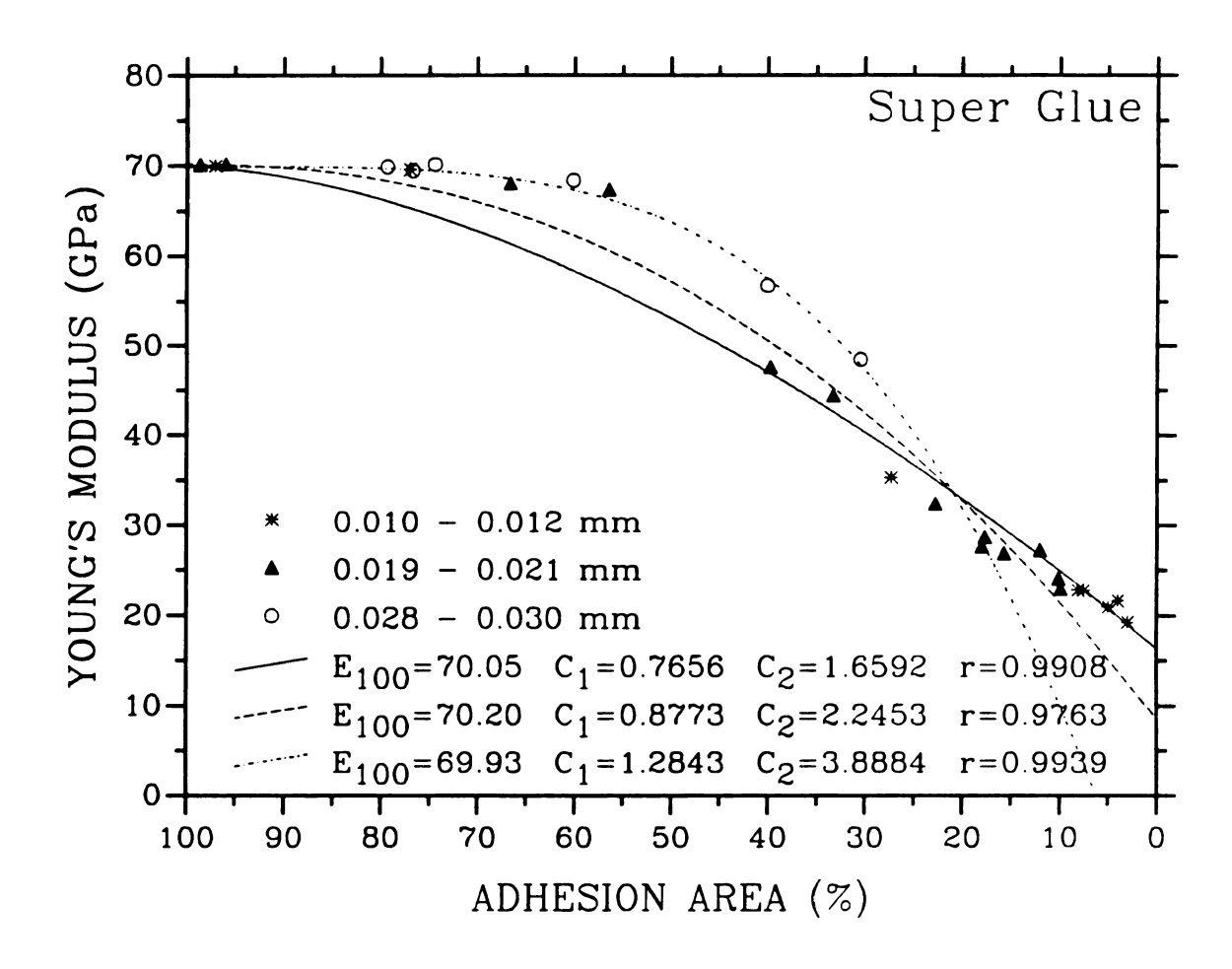


Figure 19. For a super glue bond layer, the effect of glue bond thickness of super glue on Young's modulus as a function of adhesion area(%) for specimens having one super glue spot.

The curves represent a least-squares best fit to equation 31.

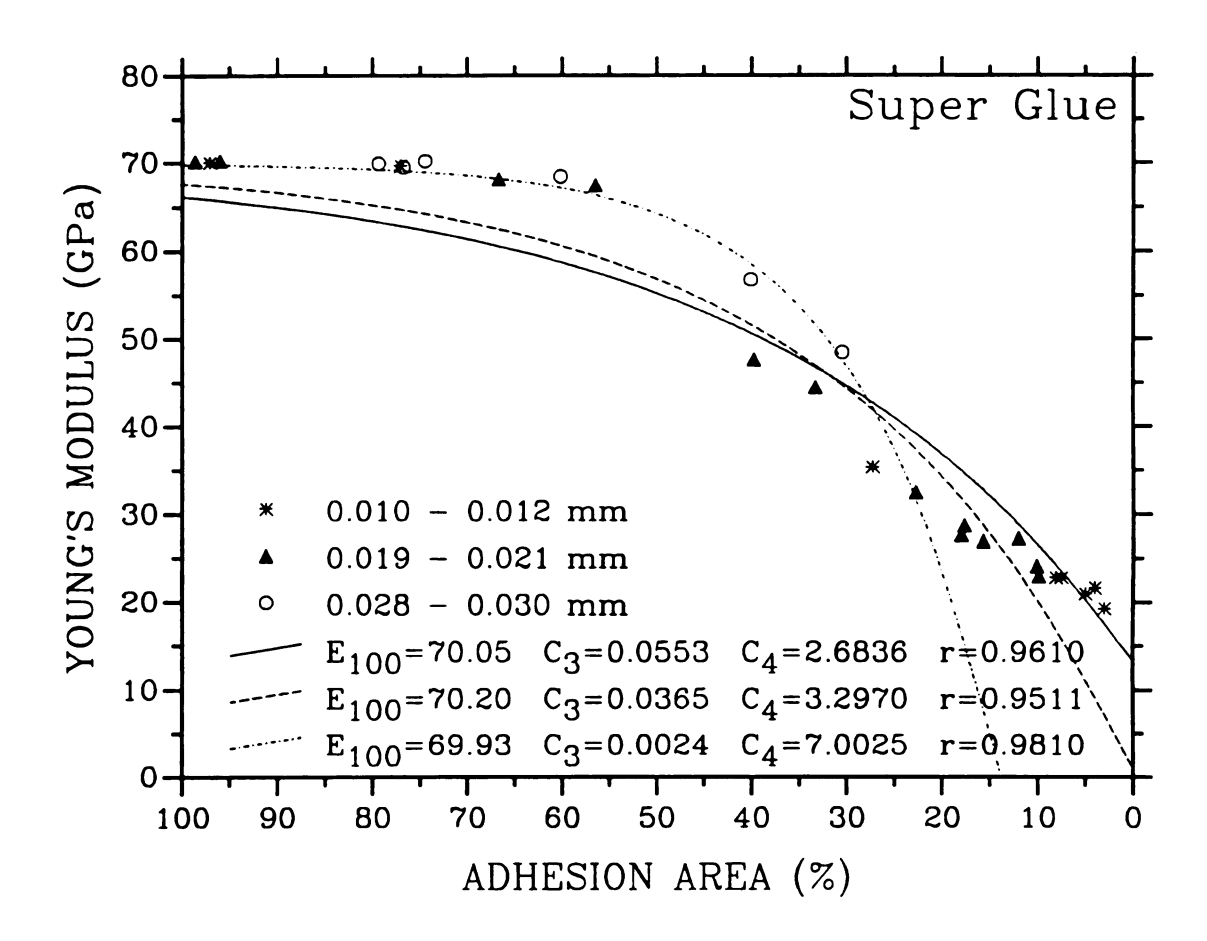


Figure 20. For a super glue bond layer, the effect of glue bond thickness of super glue on Young's modulus as a function of adhesion area(%) for specimens having one super glue spot. The curves represent a least-squares best fit to equation 32.

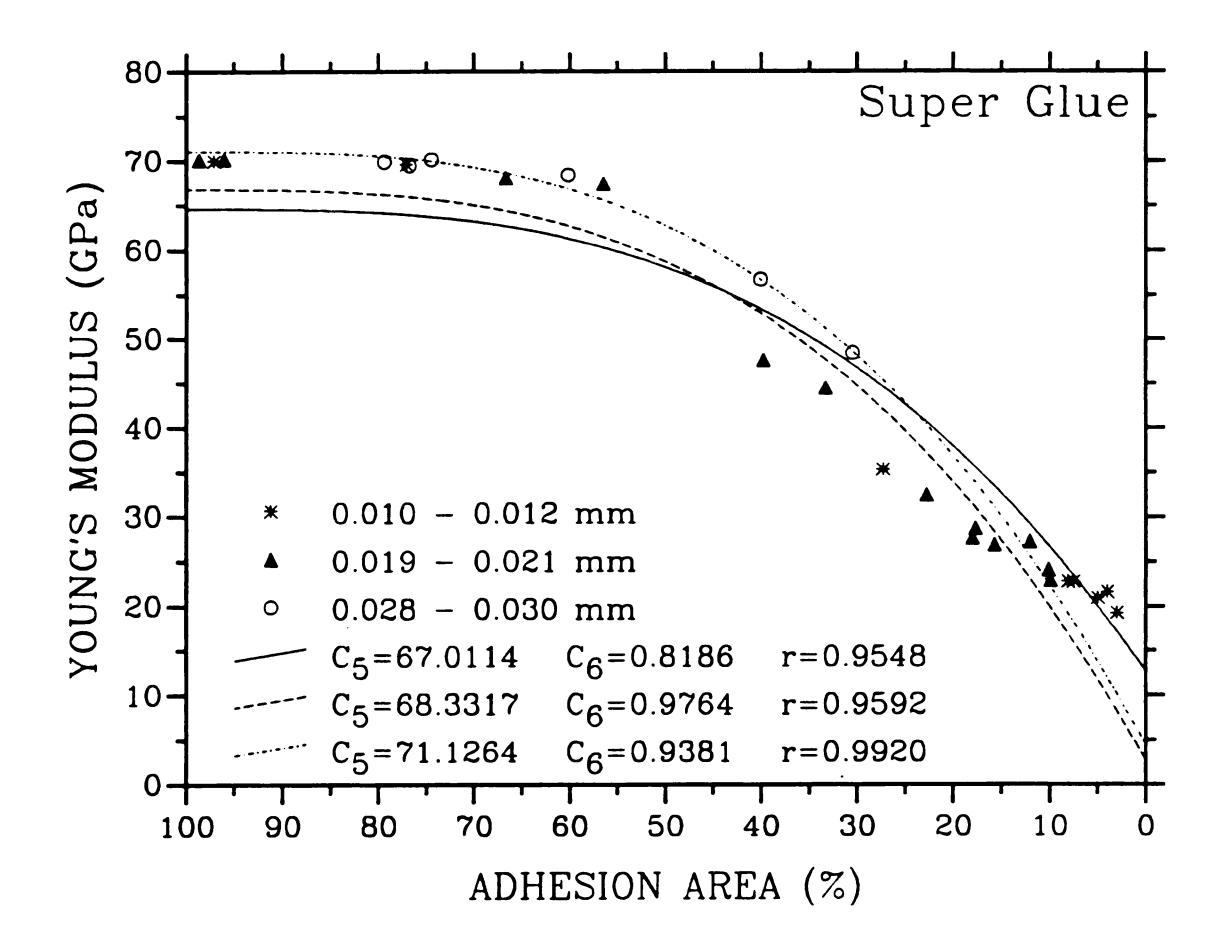


Figure 21. For a super glue bond layer, the effect of glue bond thickness of super glue on Young's modulus as a function of adhesion area(%) for specimens having one super glue spot. The curves represent a least-squares best fit to equation 33.

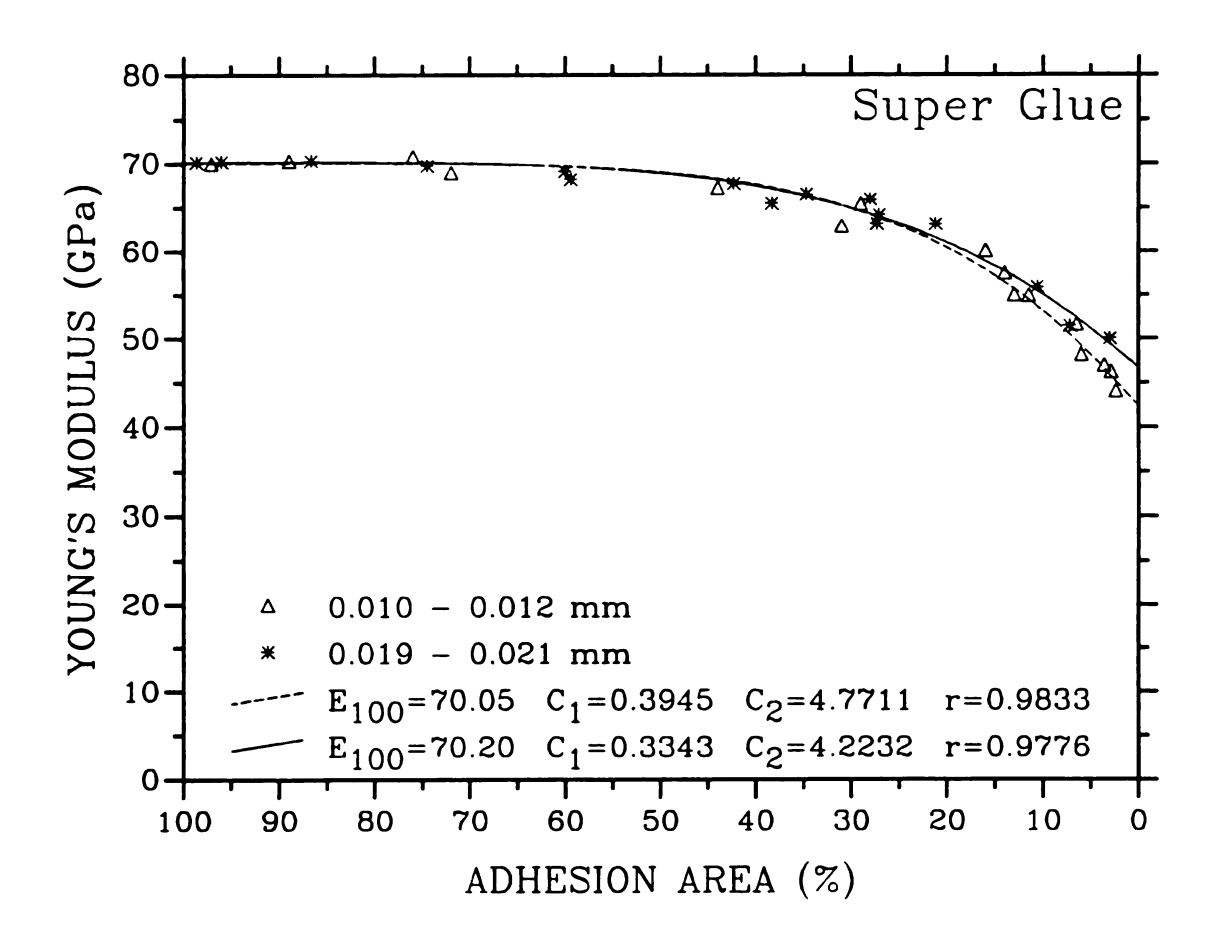


Figure 22. For a super glue bond layer, the effect of glue bond thickness of super glue on Young's modulus as a function of adhesion area(%) for specimens having two and three super glue spots. The curves represent a least-squares best fit to equation 31.

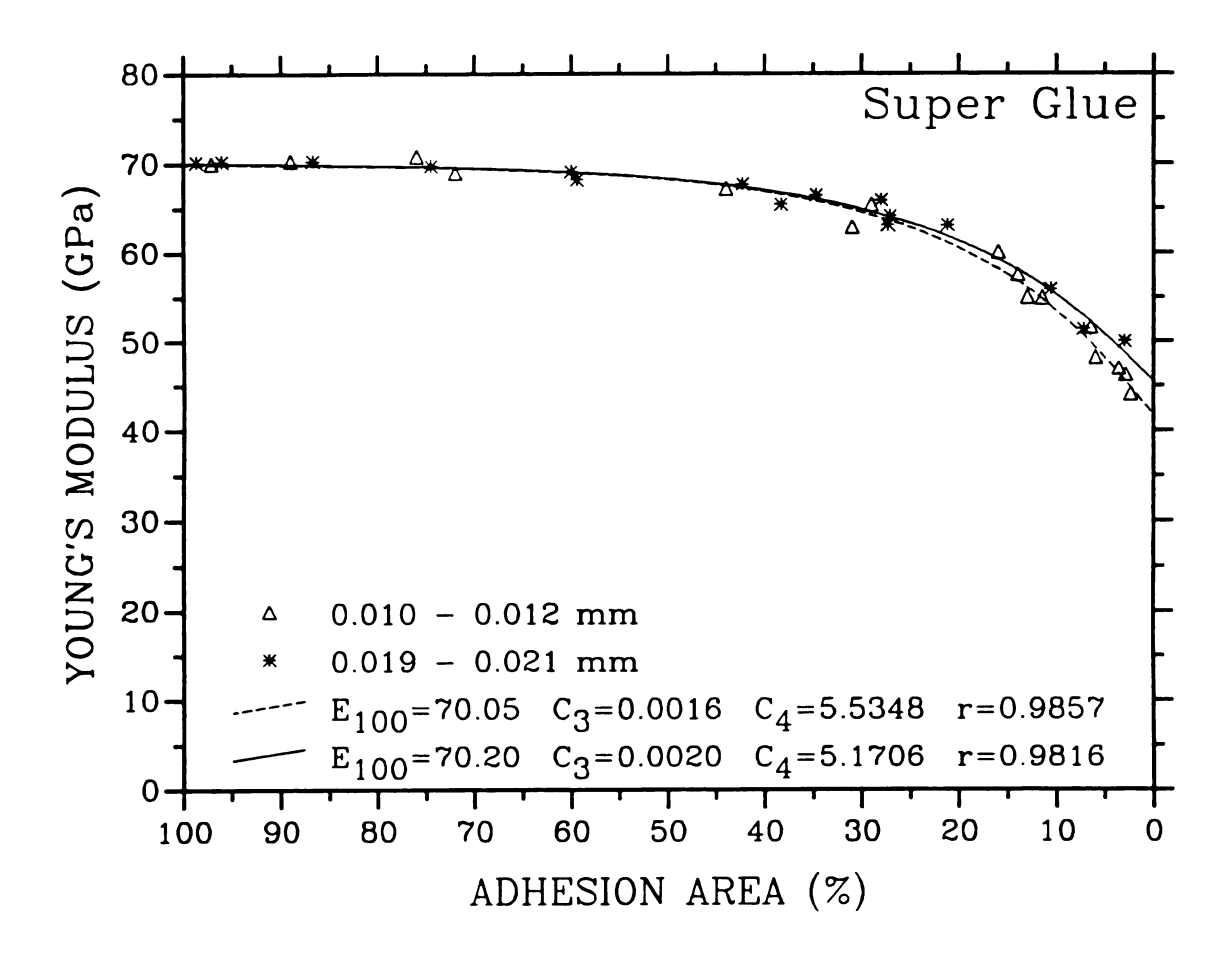


Figure 23. For a super glue bond layer, the effect of glue bond thickness of super glue on Young's modulus as a function of adhesion area(%) for specimens having two and three super glue spots. The curves represent a least-squares best fit to equation 32.

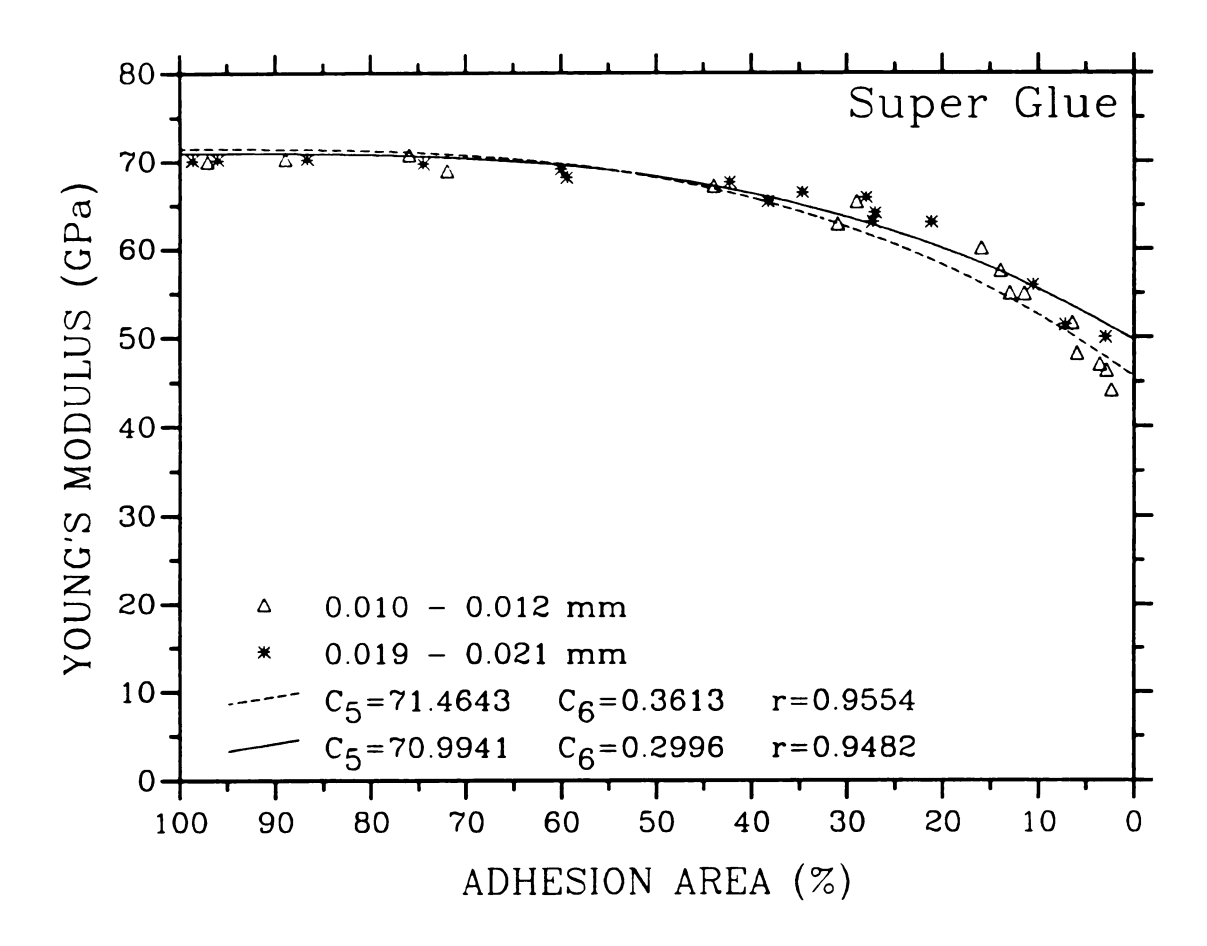


Figure 24. For a super glue bond layer, the effect of glue bond thickness of super glue on Young's modulus as a function of adhesion area(%) for specimens having two and three super glue spots. The curves represent a least-squares best fit to equation 33.

3.1.2. The Effects of Epoxy Cement Adhesion on Elastic Modulus

The effect of area fraction of the glue on elastic modulus was investigated using epoxy cement. Data from 10 glass slide/epoxy cement composite specimens having one glue spot and 10 glass slide/epoxy cement composite specimens having three glue spots show that as the adhesion area decreases, the elastic modulus decreases (Figures 25-27). A similar experimental result was obtained for the glass slide/super glue composite specimens (Section 3.1.1.).

The elastic moduli of the glass slide/epoxy cement composite specimens having one glue spot or three glue spots changed as a function of adhesion area in a manner very similar to that of the super glue. As was the case with the super-glue bonded specimens, the data for the epoxy-bonded specimens was fit to equations 31-33.

3.2. The Effects of Epoxy Resin Adhesion on Elastic Modulus

The effects of adhesion area, glue bond thickness and composition of epoxy resin were investigated. In addition, the ROM and the Dynamic Beam Vibration models were compared using the glass slide/epoxy resin composite specimens having a 100 percent adhesion area.

3.2.1. The Effect of Adhesion Area on Elastic Modulus

Without considering the effect of glue bond thickness, the Young's moduli of seventy glass slide/epoxy resin composite specimens with the

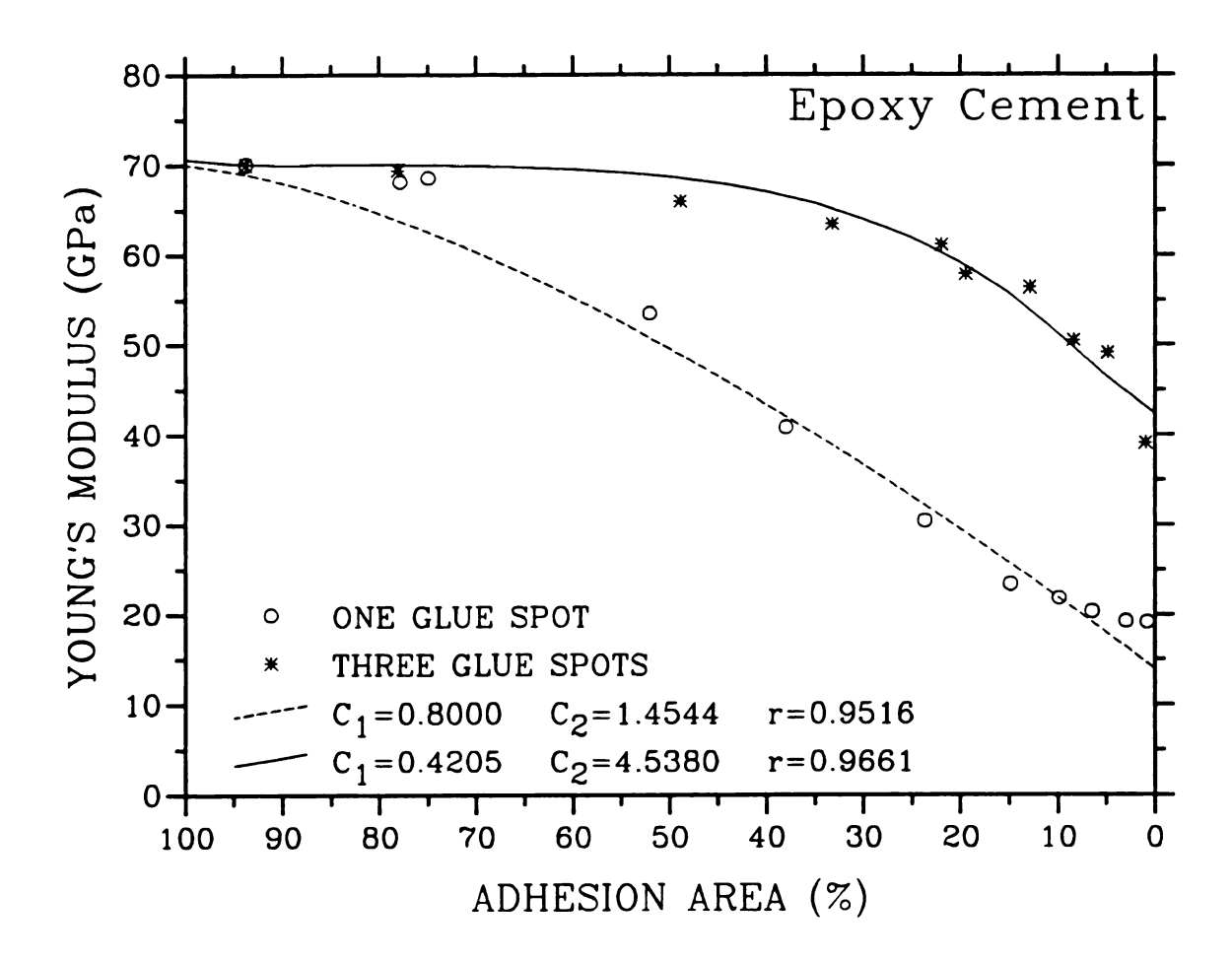


Figure 25. For an epoxy cement bond layer, the effect of epoxy cement on Young's modulus as a function of adhesion area(%) for specimens having one and three glue spots. The curves represent a least-squares best fit to equation 31.

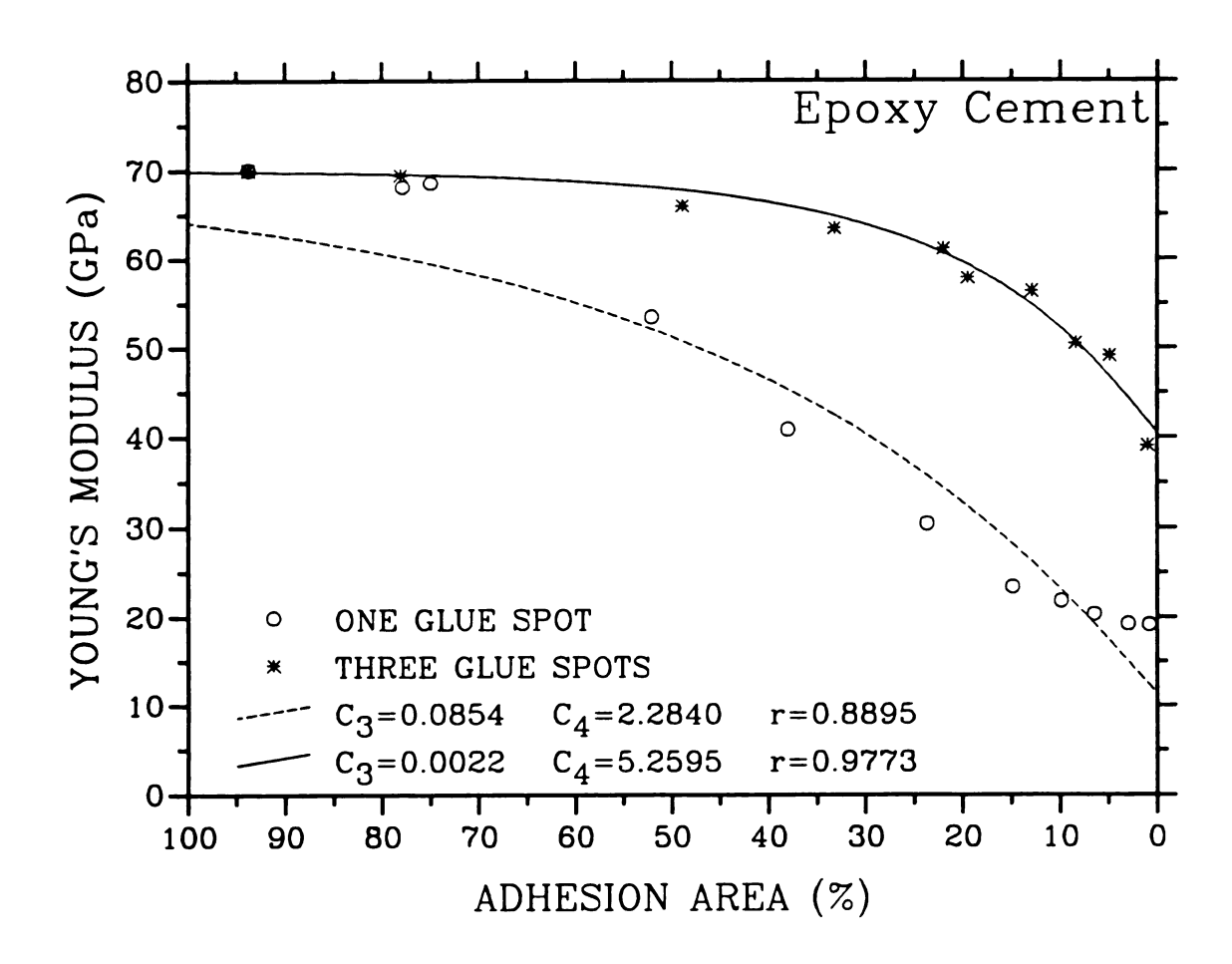


Figure 26. For an epoxy cement bond layer, the effect of epoxy cement on Young's modulus as a function of adhesion area(%) for specimens having one and three glue spots. The curves represent a least-squares best fit to equation 32.

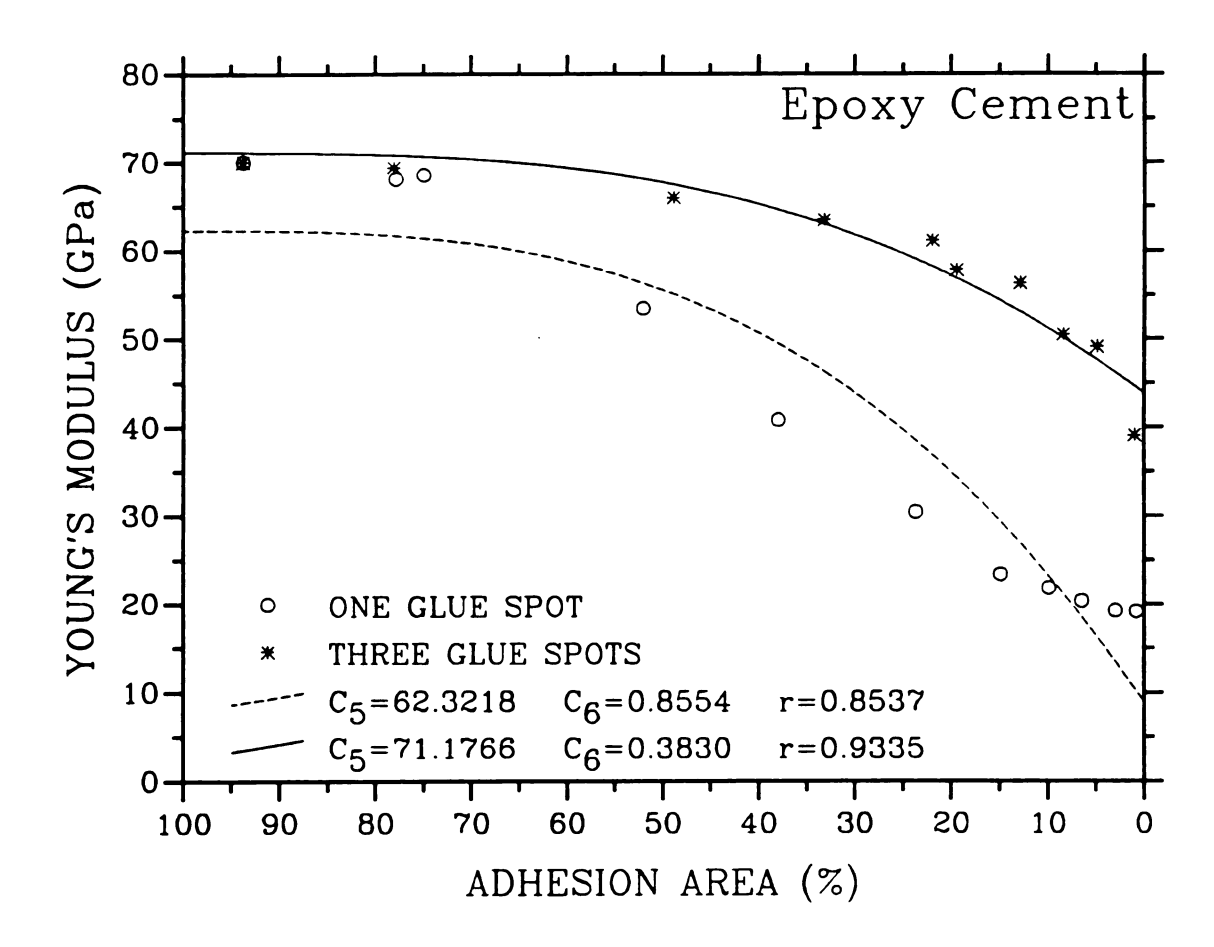


Figure 27. For an epoxy cement bond layer, the effect of epoxy cement on Young's modulus as a function of adhesion area(%) for specimens having one and three glue spots. The curves represent a least-squares best fit to equation 33.

composition of 50 percent resin and 50 percent hardener were plotted with respect to adhesion area as shown in Figures 28-30. Using a least squares best-fit procedure, the data was fit to equations 31-33 (Figure 28-30).

As in the results for super glue and epoxy cement, the Young's modulus of glass slide/epoxy resin composite specimens decreased with the decrease of adhesion area.

3.2.2. The Effect of Glue Bond Thickness on Elastic Modulus

The effect of glue bond thickness on Young's modulus are apparent through two different types of data classification: (1) fixed glue composition but varying adhered areas and (2) fixed adhesion area but varying glue composition.

3.2.2.1. Glass Slide/Epoxy Resin Composite Specimens having a Fixed Glue Composition but Different Adhesion Areas

Seventy glass slide/epoxy resin composite specimens out of a total of ninety six were made with a fixed epoxy composition of 50 percent resin and 50 percent hardener, but having differing adhesion area fractions. Using a least-squares best-fit program the Young's modulus versus area fraction of glue data was fit to equations 31-33.

When the data is sorted into three glue-bond thickness ranges

(0.225 - 0.275 mm, 0.125 - 0.175 mm, and 0.025 - 0.075 mm), the Young's modulus for each thickness range decreases as a function of area

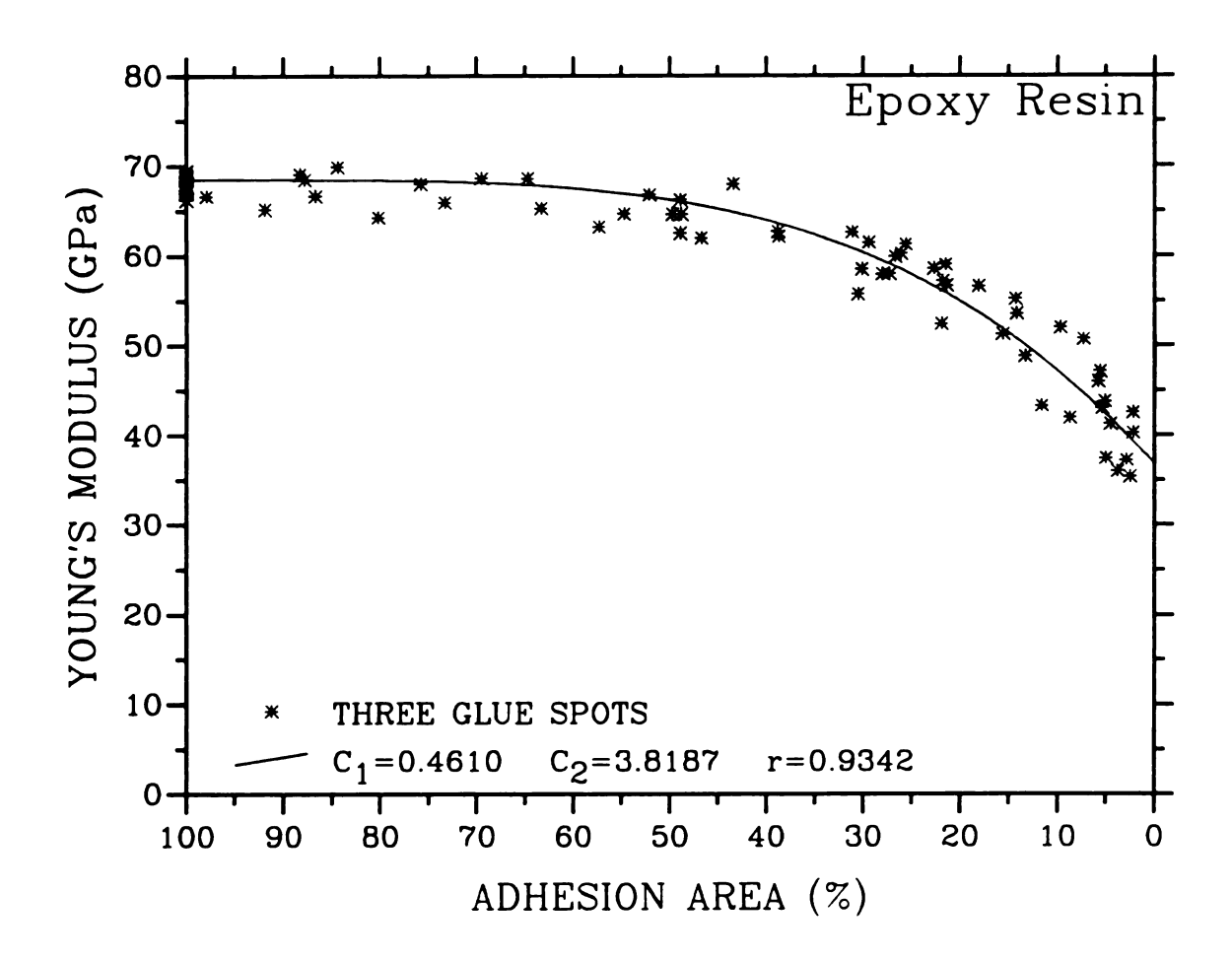


Figure 28. For an epoxy resin bond layer, the effect of epoxy resin on Young's modulus as a function of adhesion area(%). The curve represents a least-squares best fit to equation 31.

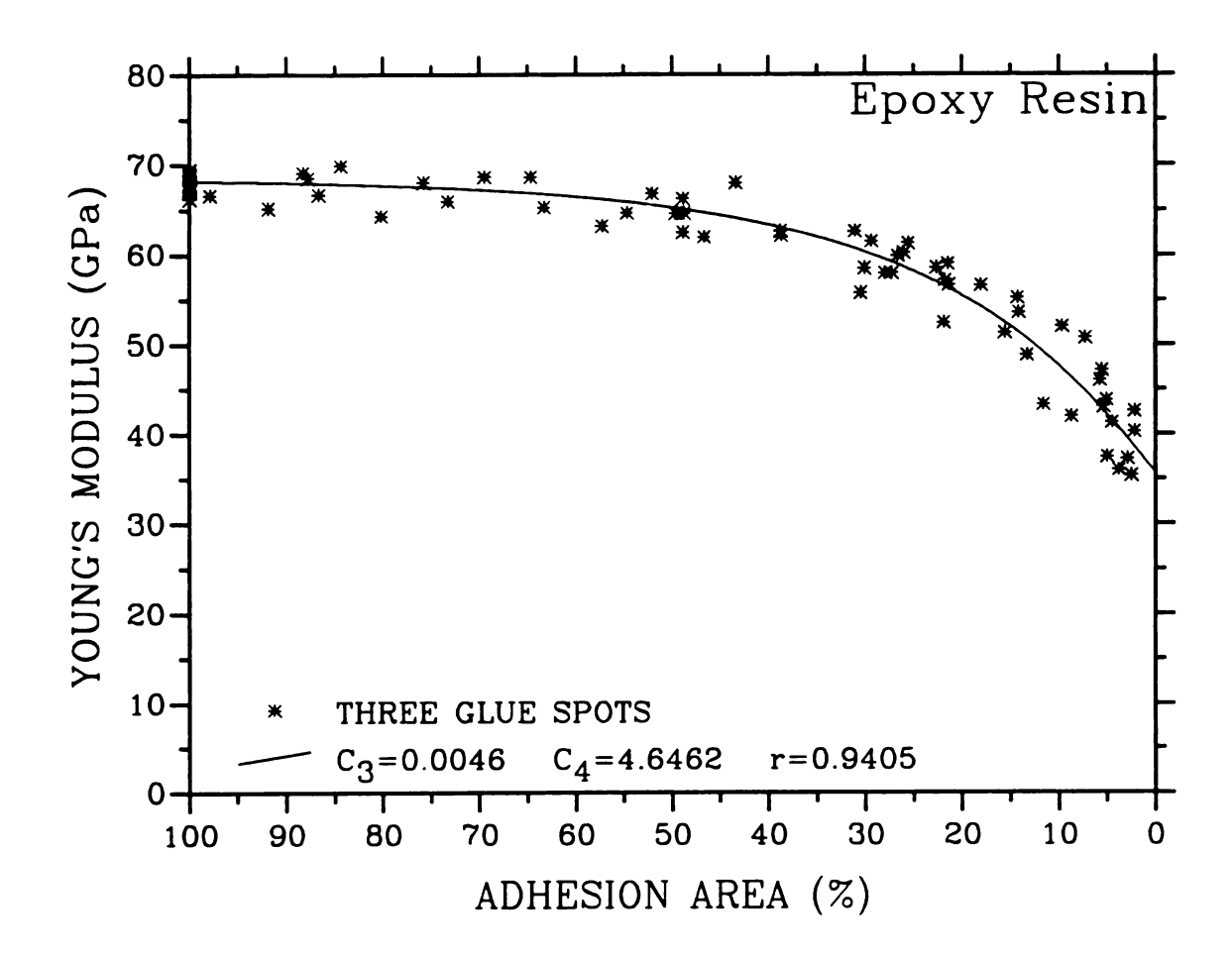


Figure 29. For an epoxy resin bond layer, the effect of epoxy resin on Young's modulus as a function of adhesion area(%). The curve represents a least-squares best fit to equation 32.

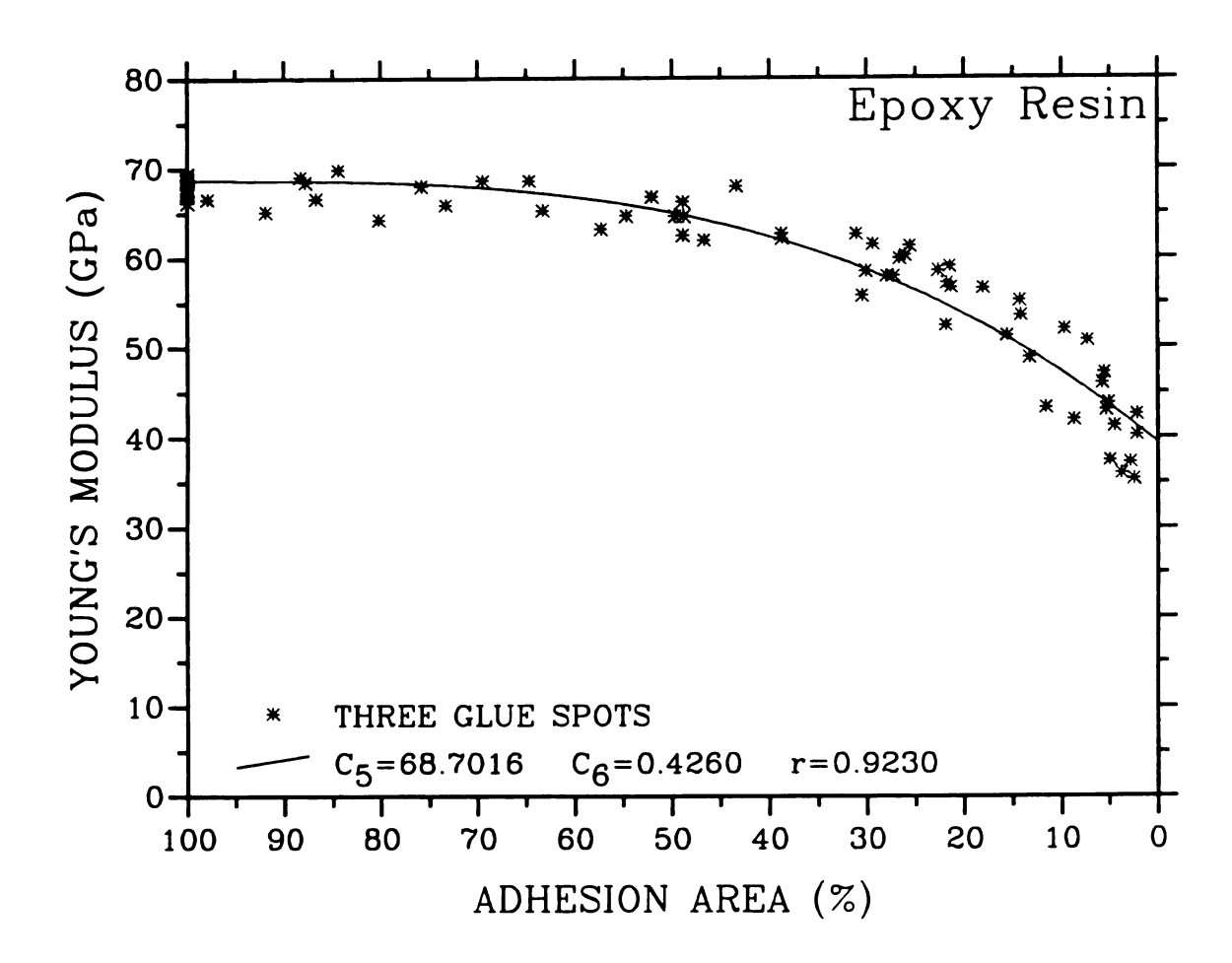


Figure 30. For an epoxy resin bond layer, the effect of epoxy resin on Young's modulus as a function of adhesion area(%). The curve represents a least-squares best fit to equation 33.

fraction of glue (Figures 31-33). In addition, for each thickness range, the elastic modulus decreases as the glue bond thickness increases.

Qualitatively, the observed decrease in Young's modulus with an increase in glue bond thickness can be understood in terms of a sandwich "layer" model. The outer two layers of each glass slide/epoxy resin composite specimen are glass slides having a Young's modulus of approximately 70.53 ± 0.32 GPa (average value calculated from 140 individual glass slides). In contrast, the elastic modulus of the epoxy layer is only 2.977 to 3.428 GPa (Table 6). Thus the considerably lower modulus of the epoxy indicates that as the relative thickness of the epoxy bond increases, the overall modulus of the glass slide/epoxy resin composite specimen should decrease. However, for the glass slide/epoxy resin composite specimens having a glue bond that cover less than 100 percent of bonded surface, the quantitative analysis of the effect of the epoxy bond thickness is not straightforward.

3.2.2.2. Glass Slide/Epoxy Resin Composite Specimens of Differing Glue Composition and Fixed Adhesion Areas

Thirty nine specimens out of the total of ninety six epoxy bonded specimens were made with five different epoxy compositions but with 100 percent adhesion area (See Section 2.4.3.). The elastic modulus decreased with increasing epoxy bond thickness for each of the four different epoxy compositions (Figure 34).

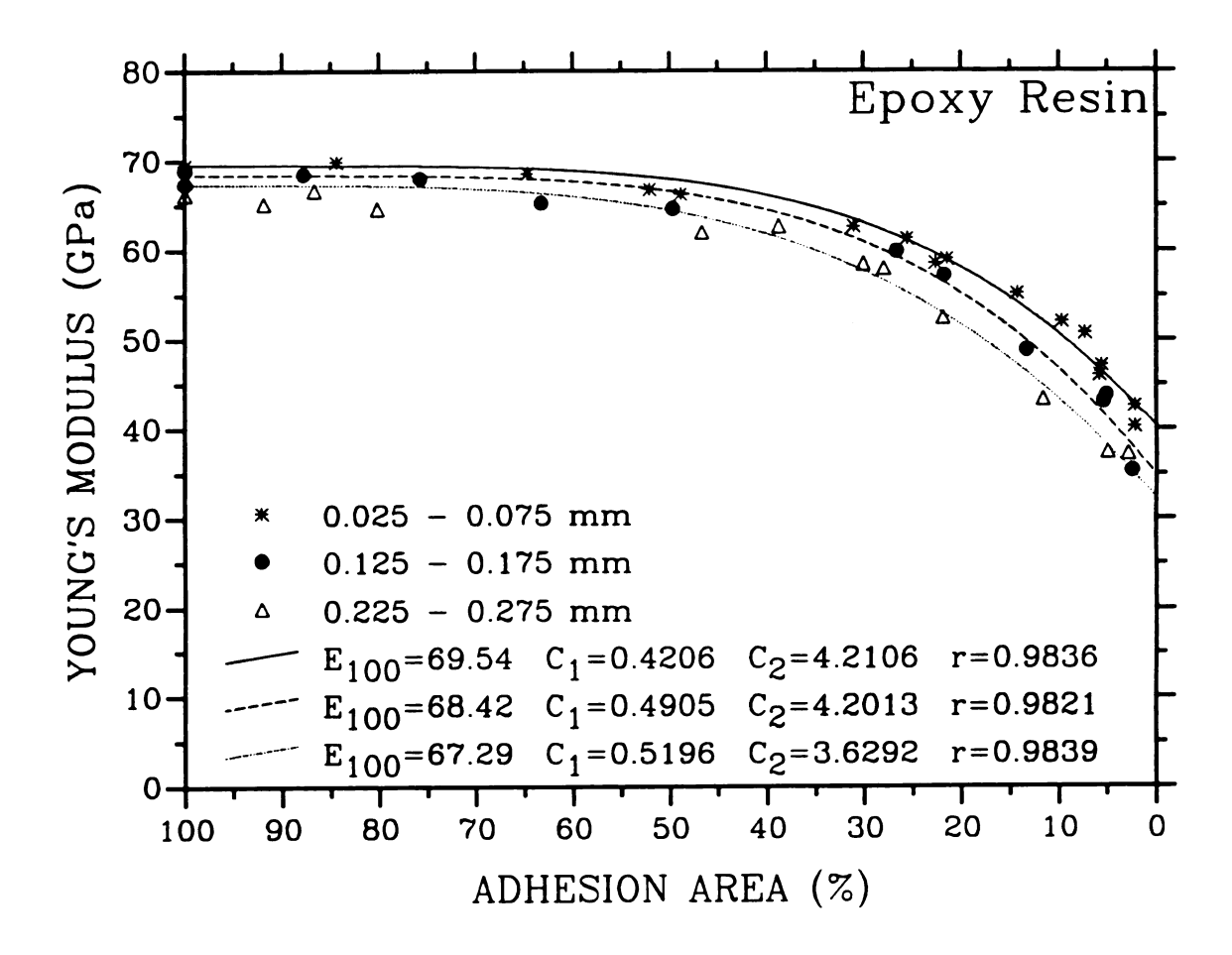


Figure 31. For an epoxy resin bond layer, the effect of glue bond thickness of epoxy resin on Young's modulus as a function of adhesion area(%). The curves represent a least-squares best fit to equation 31.

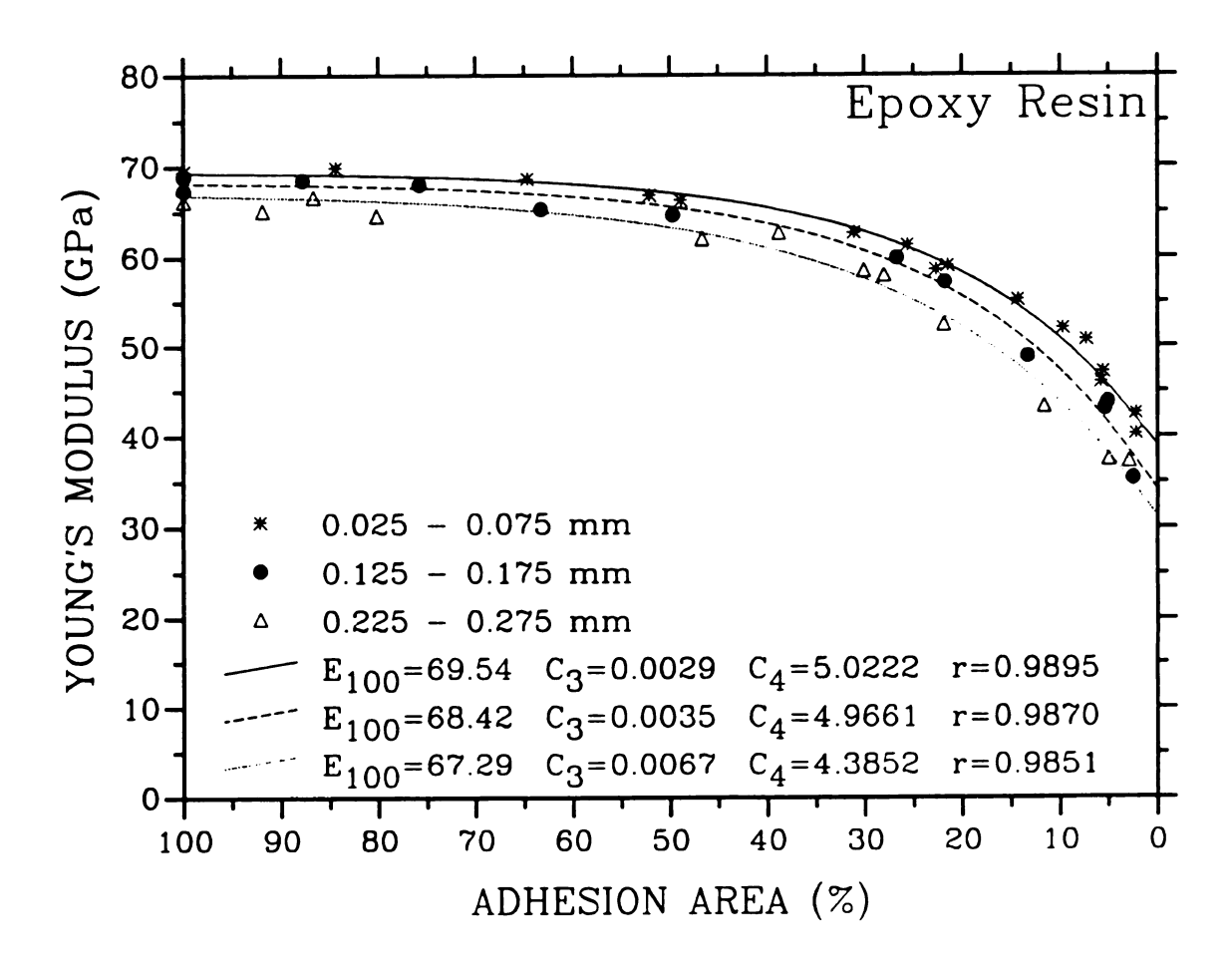


Figure 32. For an epoxy resin bond layer, the effect of glue bond thickness of epoxy resin on Young's modulus as a function of adhesion area(%). The curves represent a least-squares best fit to equation 32.

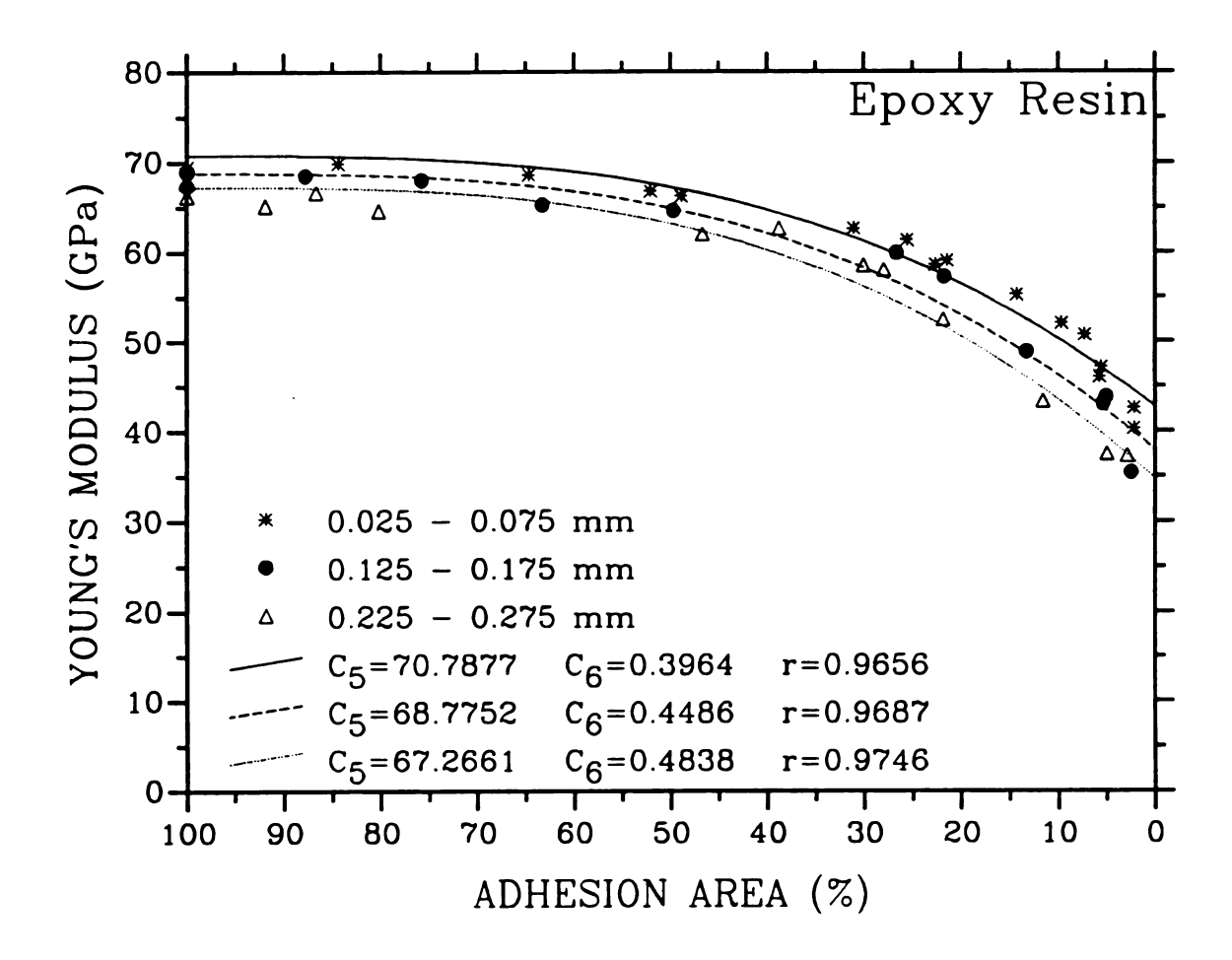


Figure 33. For an epoxy resin bond layer, the effect of glue bond thickness of epoxy resin on Young's modulus as a function of adhesion area(%). The curves represent a least-squares best fit to equation 33.

Table 6. Comparison of experimentally obtained elastic moduli, densities and Poisson's ratios with reference values.

COMPOSITION (Resin : Hardener)	ELASTIC MODULUS (GPa)	DENSITY (gm/cm³)	POISSON'S RATIO	Reference
50% : 50%	2.977	1.133	0.27	This study
65% : 35%	3.174	1.136	0.29	This study
80% : 20%	3.428	1.164	0.31	This study
*	2.7 - 4.1	**	0.34	[17]
***	3.0 - 6.0	1.1 - 1.4	0.38 - 0.4	[18]

^{*} Specific composition not specified, material listed as "cured epoxy resins"

^{**} Mass density not specified

^{***} Specific composition not specified, material listed as "epoxy resins".

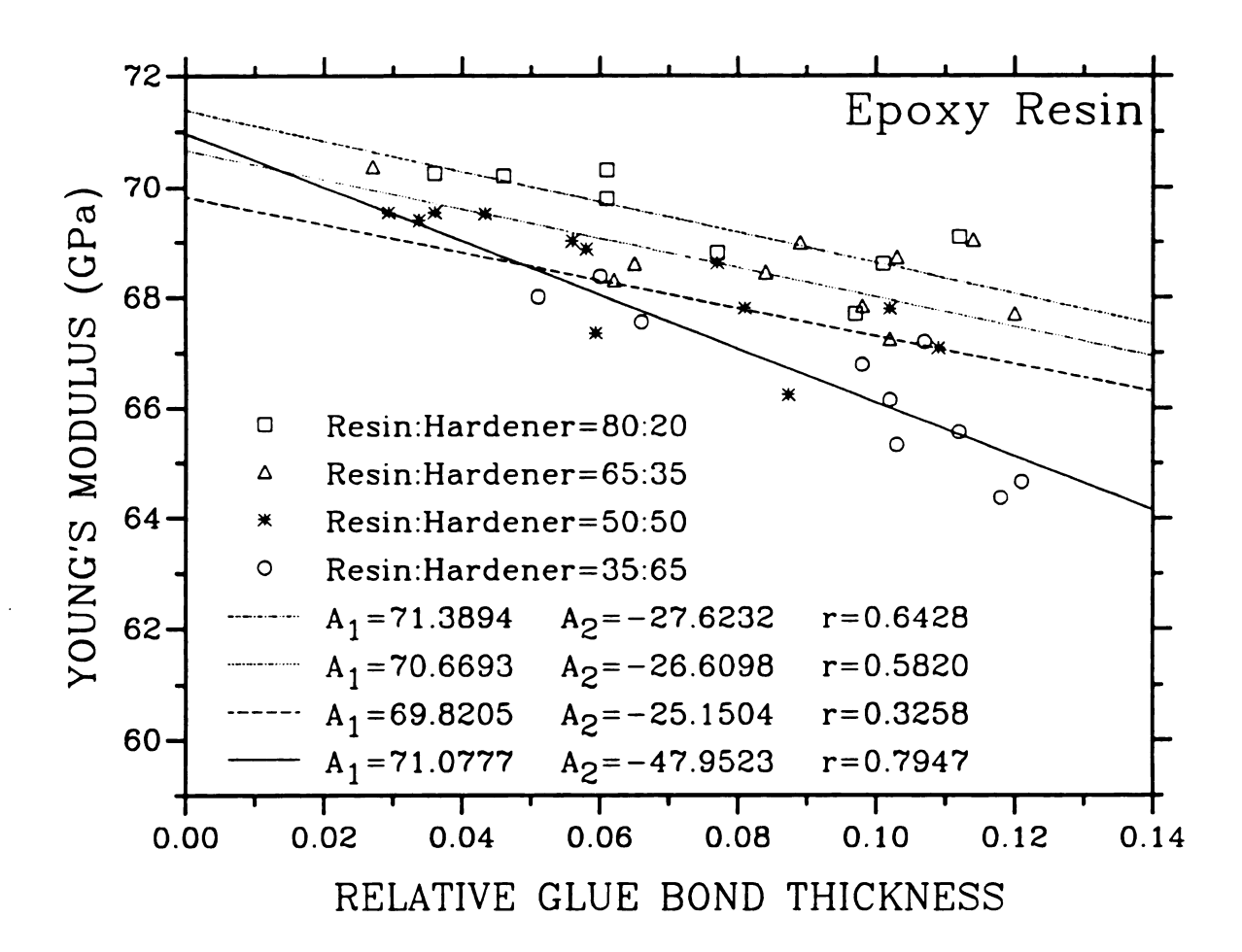


Figure 34. For an epoxy resin bond layer, the effect of composition of epoxy resin on Young's modulus as a function of relative glue bond thickness. The curves represent a least-squares best fit to equation 34.

3.2.3. The Effect of Epoxy Resin Composition on Elastic Modulus

For the investigation of the effect of epoxy resin composition on Young's modulus, thirty nine glass slide/epoxy resin composite specimens with varying compositions of resin and hardener were fabricated (Section 2.4.3.).

The effect of epoxy resin composition on the elastic modulus was analyzed in terms of the linear relation

$$E = A_1 + A_2 t_R \tag{34}$$

where E = Elastic Modulus

 A_1 and A_2 = constants

t_R = relative thickness of the glue bond

= thickness of the glue bond/total thickness of the glass slide/glue composite specimen.

The data for the various glue composition specimens were fit to equation 34 using a least-squares best-fit program. As the content of resin in the glue decreased from 80 percent to 35 percent, the elastic modulus decreased over the entire range of glue bond thickness except for 35 percent resin and 65 percent hardener composition (Figure 34).

The effect of glue composition on Young's modulus can be reconfirmed directly from the data about the epoxy resin specimens shown in Table 6.

3.2.4. Experimentally obtained Elastic Moduli, Densities and Poisson's Ratios of Epoxy Resin Specimens

The Young's moduli of epoxy resin specimens were determined using the sonic resonance technique. The densities and Poisson's ratios also were calculated. Table 6 compares the experimental mass density and elastic modulus data with reference values [17, 18]. As the content of resin in the glue increases, the elastic modulus increases (Table 6). Also, the experimental value of Young's moduli and densities obtained in this study are reasonable when compared to the values from two different references.

3.2.5. Comparison of Rule of Mixtures and Dynamic Beam Vibration models

The Rule of Mixtures and the Dynamic Beam Vibration models were compared to data for glass slide/epoxy resin composite specimens having an 100 percent adhesion area. The glass slide/epoxy resin composite specimens with 100 percent adhesion area can be considered as a continuous glue bond layer between two glass slide layers. The elastic moduli of such glass slide/epoxy resin composite specimens were calculated using equation 17 for the ROM model and equation 25 for the Dynamic Beam Vibration model.

The relative differences, δ_R , between the experimentally determined Young's modulus, $E_{\rm exp}$, and the predicted Young's modulus, E, from the ROM and Dynamic beam vibration models were calculated as

$$\delta_R = \frac{(E - E_{\rm exp})}{E_{\rm exp}} . \tag{35}$$

Plotting δ_R as a function of t_R , the relative thickness of the glue bond results in an approximately linear relationship for both the ROM and Dynamic beam vibration models (Figures 35-37). The δ_R versus t_R relations (which show opposite slopes for the ROM and Dynamic beam vibration models) was fit to the relationship

$$\delta_R = \frac{(E - E_{\text{exp}})}{E_{\text{exp}}} = B_1 + B_2 t_R$$
 (36)

where B_1 and B_2 are constants.

The moduli calculated from equations 17 and 25 were compared with the experimentally obtained Young's moduli using equation 35 and the moduli obtained from a least-squares fit to equation 36 (see Figures 35-37 for 50%, 65%, 80% resin, respectively). Also, the calculated moduli were directly compared with the measured Young's moduli using the regression curves fit to the linear relationship given by (Figures 38-40 for 50%, 65%, and 80% resin, respectively)

$$E = B_3 + B_4 t_R \tag{37}$$

where E = elastic modulus (GPa)

 B_3 and B_4 are constants

 t_R = relative thickness.

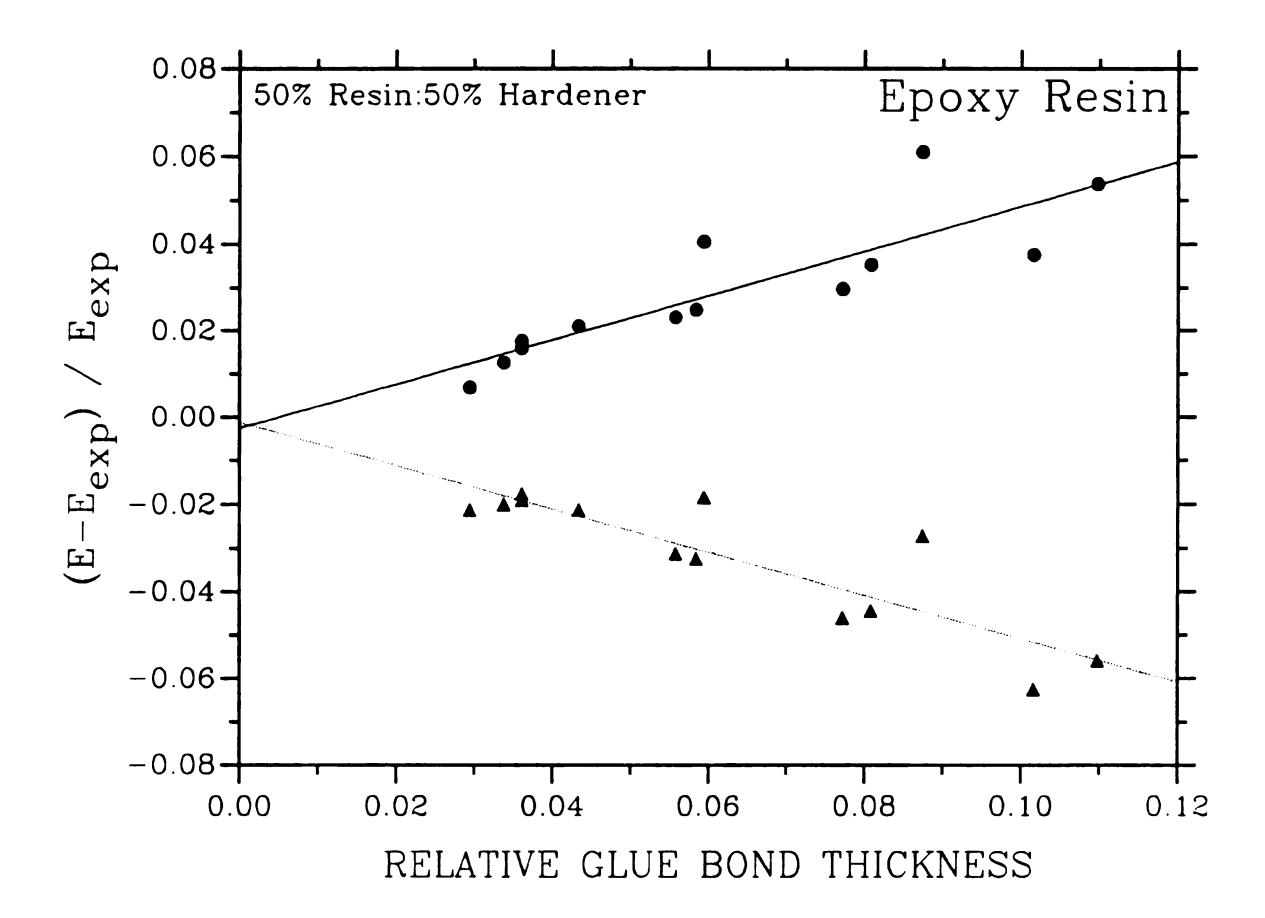


Figure 35. Comparison of ROM and Dynamic Beam Vibration models for epoxy bonds made from an initial composition of 50% resin and 50% hardener. The curves represent a least-squares best fit to equation 36. (— Dynamic Beam Vibration model: $B_1=-0.0025$, $B_2=0.5106$, r=0.7446 and …… Rule of Mixtures model: $B_1=-0.0012$, $B_2=-0.4959$, r=0.7603)

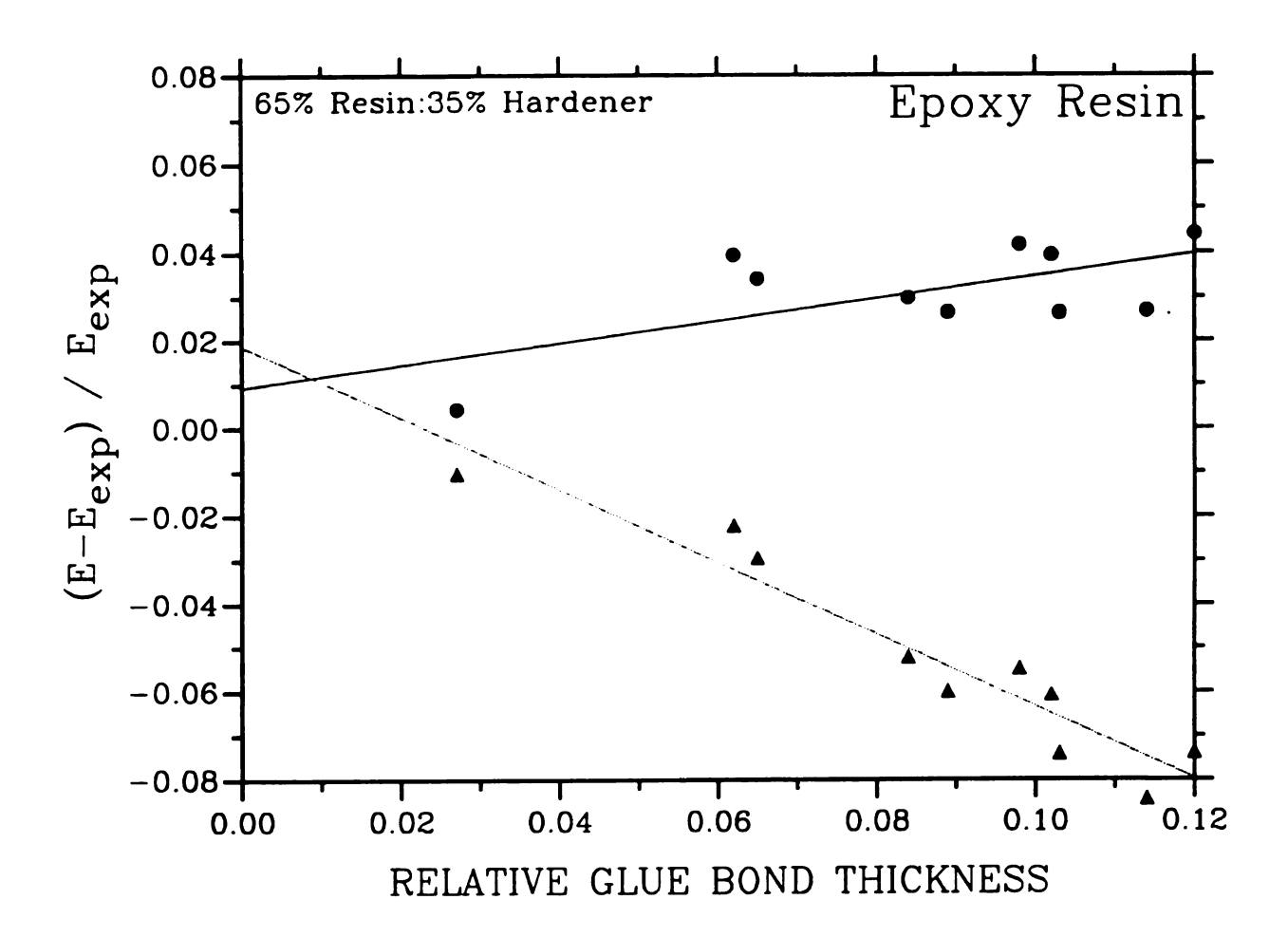


Figure 36. Comparison of ROM and Dynamic Beam Vibration models for epoxy bonds made from an initial composition of 65% resin and 35% hardener. The curves represent a least-squares best fit to equation 36. (— Dynamic Beam Vibration model: $B_1=0.0094$, $B_2=0.2590$, r=0.3763 and \cdots Rule of Mixtures model: $B_1=0.0189$, $B_2=-0.8209$, r=0.9108)

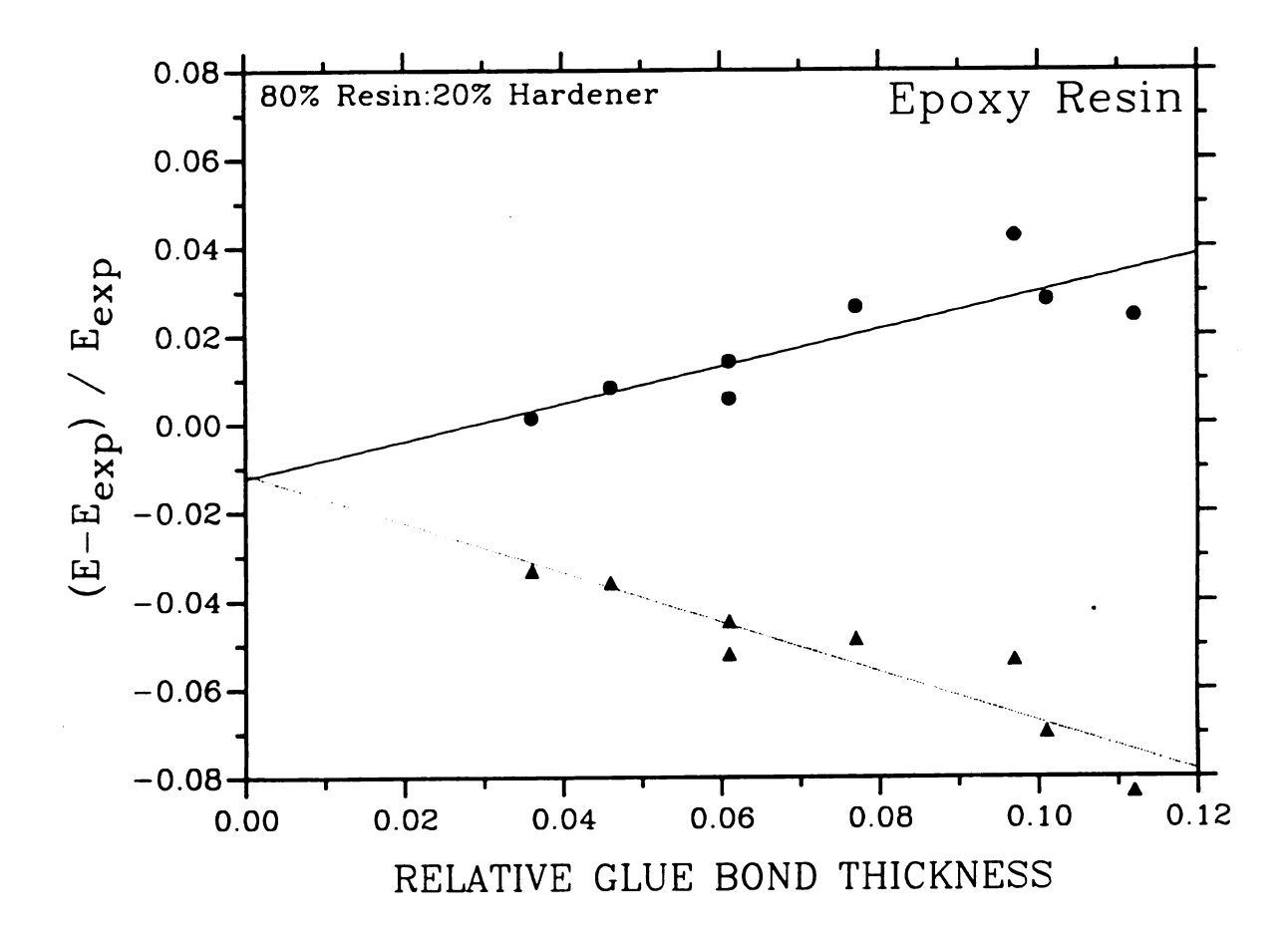


Figure 37. Comparison of ROM and Dynamic Beam Vibration models for epoxy bonds made from an initial composition of 80% resin and 20% hardener. The curves represent a least-squares best fit to equation 36. (— Dynamic Beam Vibration model: $B_1=-0.0122$, $B_2=0.4210$, r=0.6951 and ······ Rule of Mixtures model: $B_1=-0.0112$, $B_2=-0.5892$, r=0.8361)

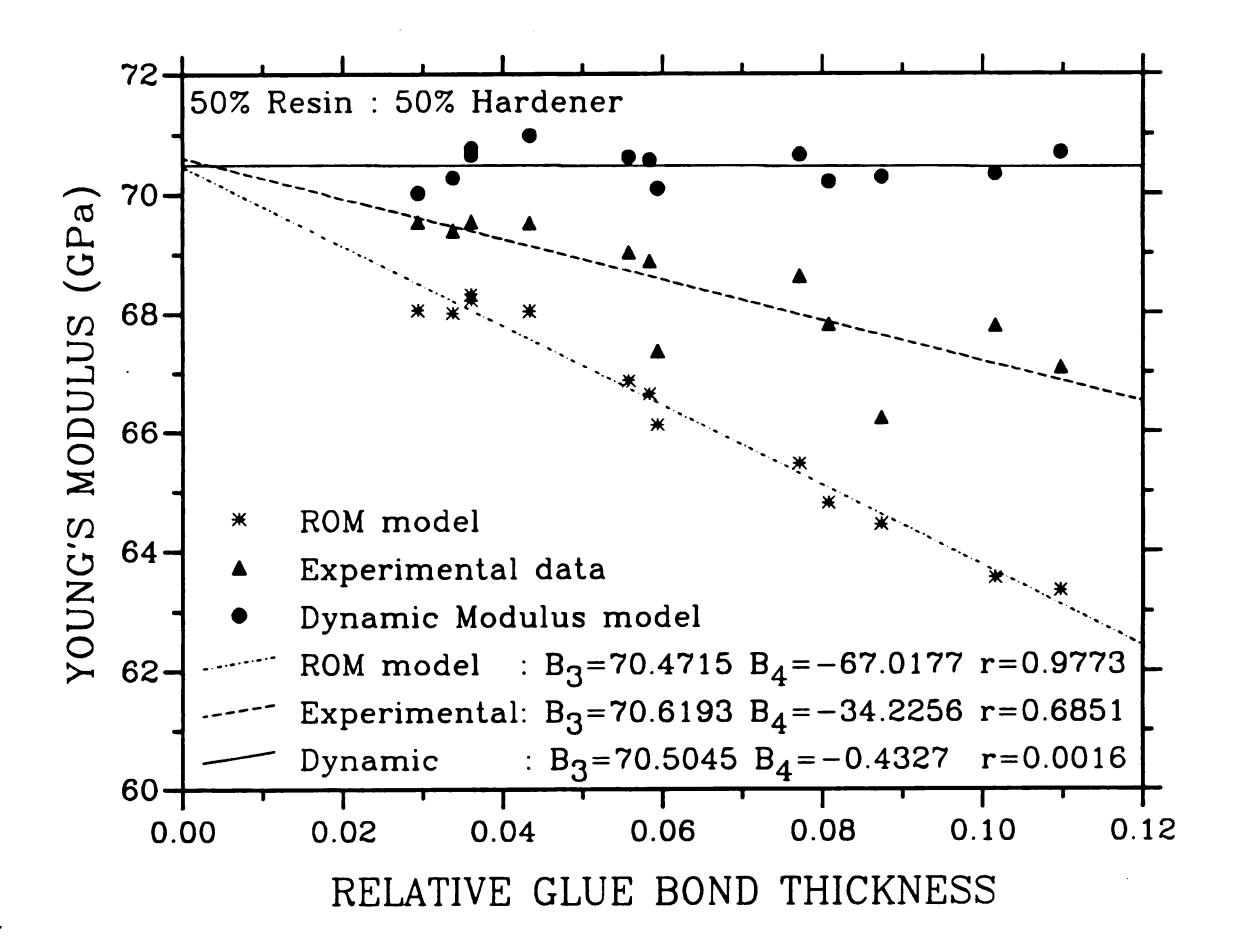


Figure 38. Comparison of experimentally determined moduli with the moduli predicted from the Rule of Mixtures and Dynamic Beam Vibration models as a function of relative glue bond thickness for 50% resin and 50% hardener. The curves represent a least-squares best fit to equation 37.

(—— Dynamic modulus model: B₃=70.5045, B₄=-0.4327, r=0.0016, ----- Experimental data: B₃=70.6193, B₄=-34.2256, r=0.6851, ---- ROM model: B₃=70.4715, B₄=-67.0177, r=0.9773)

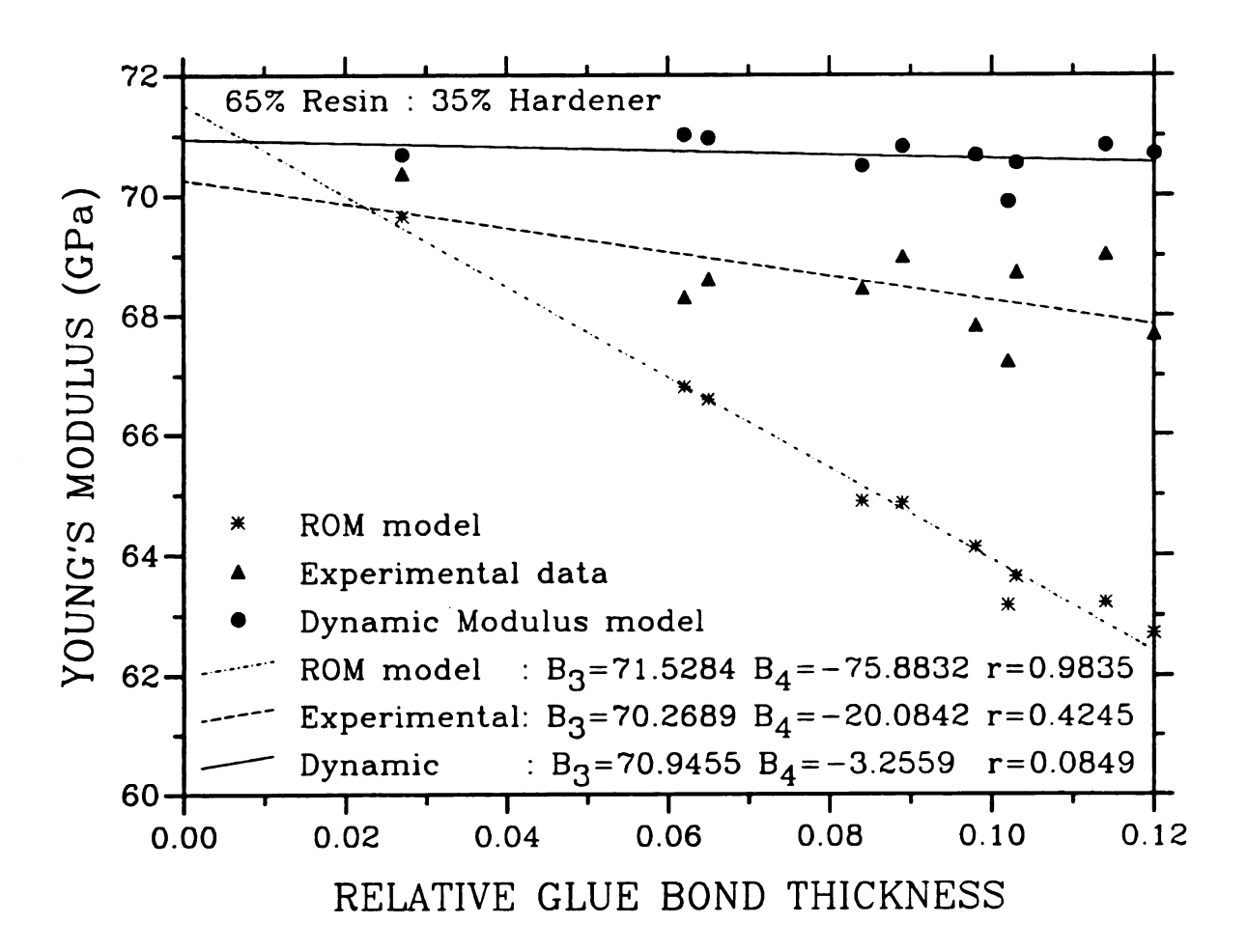


Figure 39. Comparison of experimentally determined moduli with the moduli predicted from the Rule of Mixtures and Dynamic Beam Vibration models as a function of relative glue bond thickness for 65% resin and 35% hardener. The curves represent a least-squares best fit to equation 37.

(—— Dynamic modulus model: B₃=70.9455, B₄=-3.2559, r=0.0849, Experimental data: B₃=70.2689, B₄=-20.0842, r=0.4245, ROM model: B₃=71.5284, B₄=-75.8832, r=0.9835)

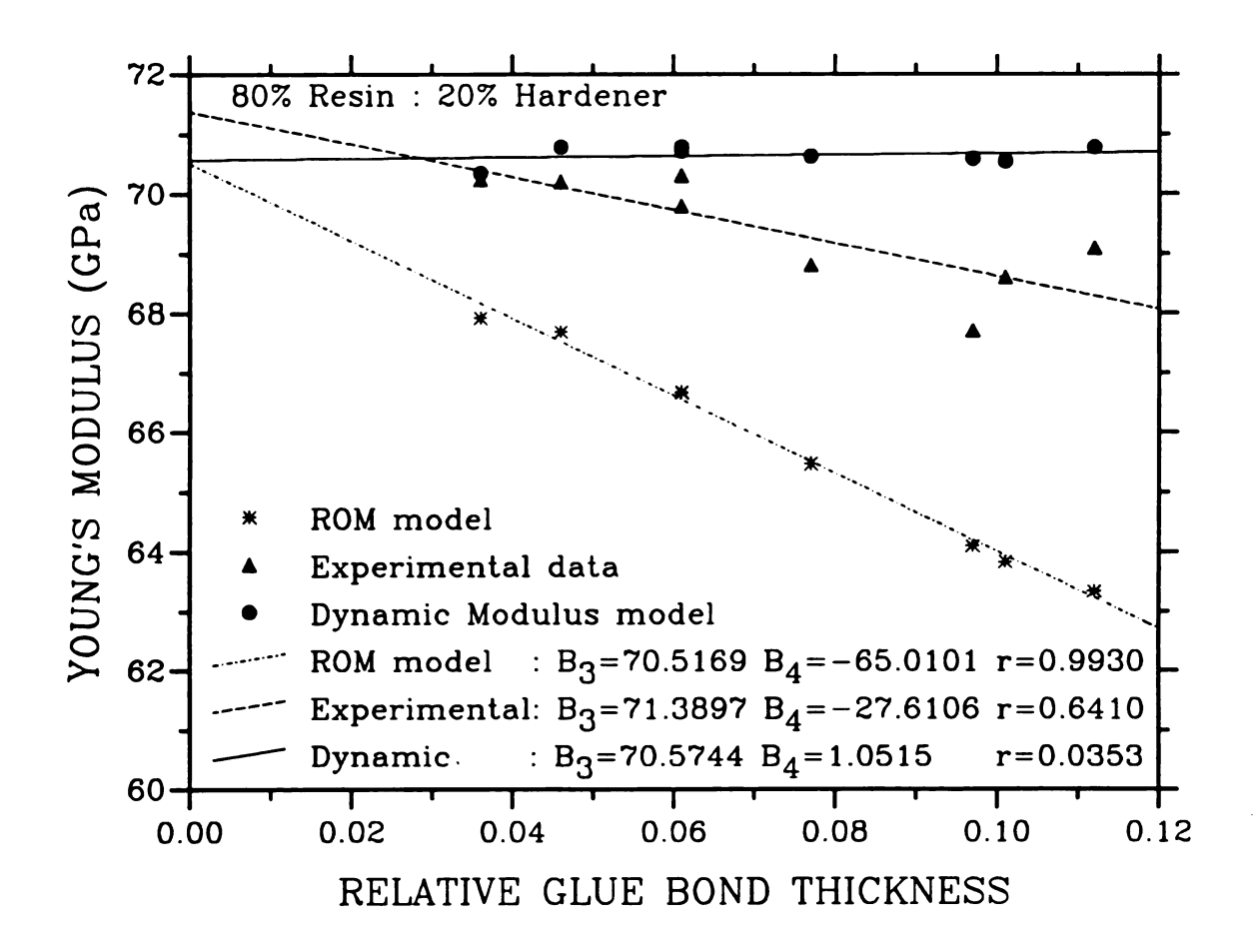


Figure 40. Comparison of experimentally determined moduli with the moduli predicted from the Rule of Mixtures and Dynamic Beam Vibration models as a function of relative glue bond thickness for 80% resin and 20% hardener. The curves represent a least-squares best fit to equation 37.

(—— Dynamic modulus model: B₃=70.5744, B₄=1.0515, r=0.0353, ····· Experimental data: B₃=71.3897, B₄=-27.6106, r=0.6410, ····· ROM model; B₃=70.5169, B₄=-65.0101, r=0.9930)

As the relative glue bond thickness increases, the deviation of the experimentally obtained Young's modulus increased with respect to the predictions of both the Dynamic Beam Vibration model and the ROM model (Figures 35-40). The curves for the deviation, δ_R , for the two models have similar slopes but the opposite algebraic signs. In addition, the deviation, δ_R , goes to zero as the relative glue bond thickness approaches zero.

The deviation of the measured elastic moduli from the moduli predicted by the ROM and Dynamic modulus models may involve imperfect interfacial bonding between two glass layers and inelastic behavior of epoxy glue layer. The glass slides, however, certainly do behave elastically. Also, unlike the ROM model, the loading in this study was not a uniaxial loading but a free-free suspension vibration by sonic resonance technique. However, the sonic resonance modulus measurement technique employed in this study is appropriate to the assumptions made for the Dynamic modulus model.

Another reason for the deviation between the experimental values and the values predicted from the Dynamic modulus model could stem from the large difference in stiffness of the glass slide layers and the glue bond layer. For our laminated glass slide/glue composite specimens, the difference in stiffness can give rise to a piecewise linear (as opposed to a linear) variation of inplane displacement through the thickness [19]. Thus, the Euler-Bernoulli assumptions are less valid as the glue bond thickness increases, such that the effect is increased with increasing the glue bond thickness.

As the relative glue bond thickness approaches zero, both models seem to successfully describe the Young's modulus of three-layer composite.

3.2.6. Change of Effective Young's Modulus of Glass Slide/Glue Specimens with respect to Glue-Bond Thickness Ranges at Fixed Adhesion Areas

The data included in the three regression curves in Figure 33 were analyzed with respect to three glue-bond thickness ranges and adhesion area percent ranging from 0% to 100% (Table 7, Figures 41 and 42).

Also, for 100% adhesion area the Young's moduli calculated from equation 33 were compared to the measured data (Figure 43).

For the entire range of adhesion area fraction, the Young's modulus decreased with the increase of the glue bond thickness (Figures 41 and 42). Also, each of the curves showed approximately the same slope. In addition, as the adhesion area increased from 0% to 100% by increments of 10%, the Young's modulus difference between two adjacent curves decreased from 10 GPa (going from 0% adhesion area to 10% adhesion area) to 0.03 GPa (going from 90% adhesion area to 100% adhesion area) (Table 7, Figure 41 and Figure 42).

The slopes of the curves for the calculated Young's modulus and the measured Young's modulus are very similar (Figure 43).

As a result, for adhesion areas less than 100%, the predicted Young's modulus from the ROM and the dynamic modulus models will show the similar deviation from the measured Young's modulus as discussed in Section 3.2.5.

Table 7. Young's moduli (GPa) of glass slide/epoxy resin composite specimens obtained from the regression curves in Figure 33. The table shows representative Young's moduli of glass slide/epoxy resin composite specimens having a given adhesion areas and a glue bond thickness within a given range of glue bond thickness.

ADHESION	RANGES OF GLUE BOND THICKNESS				
AREA (%)	R ₁ (0.025-0.075mm)	R ₂ (0.125-0.175mm)	R ₃ (0.225-0.275mm)		
100	70.79	68.78	67.27		
90	70.76	68.74	67.23		
80	70.56	68.53	67.01		
70	70.03	67.94	66.39		
60	68.99	66.80	65.18		
50	67.28	64.92	63.20		
40	64.73	62.11	60.24		
30	61.16	58.19	56.10		
20	56.42	52.97	50.60		
10	50.33	46.28	43.54		
0	42.73	37.92	34.72		

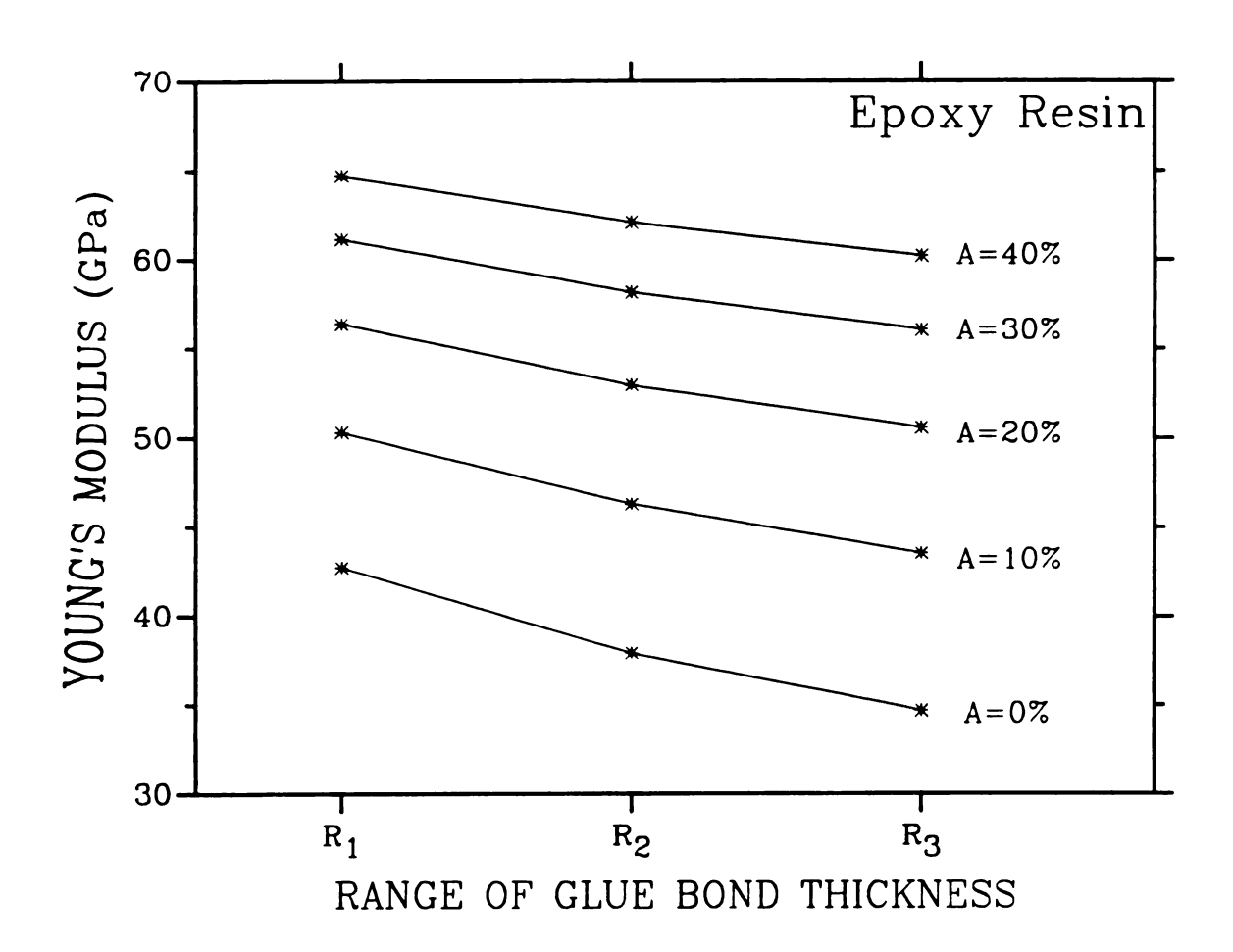


Figure 41. Change of Young's modulus with respect to glue-bond thickness ranges ($R_1:0.025-0.075$ mm, $R_2:0.125-0.175$ mm, $R_3:0.225-0.275$ mm) at adhesion area percent, A, ranging from 0% to 40%. The data were obtained from the three regression curves using equation 33 in Figure 33.

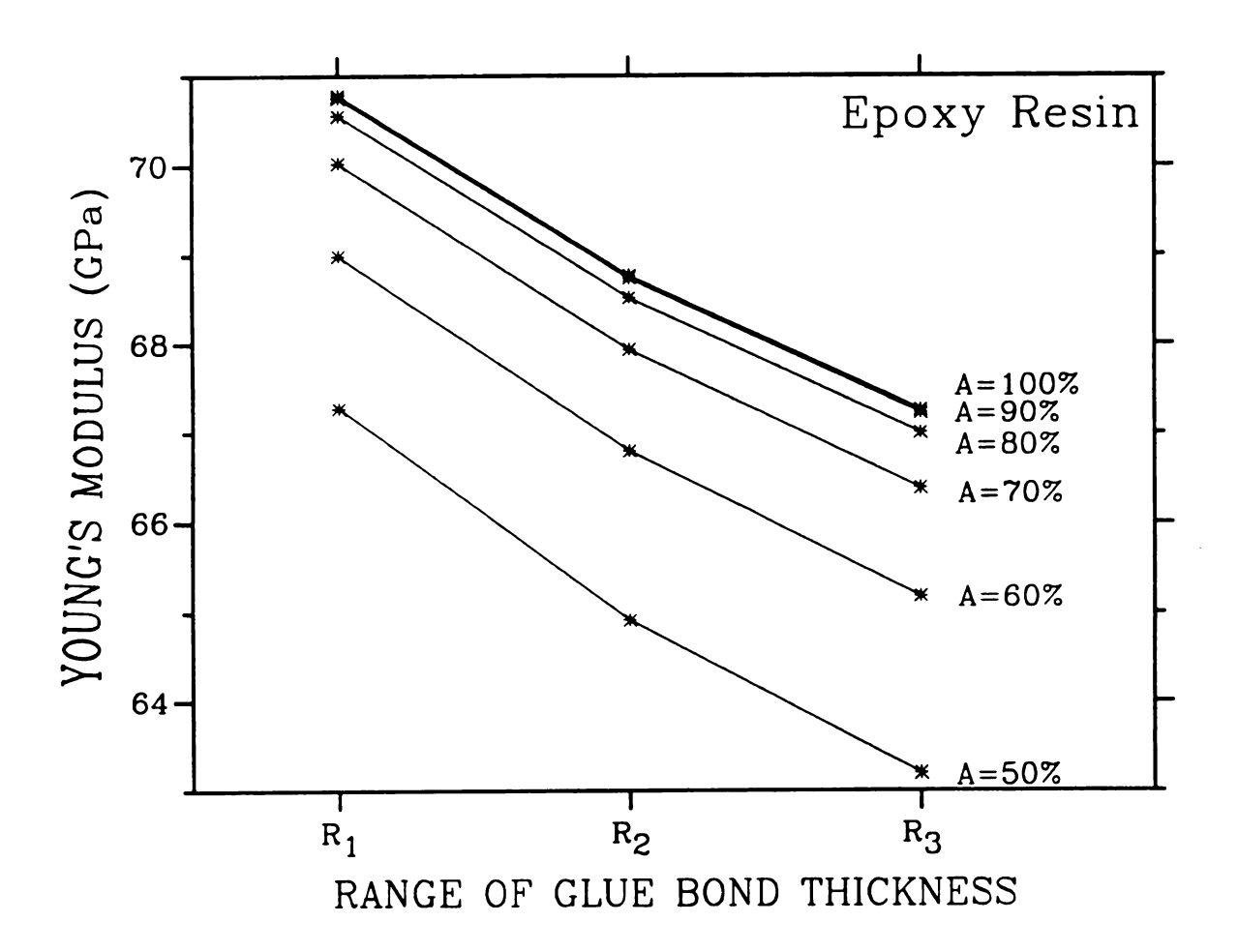


Figure 42. Change of Young's modulus with respect to glue-bond thickness ranges ($R_1\colon 0.025-0.075$ mm, $R_2\colon 0.125-0.175$ mm, $R_3\colon 0.225-0.275$ mm) at adhesion area percent, A, ranging from 50% to 100%. The data were obtained from the three regression curves using equation 33 in Figure 33.

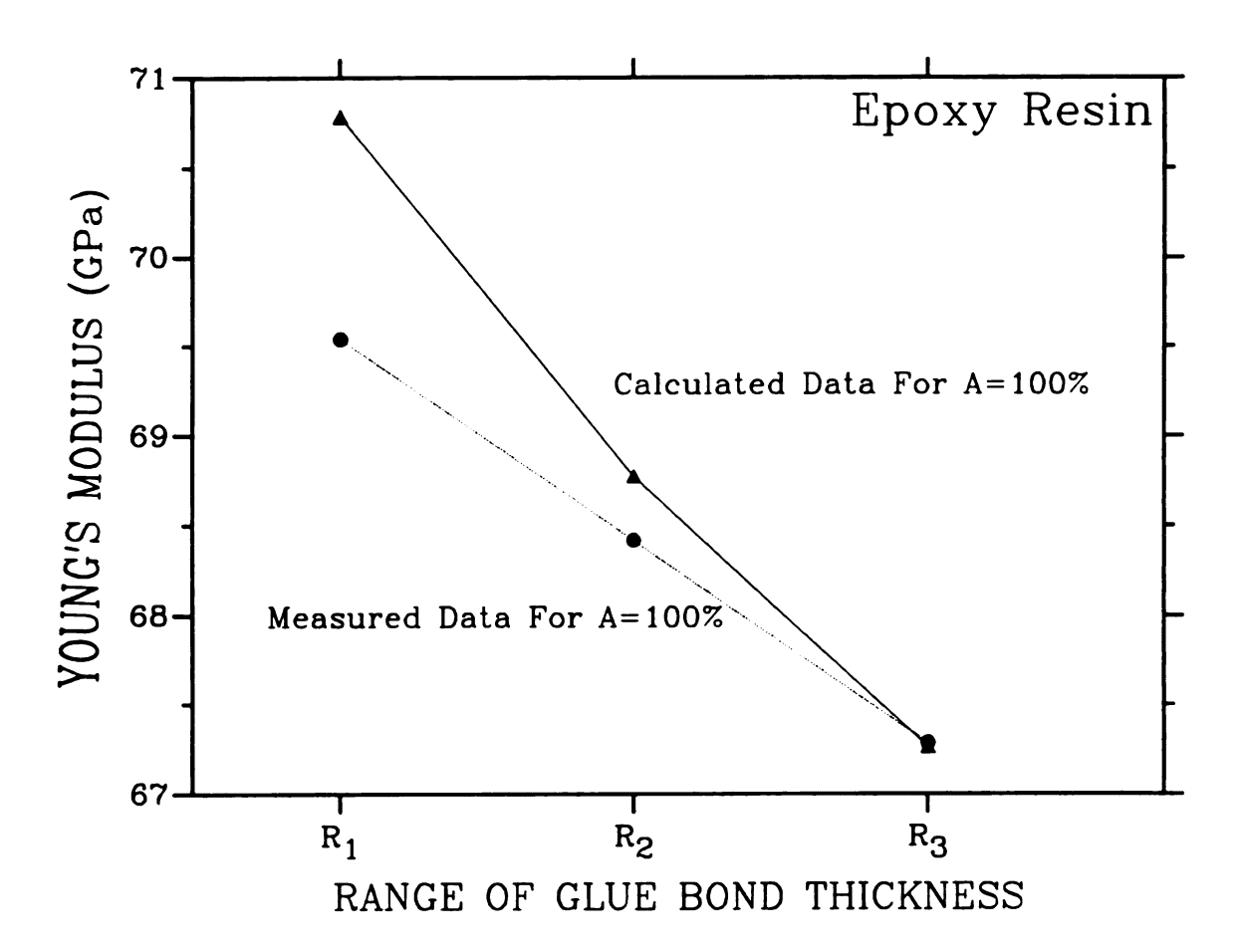


Figure 43. Change of the measured and the calculated Young's modulus with respect to glue-bond thickness ranges (R_1 :0.025-0.075 mm, R_2 :0.125-0.175 mm, R_3 :0.225-0.275 mm) at 100% adhesion area. The calculated data were obtained from the three regression curves using equation 33 in Figure 33.

3.2.7. Possible Physical Mechanisms for the Difference between the Measured Modulus of the Glass Slide/Glue Composite Specimens and the Predictions of the ROM and Dynamic Modulus Models

We shall consider two types of possible mechanisms that could potentially explain the differences (Figures 35-40) between the experimental data and the theoretical predictions of the ROM and dynamic modulus models. The two mechanisms are: (1) A change in the elastic modulus of the glue bond layer itself, perhaps due to residual stresses induced by shrinkage of the bond layer, or (2) an adhesion area less than the 100 percent adhesion area assumed in the experiment. (Note that the ROM and dynamic modulus models were only applied to the case where the experimentally determined adhesion area was nominally 100 percent, or nearly 100 percent (Figures 35-40)).

If the actual adhesion area is less than 100 percent, the effective modulus of the specimens would be lower than predicted by the ROM and dynamic modulus models. However, the feasibility of a residual-stress induced change in the modulus of the bond layer must be considered in terms of the relative modulus changes observed in a literature.

We shall briefly review stress (or pressure) induced changes in elastic modulus, using examples from the thermal quenching of a polymer glass [20] and the pressure induced changes in stiffness for crystalline ceramics [21-23].

Vega and Bogue [20] measured residual stresses in terms of residual Optical birefringence induced into polymer glasses by thermal quenching into several media. Vega and Bogue reported a decrease of elastic modulus as a function of the quench medium temperature (Table 8). With respect to the slow cooling of 30°C medium, the elastic modulus of the

Table 8. Elastic modulus of quenched polymer glass as a function of the quench medium temperature [20].

Quenching Medium	Temperature of Medium	Elastic Modulus (GPa)
Slow cool *	30	1.7
Water quench **	30	1.5
Slow cool *	70	1.5
Water quench **	70	0.95
Nitrogen quench	70	1.0

^{*} Slow cooling is at 0.01°C/s.

^{**} Water quench is at 160°C/s.

polymer glass quenched into the other media decreased by approximately 12% (0.2 GPa) to 44% (0.75 GPa).

The pressure dependence of elastic modulus has been reported in terms of elastic stiffness for crystalline ceramics such as magnesium oxide, sodium chloride, potassium chloride, and quartz (Table 9) [21-23]. Anderson and Andreatch [21] observed that an elastic stiffness of single-crystal magnesium oxide increased by up to 0.66% (20 MPa) with increasing the hydrostatic pressure from 1 atm to 20 MPa at 23°C.

We shall now discuss (section 3.2.8.and section 3.2.9) the particular differences between the experimentally determined moduli for the glass slide/glue composite specimens and the moduli predicted from the ROM and dynamic modulus models, respectively. In each section, we shall discuss whether it is feasible that the observed differences can be explained in terms of (1) a shift in the modulus of the bond layer or (2) an adhesion area that is less than the nominal 100 percent adhesion area.

3.2.8. Possible Changes in Effective Young's Modulus of a Bond Layer
for the Difference between the Experimentally Determined Modulus
and the Moduli Predicted from the ROM Model

The experimentally determined Young's moduli of the epoxy resin specimens (Table 6) were used to calculate the Young's moduli predicted from the ROM models. Assuming the ROM model was correct, the Young's modulus of epoxy resin bond layer in a glass slide/epoxy resin composite specimen was calculated by using measured dimensions of each layer (the glue bond layer thickness and the thickness of each glass slide) and

Table 9. Pressure derivatives of elastic constants of MgO at 23°C, NaCl, KCl at 22°C, and Quartz at 25°C [21-23]. Units of all elastic constant values are MPa.

MATERIALS	ELASTIC CONSTANTS	At P=1 (Pa) (=1 bar)	At P (Pa) *	PRESSURE ** DERIVATIVE
MgO [21]	C ₁₁	2964.7	2984.3	9.50
	C ₁₂	950.68	954.8	1.99
	C44	1558.9	1561.3	1.16
	В,	1622.0	1631.3	4.50
NaCl [22]	C ₁₁ ′	43500	***	7.24
	c'	18210	***	4.79
	C4	12720	***	0.37
	В,	24710	**	5.27
KC1 [23]	C ₁₁ ′	30040	***	6.83
	c'	16760	***	5.61
	C44	6300	***	-0.39
	B,	18150	***	5.34
Quartz [23]	C ₁₁	86800	***	3.28
	C ₁₂	7040	***	8.66
	C44	58200	***	2.66
	B _s	37410	***	6.30

where C_{11} , C_{12} , and C_{44} = elastic stiffnesses $B_s = (C_{11} + 2C_{12})/3$ = adiabatic bulk modulus $C_{11}' = (C_{11} + C_{12} + 2C_{44})/2$

 $C_{12}' = (C_{11} - C_{12})/2.$

^{*} Pressure, P, is 20.681 MPa for MgO, NaCl and KCl, and 15 MPa for Quartz.

^{**} Pressure derivative represents dC/dP for elastic stiffness and dB_a/dP for bulk modulus.

^{***} Elastic constants not specified.

Young's moduli of each glass slide layer. The results are plotted as a function of the relative glue bond thickness (Table 10 and Figure 44).

The calculated Young's moduli of epoxy resin layers were about 700% to 1700% higher than the measured Young's modulus of the epoxy resin specimen with composition of 50% resin, 2.977 GPa (Table 6 and 10). A 700% to 1700% shift of the calculated moduli of the bond layer from the experimentally determined modulus can not be considered as reasonable values compared to Vega and Bogue's [20] stress-induced changes (section 3.2.7. and Table 8), and Anderson and Andreatch's pressure-induced changes (section 3.2.7. and Table 9). Therefore, possible changes in Young's modulus of epoxy resin layer do not alone account for the deviation of experimentally determined Young's moduli from the ROM model.

3.2.9. Dependence of the ROM and the Dynamic Modulus Models on the

Relative Glue Bond Thickness and Comparison with Experimental

Results

To see the dependence of both models on relative glue bond thickness (Figures 45-47), the Young's moduli for the ROM and the Dynamic Modulus models were calculated using reasonable data representing mean values of measured moduli and specimen dimensions. Also, both models were compared to experimentally determined data.

The used elastic moduli for layers 1 and 2 (glass slides) were 70.53 GPa, which corresponds to the experimentally determined average Young's modulus of 140 individual glass slides (See Section 3.2.2.1.). The thicknesses and width assumed for layers 1 and 2 were 1.2 mm

Table 10. Young's modulus of epoxy resin layer in a glass slide/epoxy resin composite specimen to compensate for the ROM model.

	50% Resin : 50% Hardener		65% Resin : 35%Hardener		esin : ardener
t _R *	E _b **(GPa)	t _R	E _b (GPa)	t _R	E _b (GPa)
0.029	53.35	0.027	59.10	0.046	57.99
0.034	44.18	0.062	27.42	0.061	63.64
0.036	39.54	0.065	34.52	0.061	54.32
0.036	36.78	0.084	45.77	0.077	46.64
0.043	37.05	0.089	49.72	0.097	40.48
0.056	41.56	0.098	41.07	0.101	50.75
0.058	41.15	0.102	43.21	0.112	54.87
0.059	23.80	0.103	52.33		
0.077	43.80	0.114	54.26		
0.081	40.23	0.120	44.86		
0.087	23.47				
0.102	23.27				
0.1097	37.06				

^{*} t_R = relative glue bond thickness
** E_b = elastic modulus of glue bond layer

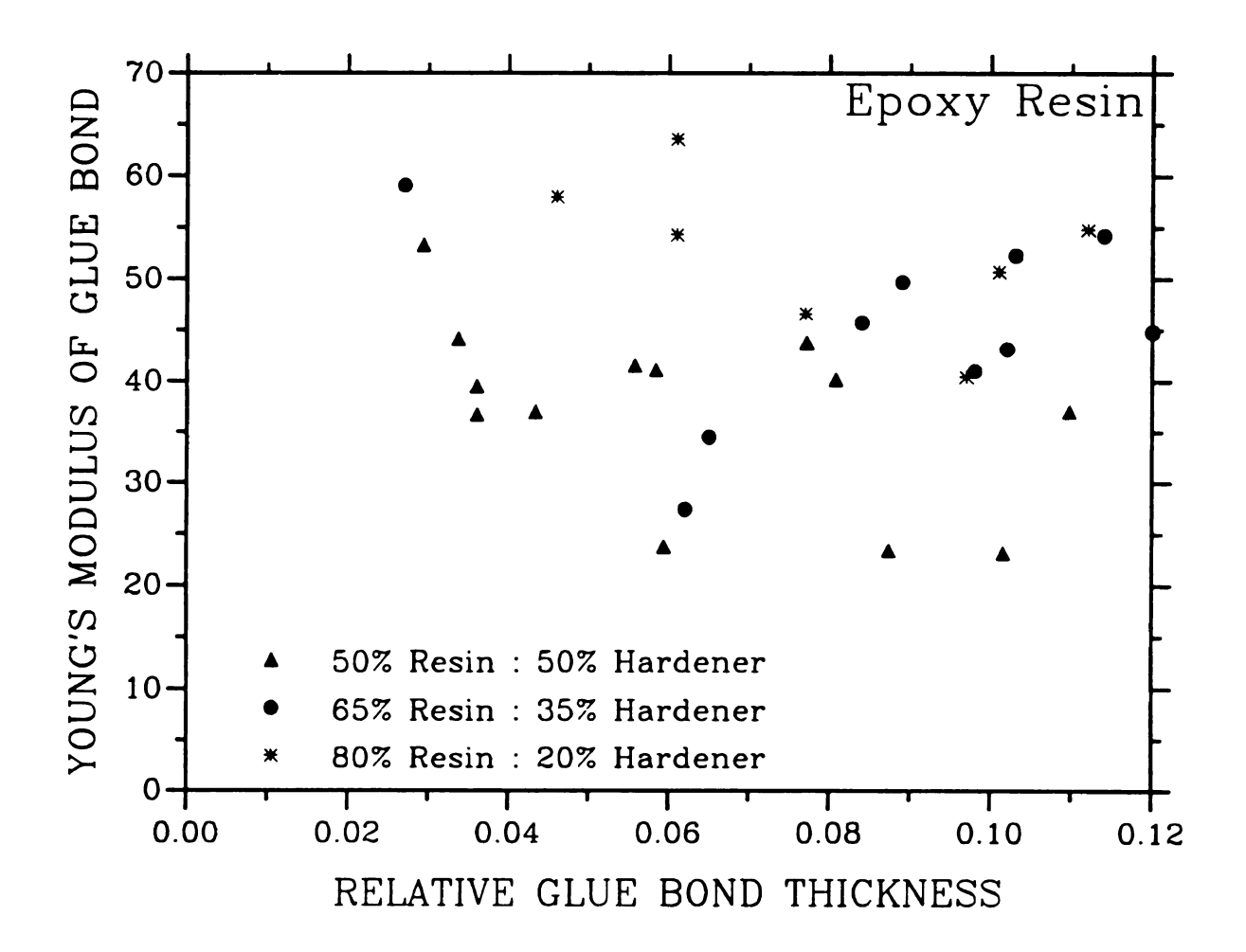


Figure 44. Calculated Young's moduli of epoxy resin bond layer to compensate for the Rule of Mixtures model.

- represents 50% resin and 50% hardener.
- A represents 65% resin and 35% hardener.
- . represents 80% resin and 20% hardener.

(approximate thickness of single glass slide) and 25.4 mm (approximate width of single glass slide). The experimentally determined Young's modulus for the epoxy resin specimen (Table 6) was assumed as the Young's modulus of epoxy resin bond layer. The value of the epoxy resin bond layer is a function of the epoxy's composition.

The Young's modulus calculated from the ROM model decreased linearly with the increase of the relative glue bond thickness without regard to the composition of epoxy resin layer (Figure 45-47). Also, the Young's modulus calculated from the Dynamic Modulus model decreased even though the dependence was very weak. Where the relative glue bond thickness was almost zero, the calculated Young's moduli from both the ROM and the Dynamic modulus models coincided. As the relative glue bond thickness increased, the difference between the calculated Young's moduli from both models increased. The experimentally determined Young's moduli fall between the curves predicted from the ROM model and the Dynamic modulus model (Figures 45-47).

3.2.10. Possible Changes in Effective Young's Modulus of a Glass
Slide/Glue Specimen for the Difference between the Measured
Moduli and the Moduli Predicted from the Dynamic Modulus Model

In section 3.2.7., we discussed the Vega and Bogue's work on the decrease of the Young's modulus due to residual stresses induced by a quenching of polymeric materials (Table 8) [20]. In the current study, when a glass slide/epoxy resin specimen was fabricated, the volume contraction of the glue bond layer might have induced residual stresses. Assuming the Dynamic modulus model is correct, we could imagine two

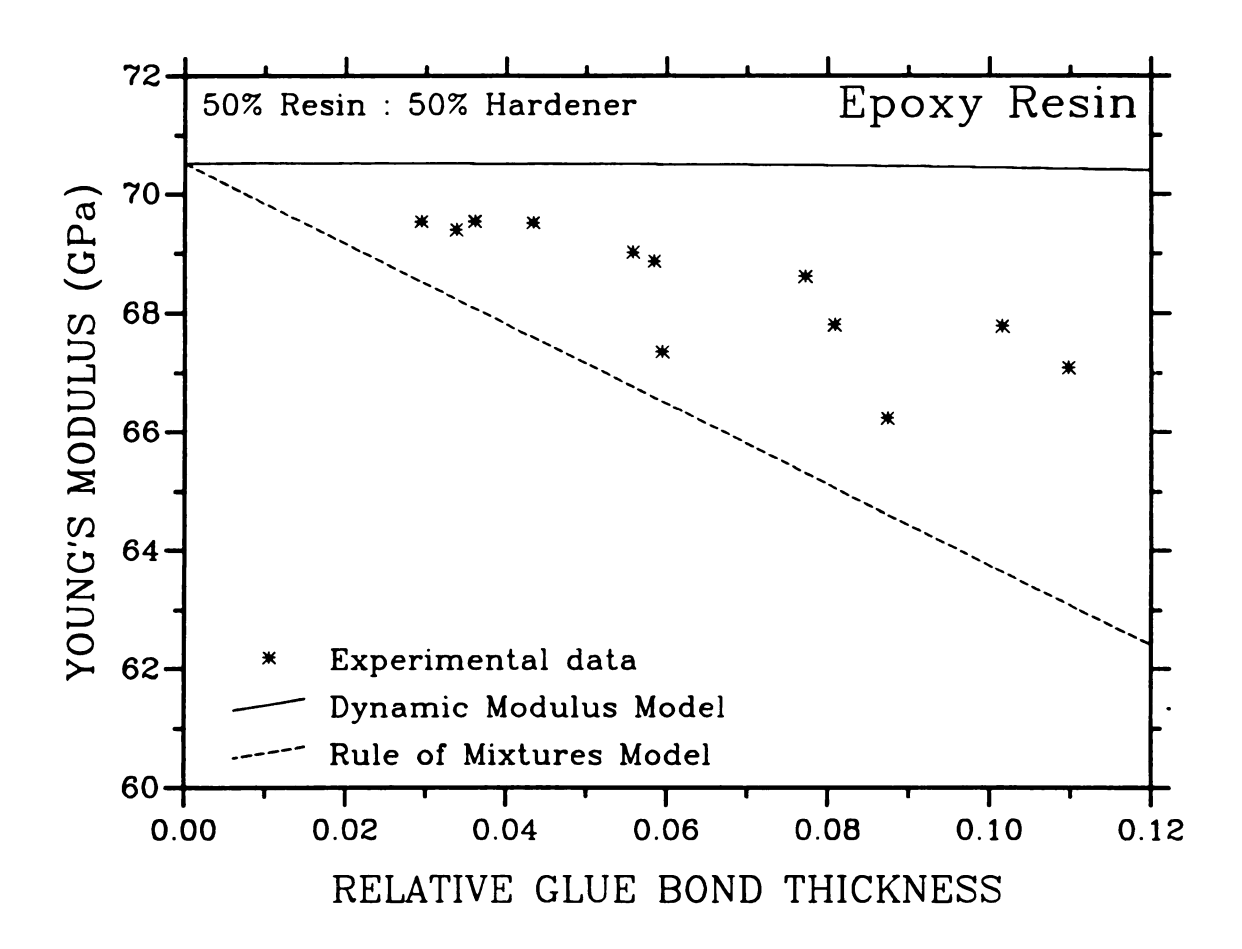


Figure 45. Comparison of experimentally determined Young's modulus (.) and calculated Young's modulus from the Dynamic Modulus model (----) and the ROM model (----) for 50% resin and 50% hardener.

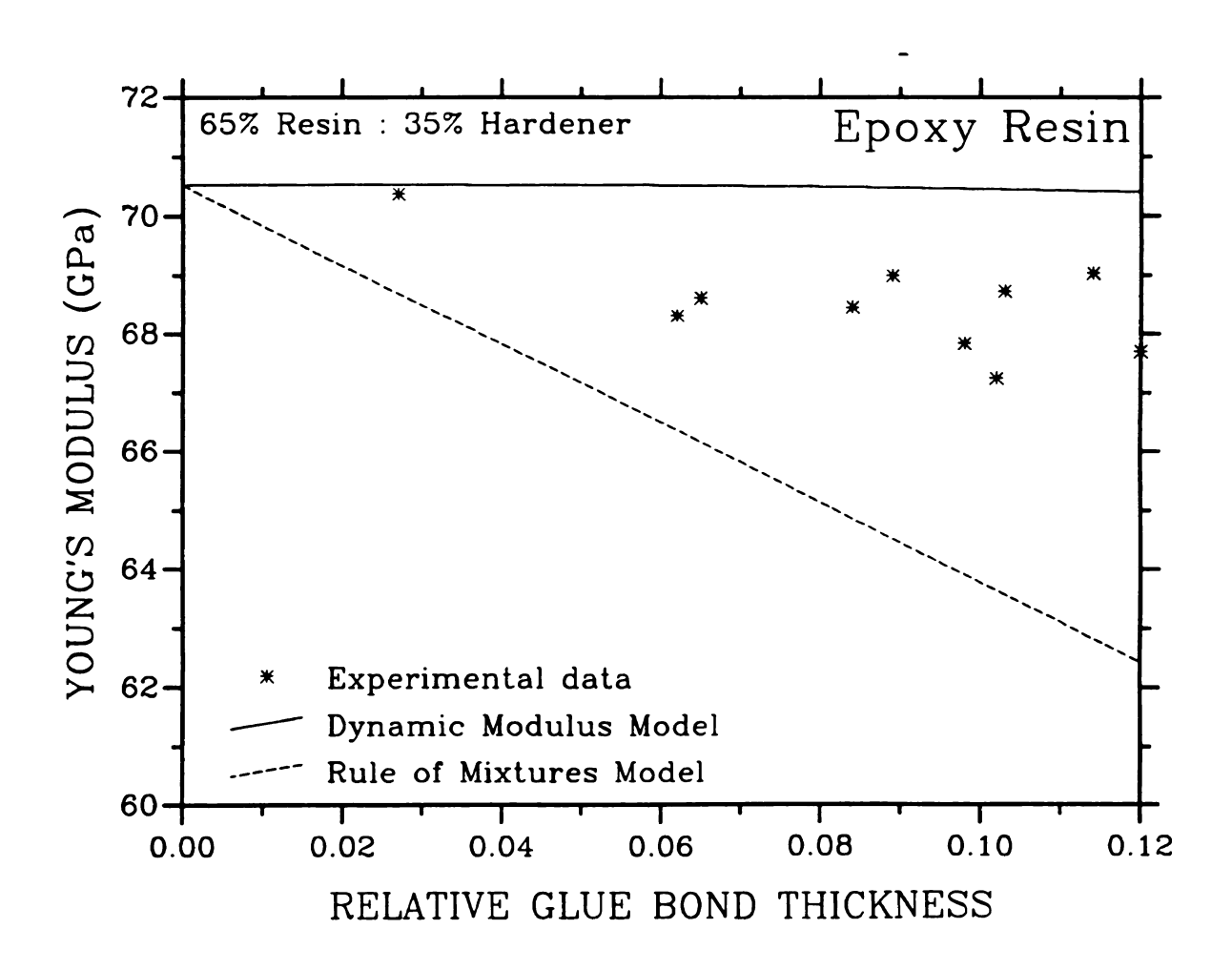


Figure 46. Comparison of experimentally determined Young's modulus (.) and calculated Young's modulus from the Dynamic Modulus model (----) and the ROM model (----) for 65% resin and 35% hardener.

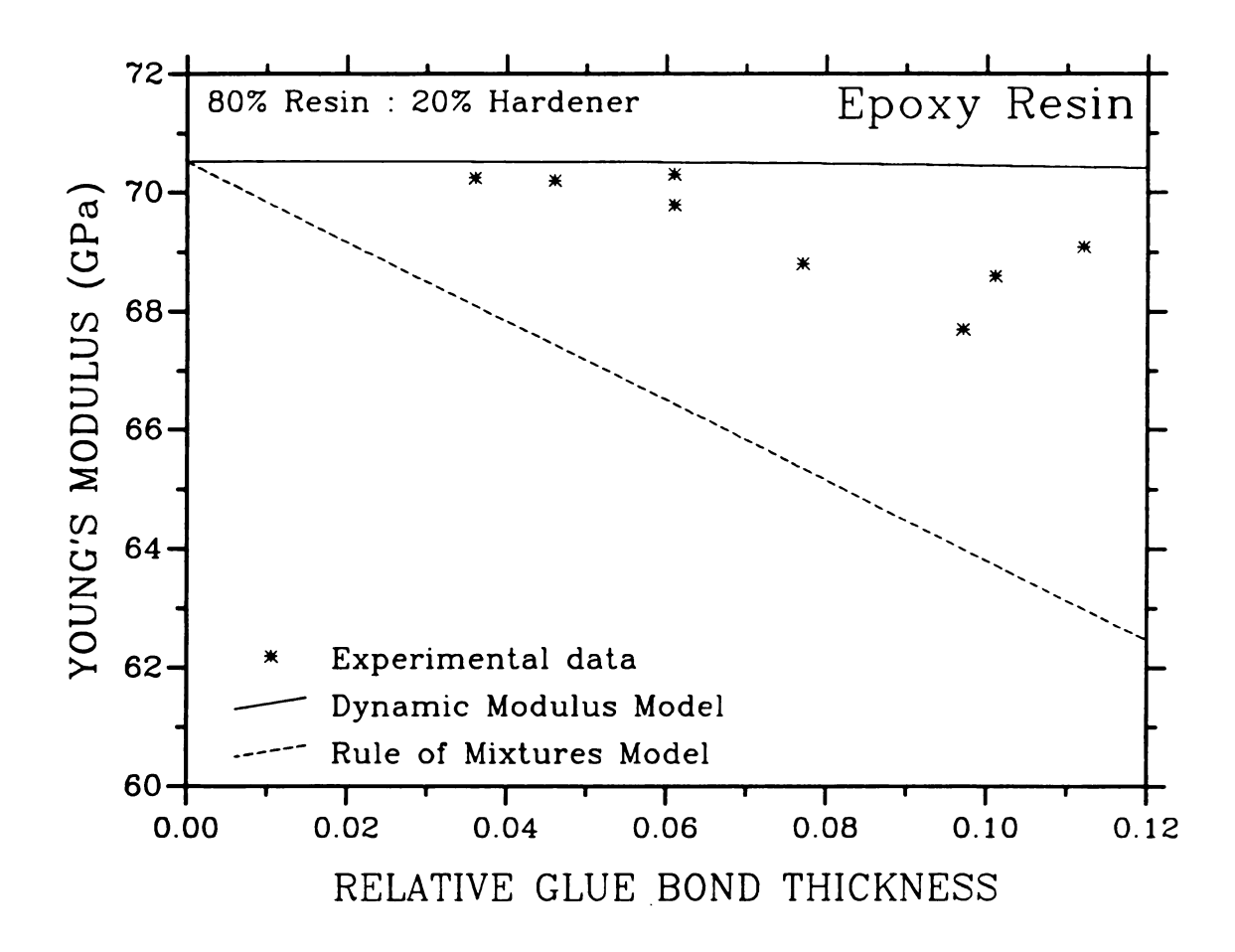


Figure 47. Comparison of experimentally determined Young's modulus (.) and calculated Young's modulus from the Dynamic Modulus model (----) and the ROM model (----) for 80% resin and 20% hardener.

possible ways the effective Young's modulus might deviate from the modulus predicted by the Dynamic modulus model (section 3.2.5.): (1) change of the elastic moduli of glass slide layers, (2) change of the elastic modulus of glue bond layer.

To investigate the possibilities of changes in Young's moduli of the glass slide layers and the glue bond layer, two modulus data were picked up from the regression curve for experimentally measured modulus values in Figure 38, which were 68.57 GPa and 66.51 GPa corresponding to the relative glue bond thickness, 0.06 and 0.12, respectively. The same reasonable data as in section 3.2.9. were used for calculations of the elastic moduli of a glass slide and an epoxy resin bond layer (the elastic modulus $E_{II}=E_{II}=70.53$ GPa, for the two glass slide layers of thickness 1.2 mm, the experimentally determined elastic modulus, $E_b=2.98$ GPa, for the epoxy resin glue bond having 50% resin composition, and the width of a composite specimen, 25.4 mm).

First, using the assumed data and equations 22a-22c, 24, and 25 (dynamic modulus model) the elastic modulus of a glass slide layer required to obtain the measured moduli, 68.57 GPa and 66.51 GPa at the relative glue bond thicknesses, 0.06 (=0.144 mm) and 0.12 (=0.288 mm) were calculated assuming the constant elastic modulus of the glue bond layer, 2.98 GPa. The data calculated by the dynamic modulus equation 25 were 68.58 Gpa for 0.144 mm thick glue bond and 66.59 Gpa for 0.288 mm thick glue bond (Table 11). The resulting data indicate that the elastic modulus of a glass slide with the assumed dimensions decreased by about 2 GPa (=70.53 GPa - 68.58 GPa) as the relative glue bond thickness increased from 0.00 to 0.06. Likewise, as the relative glue bond thickness increased from 0.00 to 0.12, the elastic modulus of a glass slide decreased by about 4 GPa (=70.53 GPa - 66.59 GPa). As we

can see easily, the relative glue bond thickness, 0.06 falls in half way between 0.00 and 0.12. Thus by this brief calculation, we could expect the linear change of the elastic modulus of a glass slide. Therefore a linear deviation of the effective Young's modulus of a composite specimen as a function of the relative glue bond thickness could be expected as shown in Figures 35-40.

Secondly, for the possibility of the change in elastic modulus of a glue bond layer within a composite specimen, the elastic moduli of the glue bond layers having the relative glue bond thicknesses, 0.06 and 0.12 were calculated by the assumed reasonable data and the equations from the dynamic modulus model assuming the fixed modulus value of each glass slide, 70.53 GPa. The resulting modulus values were -10736 GPa and -3198 GPa at the relative glue bond thickness, 0.06 and 0.12, respectively (Table 12). However, according to a basic mechanical theory, elastic moduli must be positive. Also the absolute values 10736 GPa and 3198 GPa are too high to be considered as the elastic modulus for the epoxy resin compared to the experimentally determined elastic modulus, 2.98 GPa. Thus we can conclude that the change of the elastic modulus of glue bond layer is physically impossible.

Table 11. Comparison of measured Young's moduli of a glass slide layer with Young's moduli of the glass slide layer calculated from the Dynamic modulus model required to obtain the measured effective Young's moduli.

RELATIVE GLUE BOND THICKNESS	GLUE BOND THICKNESS (mm)	Ē _{mp} (GPa)	E _{l,max} (GPa)	E _{I,DYN} (GPa)	E _{l,mo} -E _{l,DYN} (GPa)
0.06	0.144	68.57	70.53	68.58	1.95
0.12	0.288	66.51	70.53	66.59	3.94

where \bar{E}_{exp} = experimentally determined effective elastic modulus $E_{l,exp}$ = assumed elastic modulus of a glass slide layer

 $\mathbf{E}_{\mathrm{LDYN}}$ = elastic modulus of a glass slide layer calculated from

the Dynamic modulus model

 $E_{l,m}-E_{l,DYN}$ = difference between assumed and calculated elastic moduli of a glass slide layer.

Table 12. Comparison of measured Young's moduli of a glue bond layer with Young's moduli of the glue bond layer calculated from the Dynamic modulus model required to obtain the measured effective Young's moduli.

RELATIVE GLUE BOND THICKNESS	GLUE BOND THICKNESS (mm)	E _{exp}	E _{b,sup} (GPa)	E _{b,DYN} (GPa)	E _{b,exp} -E _{b,DYN} (GPa)
0.06	0.144	68.57	2.98	-10736	10739
0.12	0.288	66.51	2.98	-3198	3201

where \bar{E}_{exp} = experimentally determined effective elastic modulus $E_{b,exp}$ = experimentally determined elastic modulus of the epoxy resin specimen having 50% resin composition

 $E_{b,DYN}$ = elastic modulus of a glue bond layer calculated from the Dynamic modulus model

 $E_{b,mp}-E_{b,DYN}$ = difference between measured and calculated elastic moduli of a glue bond layer.

3.2.11. Consideration of Insufficient Bonding as a Possible Factor for Deviation of Measured Elastic Moduli from the Moduli predicted by ROM Model

The deviation of the measured Young's modulus from the moduli calculated by the ROM model was analyzed related to the effect of adhesion area on the Young's modulus. The data obtained from regression curves for the measured Young's moduli and the moduli predicted from the ROM model (Figure 38 and Table 13) were compared with the data obtained from a regression curve for Young's moduli (Figure 28 and Table 14).

Comparing Table 13 and Table 14, the differences between the measured Young's moduli and the moduli predicted from the ROM model as a function of relative thickness ranging from 0.00 to 0.12 approximately correspond to the differences between the Young's modulus for 100% adhesion area and the moduli for adhesion areas of 75% to 48%.

However, the modulus values in Table 10 were obtained for the glass slide/epoxy resin composite specimens having apparent adhesion area of 100%. Therefore, in this comparison the adhesion areas, 75% to 48% are too small to regard the insufficient bonding as a main factor for the deviation of measured moduli from the moduli predicted by the ROM model.

Measured Young's moduli and moduli predicted from the ROM and Table 13. the Dynamic Modulus models as a function of relative thickness obtained from the corresponding regression curves in Figure 38.

Relative Glue Bond Thickness	E _{exp} *	E _{DYN} * (GPa)	E _{ROM} *	E _{eep} -E _{DYN} ** (GPa)	E _{exp} -E _{ROM} *** (GPa)
0.00	70.62	70.50	70.47	0.12	0.15
0.01	70.28	70.50	69.80	-0.22	0.48
0.02	69.94	70.50	69.13	-0.56	0.80
0.03	69.59	70.49	68.46	-0.90	1.13
0.04	69.25	70.49	67.79	-1.24	1.46
0.05	68.91	70.48	67.12	-1.57	1.79
0.06	68.57	70.48	66.45	-1.91	2.12
0.07	68.22	70.47	65.78	-2.25	2.44
0.08	67.88	70.47	65.11	-2.59	2.77
0.09	67.54	70.47	64.44	-2.93	3.10
0.10	67.20	70.46	63.77	-3.26	3.43
0.11	66.85	70.46	63.10	-3.61	3.75
0.12	66.51	70.45	62.43	-3.94	4.08

 $[\]mathbf{E}_{exp}\text{, }\mathbf{E}_{DYN}\text{, and }\mathbf{E}_{ROM}$ represent the best-fit elastic moduli values of the experimentally measured moduli and the moduli calculated from the ROM and the Dynamic modulus models to equation 37, respectively (Figure 38).

^{**} E_{exp} - E_{DYN} is the difference between E_{exp} and E_{DYN} .

*** E_{exp} - E_{ROM} is the difference between E_{exp} and E_{ROM} .

Table 14. Young's moduli obtained from a regression curve in Figure 28 and the difference between the Young's moduli, E_{100} , for adhesion area of 100% and the Young's moduli, E, for adhesion area ranging from 0% to 100%.

Adhesion Area (%)	E (GPa)	E ₁₀₀ - E (GPa)
100	68.49	0.00
95	68.49	0.00
90	68.49	0.00
85	68.47	0.02
80	68.42	0.07
75	68.33	0.16
70	68.17	0.32
65	67.92	0.57
60	67.54	0.95
55	66.99	1.50
50	66.25	2.24
45	65.27	3.22
40	64.00	4.49
35	62.40	6.09
30	60.40	8.09
25	57.96	10.53
20	55.02	13.47
15	51.52	16.97
10	47.37	21.12
5	42.53	25.96
0	36.92	31.57

3.3. General Trends in Effective Young's Modulus on Adhesion

Experimentally, the glass slide/glue composite specimens adhered by different types of adhesives showed similar trends in the effective Young's modulus dependence on adhesion area and glue bond thickness.

First, for each of the types of adhesive agents used in this study, similar trends in the effective Young's modulus was observed as a function of adhesion area (Figures 48-50). For one glue spot, the Young's modulus of the super glue and epoxy cement adhered specimens nearly coincide at 100% and 0% adhesion areas (Figure 48).

For two or more glue spots, the experimentally obtained Young's modulus data for glass slide/super glue, epoxy cement, and epoxy resin composite specimens show very similar trend of decreasing Young's modulus with decreasing adhesion area (Figure 49). However, the trend for the one glue spot specimens is different from that for two or more glue spots (see section 4.2).

Secondly, if we lump together the data for two or more glue spots for the epoxy cement (10 specimens), the super glue (50 specimens), and epoxy resin (70 specimens), we observe that the super glue bond thickness tends to be relatively thin (about 0.015 mm on average), the epoxy resin bond thickness is relatively thick (0.165 mm on average), while the epoxy cement is of intermediate thickness (about 0.060 mm on average). Thus, compared to the effect of the epoxy resin bond thickness, the difference of about 3 GPa to 8 GPa between the two curves in Figure 50 was, in part, caused by the effect of the glue bond thickness on Young's modulus.

To investigate the effect of the glue bond thickness on the effective Young's modulus among the three different types of adhesive s

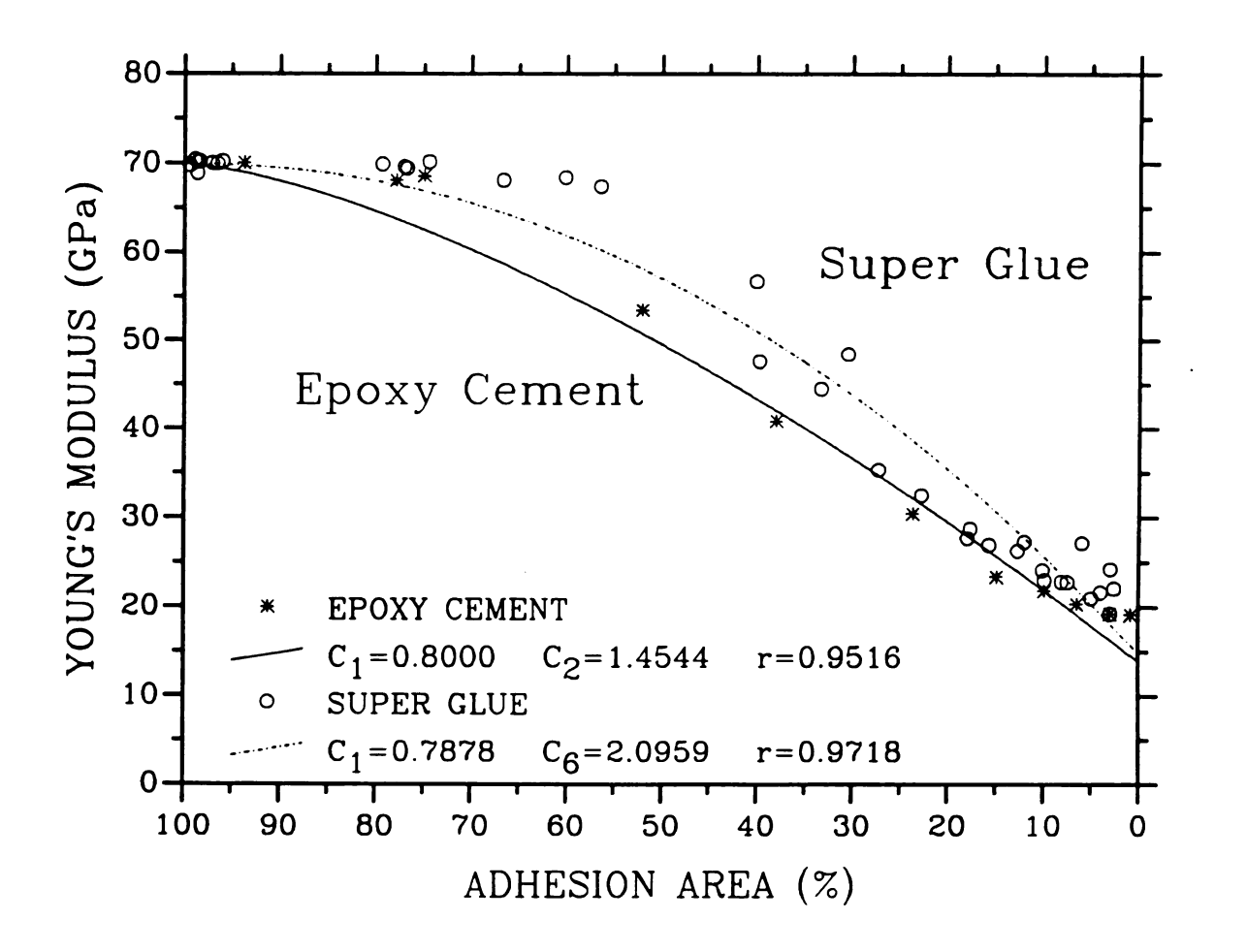


Figure 48. The general trend in Young's modulus between super glue adhered specimens and epoxy cement adhered specimens for one glue spot as a function of adhesion area(%).

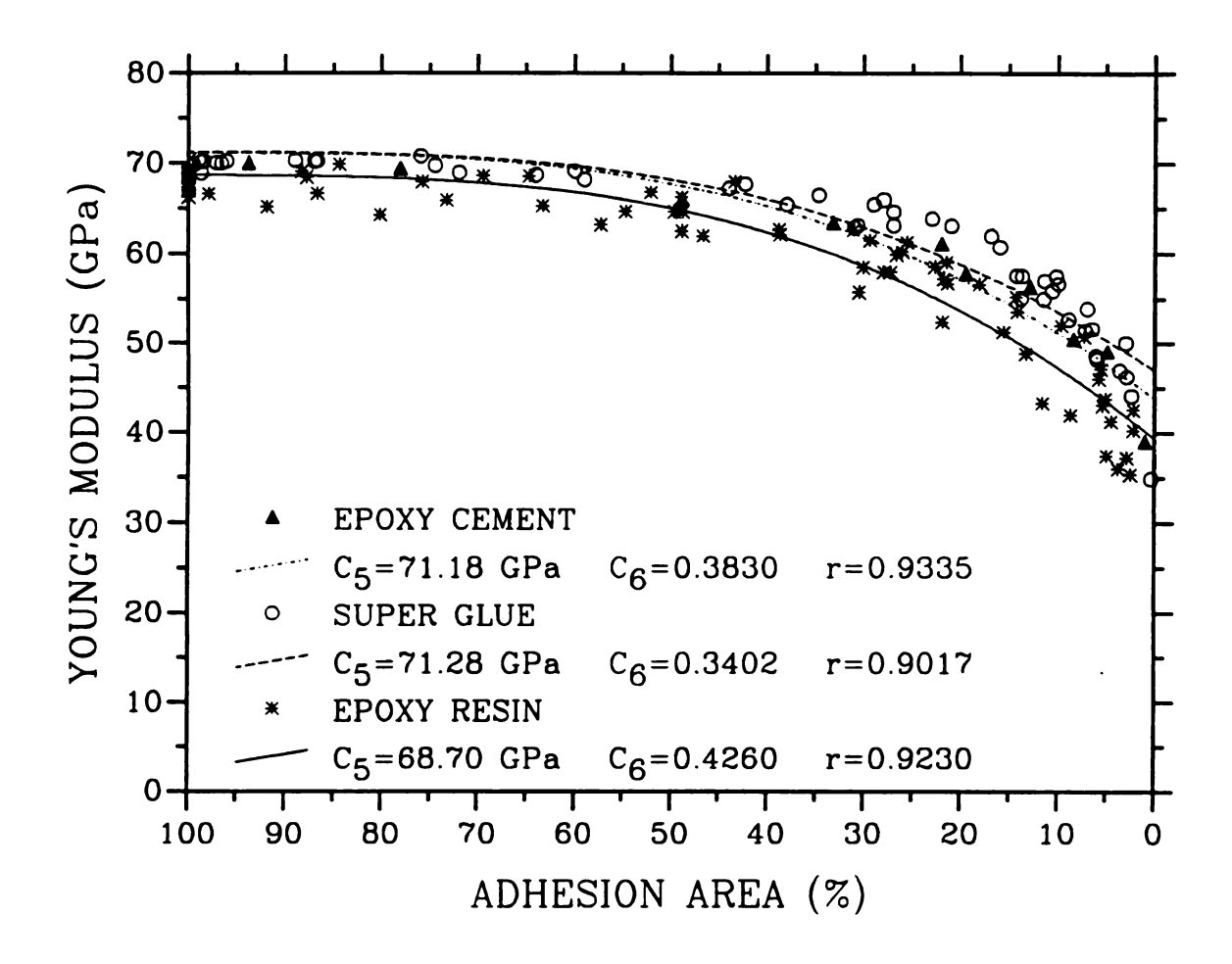


Figure 49. The general trend in Young's modulus of glass slide/super glue, epoxy cement, and epoxy resin composite specimens having two or more glue spots as a function of adhesion area(%).

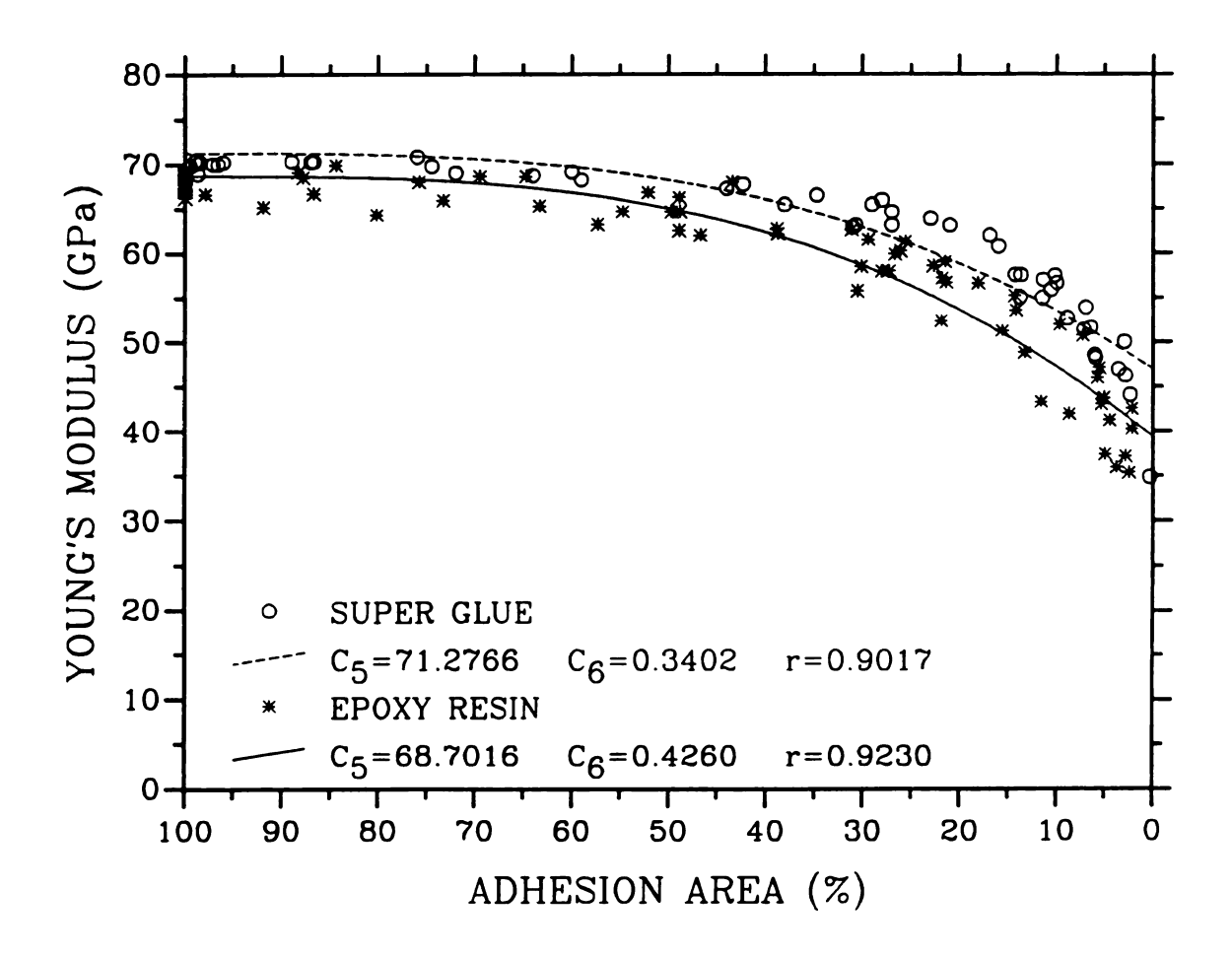


Figure 50. The effect of the glue bond thickness on Young's modulus between the super glue and the epoxy resin adhered composite specimens as a function of adhesion area(%).

agents ((1) super glue, (2) epoxy cement, and (3) epoxy resin), some numerical analysis was conducted by using the average glue bond thickness of each type of the adhesives and equation 17 obtained from the ROM model based on a 'sandwich model' in a three-layer composite.

The elastic modulus of a glass slide layer used for the calculation was 70.53 GPa which was an average elastic modulus of a single glass slide calculated from the elastic moduli of 140 single glass slides. For the thickness of each glass layer, an approximate thickness of a single slide, 1.2 mm was used. The elastic moduli of the super glue and the epoxy cement themselves were not determined in our study while the modulus measured for the epoxy resin was 2.98 GPa for the 50% composition (Table 6). For this analysis, we assumed that the elastic moduli of both the super glue and the epoxy cement were 3 GPa and 6 GPa. In Table 15, the resulting effective Young's moduli are tabulated and compared with the modulus values obtained from the three regression curves based on experimental values at 100% adhesion area in Figure 49. The differences of the data among different adhesives were calculated (Table 16).

From Tables 15 and 16, we can see that as the glue bond thickness increases from 0.015 mm (for super glue) to 0.060 mm (for epoxy cement), then to 0.165 mm (for epoxy resin), the calculated effective Young's modulus decreased by about 1.2 GPa for a glue bond modulus of 3 GPa.

For a glue bond modulus of 6 GPa, the calculated effective modulus decreased by 2.8 GPa. The experimentally measured modulus decreased by about 0.1 GPa, and then 2.5 GPa corresponding to the change of the glue bond thickness.

From this analysis, the ROM model demonstrates the effect of the glue bond thickness. Thus we can conclude that the effect of the glue

Table 15. Effective Young's modulus calculated from the ROM model and comparison with the experimental modulus values based on Figure 49.

ADHESIVE	GLUE BOND THICKNESS (mm)	E _{k, exp} (GPa.)	_ E _{exp} (GPa)	E _{3ROM} (GPa) (E _b =3 GPa)	E_{3ROM} (GPa) (E_b =6 GPa)
Super Glue	0.015	*	71.28	70.11	70.13
Epoxy Cement	0.060	*	71.18	68.88	68.96
Epoxy Resin	0.165	2.98	68.70	66.18 **	66.18 **

where $\underline{E}_{b,exp}$ = Experimentally determined elastic modulus of an adhesive \underline{E}_{sep} = Experimentally determined elastic modulus of a composite \underline{E}_{sgom} = Calculated elastic modulus of a composite by the ROM model

^{*} The elastic moduli of the super glue and the epoxy cement were not determined experimentally.

^{**} The values are based on $E_{b, exp}=2.98$ GPa.

Table 16. Differences between the data of the super glue, the epoxy cement and the epoxy resin shown in Table 15.

ADHESIVE	DIFFERENCE IN GLUE BOND THICKNESS (mm)	AE _{eep}	ΔE _{3ROM} (GPa) (E _b =3 GPa)	ΔE _{3ROM} (GPa) (E _b =6 GPa)
*	0.045	0.10	1.23	1.17
**	0.105	2.48	2.72	2.78
***	0.150	2.58	3.93	3.95

^{*} Absolute value of difference between the epoxy cement and the super glue

^{**} Absolute value of difference between the epoxy resin and the epoxy cement

^{***} Absolute value of difference between the epoxy resin and the super glue

bond thickness for the experimental results is consistent with the effect of the glue bond thickness predicted by the ROM model.

However, the measured modulus and the calculated modulus differ. As one possible factor, we can think the change of the elastic modulus of a glass slide layer as a function of the glue bond thickness. Using equation 17 for the ROM model, the elastic modulus of a glass slide layer required to obtain the experimental modulus values for the super glue (E₆=3 GPa), the epoxy cement (E₆=3 GPa), and the epoxy resin (

E_{6,000}=2.98 GPa) were calculated. The resulting elastic moduli of a glass slide were 71.71 GPa for the super glue, 71.61 GPa for the epoxy cement, and 69.11 GPa for the epoxy resin, which correspond to the shifts of 1.18 GPa, 1.08 GPa, and -1.42 GPa from the average modulus of a glass slide (70.53 GPa). As a result, the shifts of the elastic modulus of the glass slide layer indicate that as the glue bond thickness increases from 0.015 mm (for the super glue) to 0.060 mm (for the epoxy cement), and then to 0.165 mm (for the epoxy resin), the elastic modulus of the glass slide decreases by 0.1 GPa and then 2.5 GPa.

The change in elastic modulus of quenched polymer glass as a function of the quench medium temperature was discussed in section 3.2.7. In addition, Mallinder and Proctor [24] pointed out that the elastic modulus of soda glass changed under tensile loading as a function of static strain, $E = E_0(1-5.11s)$, where low-strain elastic modulus, E_0 , was 72.5 GPa. In our study, residual strain could induce change in elastic modulus of a glass slide. Using Mallinder and Proctor's empirical relationship and assuming $E_0 = 71.71$ GPa calculated above for a glass slide in the super glue adhered composite specimen, we calculated the strain expected to cause the change of elastic modulus for a glass slide of the epoxy cement and the epoxy resin adhered

composite specimens, which were 0.0003 and 0.0071, respectively. The stresses corresponding the strain values of 0.0003 and 0.0071 were calculated for each type of glue adhered composite specimen. At the strain of 0.0003, the stresses for the super glue and the epoxy cement were 21.51 MPa and 21.48 MPa, respectively, resulting in difference of 0.03 MPa in the effective elastic modulus (Figure 51). At the strain of 0.0071, the stresses for the super glue and the epoxy resin were 509.14 MPa and 490.68 MPa, respectively, resulting in difference of 18.46 MPa in the effective elastic modulus (Figure 52).

Chiu [25] determined mean fracture strength of 239 microscope slides by three-point bend test, which was 101.38 MPa. Compared to Chiu's fracture strength, 101.38 MPa, the stresses of 21.51 MPa and 21.48 MPa at the strain, 0.0003 are much lower (Figure 51). However, the stress values of 509.14 MPa and 490.68 MPa calculated at the strain of 0.0071 for the super glue and the epoxy resin adhered composite specimens indicate that the specimens would fail (where the mean fracture strength is about 101 MPa) long before a strain of 0.0071 was obtained (Figure 52). This brief numerical analysis indicates that the residual strain induced by adhesion might be one of possible factors for the possible change in elastic modulus of a glass slide as a function of the glue-bond thickness.

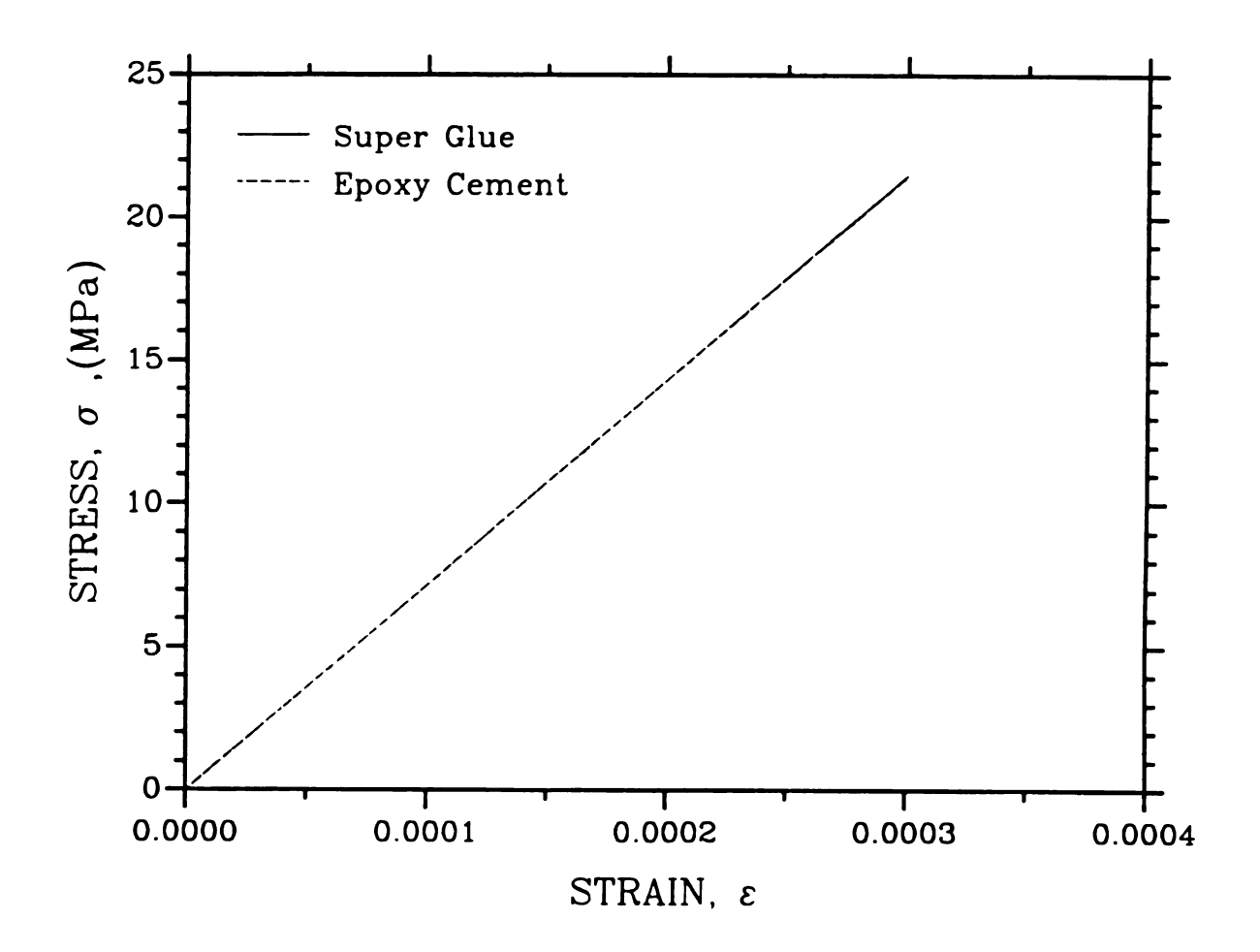


Figure 51. Change in elastic modulus of a glass slide for the super glue and the epoxy cement adhered composite specimens.

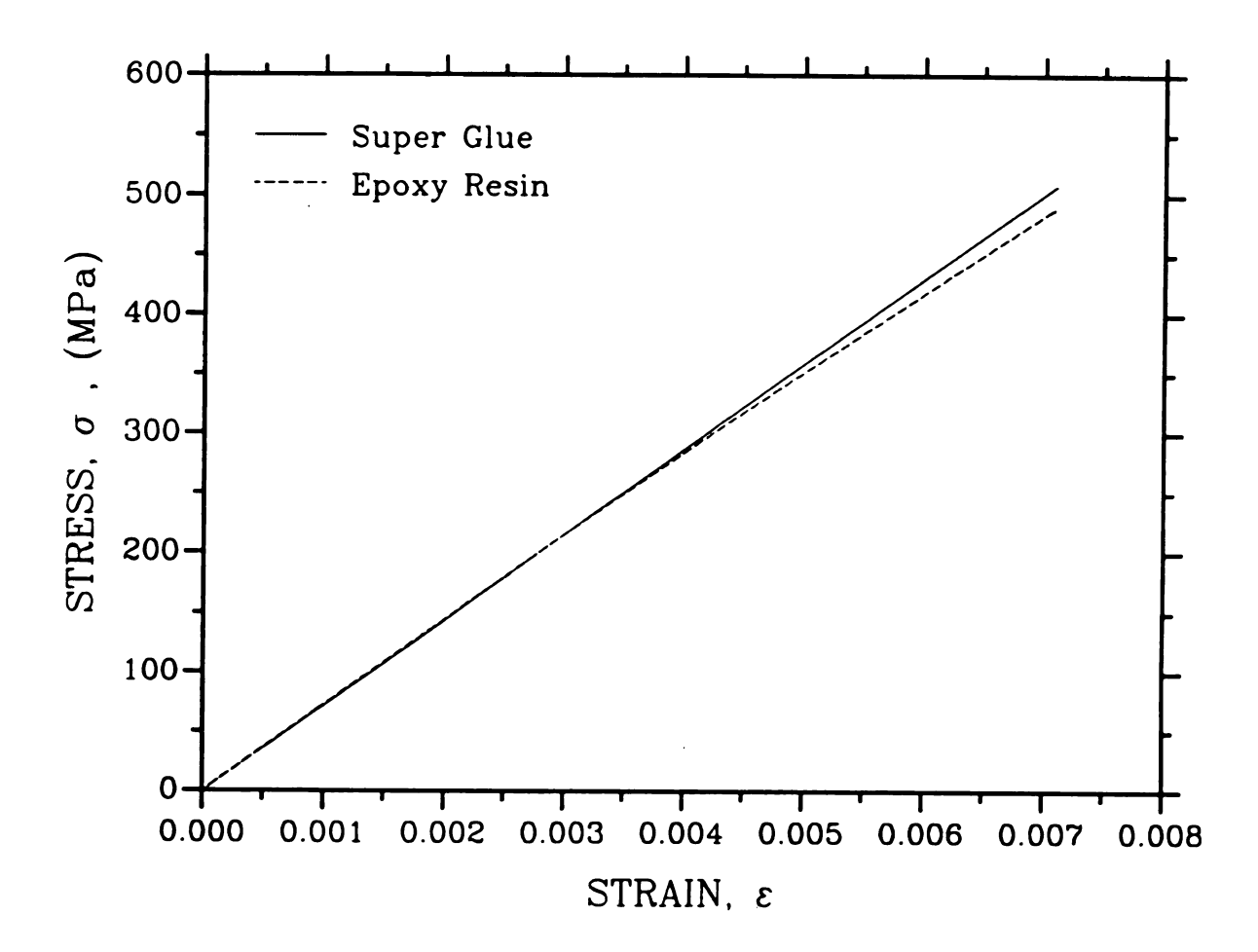


Figure 52. Change in elastic modulus of a glass slide for the super glue and the epoxy resin adhered composite specimens.

4. SUMMARY AND CONCLUSIONS

4.1. The Effect of Adhesion Area on Elastic Modulus

The change of Young's modulus of adhered soda-lime-silica microscope slides was observed as a function of adhesion area percent using three different types of adhesives: (1) super glue, (2) epoxy cement, and (3) epoxy resin. Trends in the Young's moduli of glass slide/glue composite specimens were analyzed using the least-squares best fit to equations 31-33. Young's moduli decreased continuously with decreasing the adhesion area (Figures 16-18, 25-27, 28-30, and 48-50). For an area fraction less than 30 to 35 percent the Young's moduli decreased relatively rapidly with a decrease in the adhesion area.

In this study, the unadhered regions of the glass slide surface surrounding glue spots can be considered to be similar to an external crack (Figure 1). Unlike the external cracks to which a uniaxial tension is applied in perpendicular direction (Figure 1) [1], the cracks of the current study exist at the mid-plane of a glass slide/glue composite specimen under a beam bending. It should be emphasized that the "cracks" referred to here were formed by incomplete bonding at the mid-plane of the composite specimens. Therefore the observed trends of Young's modulus versus adhesion area is analogous to the decrease in Young's modulus that accompanies an increase in the crack surface area.

4.2. The Effect of Mumber of Glue Spots on Elastic Modulus

The effect of number of glue spots on Young's modulus was investigated for glass slides adhered by super glue and epoxy cement. Glass slide/glue composite specimens having one, two, three and five glue spots were fabricated using super glue. Glass slide/glue composite specimens having one and three glue spots were fabricated using epoxy cement. For two or more glue spots, the glass slide/glue composite specimens adhered by the two different types of adhesives showed similar trends in Young's modulus as a function of adhesion area (Figures 13-15 ,25-27, and 49). Also, for one glue spot, the two types of adhesives showed similar changes in Young's modulus of glass slide/glue composite specimens as a function of adhesion area (Figures 13-15, 25-27, and 48). Glass slide/glue composite specimens having two or more glue spots had a greater Young's modulus over the entire range of glued area fraction than those glass slide/glue composite specimens having one glue spot. In addition, the difference between the Young's modulus of a glass slide/glue composite specimen with one glue spot and that of a glass slide/glue composite specimen with two or more glue spots increased as the area fraction of glue approached zero (Figures 13-15 and 25-27).

The difference in the elastic modulus behavior between the specimens having one glue spot and the specimens having two or more glue spots (Figures 13-15 and 25-27) could result from the differing physical constraints imposed on the specimens by a single glue spot as opposed to two or more glue spots. For a single glue spot located near the center of the long transverse specimen face, the two glass slides may undergo an opening and closing "duck-bill" motion. In addition, the slides may rotate with respect to one another, with the plane of rotation being

parallel to the specimen midplane. The measured elastic modulus of the glass slide/glue composite specimens is proportional to the square of the fundamental flexural frequency (equation 27 in Section 2.6. of the Experimental Procedure). Thus the relatively lower modulus for the single glue spot specimens (as opposed to the specimens having multiple spots) may result from flexural frequency perturbations caused by these ancillary vibrations (duck-beak motion and rotational motion). In a crude analysis, one could conceive of the vibrational energy associated with the flexural resonance frequency of a monolithic-bar shaped specimen being partitioned into energies for the duck-beak and rotational motions plus the energy (now reduced) for the flexural vibration. The vibrational energy could thus result in a reduced fundamental flexural frequency for the specimen (which would in turn be manifest as a lower effective Young's modulus for the composite specimen).

4.3. The Effect of Glue Bond Thickness on Elastic Modulus

The effect of glue bond thickness on Young's modulus was investigated for glass slides adhered by the super glue and the epoxy resin. In this study the selected ranges of the glue bond thickness were 0.010 - 0.012 mm, 0.019 - 0.021 mm and 0.028 - 0.030 mm for the super glue layer, and 0.025 - 0.075 mm, 0.125 - 0.175 mm and 0.225 - 0.275 mm for the epoxy resin layer. For the glass slides adhered by the epoxy resin the Young's modulus decreased by up to 5 GPa over the entire range of adhesion area fraction as the glue bond thickness increased by 0.1 mm (Figures 31-33). However, a glue-bond thickness effect was not

obvious for the glass slides adhered by the super glue (Figures 19-24). This weak dependence of Young's modulus on the glue bond thickness may result from the relative thinness of the super glue layer.

The effect of the glue-bond thickness on Young's modulus was observed by comparing the experimental results from the two different types of adhesives, the super glue and the epoxy resin. The super glue adhered specimens having average bond thickness of 0.015 mm showed the higher Young's modulus by about 3 GPa to 8 GPa than the epoxy resin adhered specimens having average bond thickness of 0.165 mm over the whole adhesion area range (Figure 50).

Since the elastic modulus of the glass slides was approximately 70 GPa and the elastic modulus of the bond layer was about 3 GPa, one observes a general trend of a decreasing effective Young's modulus with increasing bond thickness.

4.4. The Effect of Epoxy Resin Composition on Elastic Modulus

The effect of epoxy resin composition on Young's modulus of glass slide/epoxy resin composite specimens having different ratios of resin and hardener was investigated. The glass slide/epoxy resin composite specimens used for this investigation had 100 percent adhesion area, and the epoxy compositions were 80% resin:20% hardener, 65%:35%, 50%:50% and 35%:65%. The measured Young's moduli of the glass slide/epoxy resin composite specimens were analyzed as a function of relative glue bond thickness, t_R (equation 34). A least-squares fit of the data to equation 34 is given in Figure 34.

The Young's modulus decreased by 1.5 to 1.2 GPa over the entire

range of relative glue bond thickness as the content of resin in epoxy resin used for adhesion of glass slides decreased from 80 percent to 50 percent (Figure 34).

4.5. The Comparison of the ROM model and the Dynamic Beam Vibration model

The ROM model and the Dynamic beam vibration model were analyzed in terms of the fractional difference, δ_R , between the experimentally determined Young's modulus and the predicted Young's modulus from the ROM and Dynamic beam vibration models. This segment of the study utilized the same glass slide/epoxy resin composite specimens used to investigate the effect of epoxy resin composition (equations 17, 23, 35, 36, and 37, and Figures 35-40).

As the relative glue bond thickness increased, the experimentally determined Young's modulus deviated more increasingly for the Dynamic beam vibration model and decreasingly for the Rule of Mixtures model. Also, the curves for the relative deviation, δ_R , have similar slopes for the two models but opposite algebraic signs. As the relative glue bond thickness approached zero, the deviation also approached zero.

4.6. Future Work and Practical Applications of This Study

In this study, some general trends of the effective Young's modulus of glass/epoxy and glass/glue laminates on adhesion area and glue bond thickness were observed and analyzed by three experimental equations.

Even though other ceramic materials were used instead of glass slides in this study, the same general trends of the effective Young's modulus would be observed as a function of adhesion area and the glue bond thickness. In this sense, the importance of perfect adhesion in engineering applications of laminated ceramic materials should be reilluminated.

The current study shall have to be followed by the work which develop the experimental results obtained in this study to model the external cracks in a three layer composite material.

Appendix A. Calculation of Adhesion Area by a Template Method

For a single circle-shape glue spot with diameter less than width of slide, a template having forty one circles of various sizes from 1.5 mm to 35 mm was used to measure the glue area fraction. The size increment between adjacent circles on the template was 0.5 mm for circles smaller than 12 mm in diameter and 1 mm for circles greater than 12 mm (Figure 8). The size of a glass slide/glue composite specimen was 25.4 mm by 76.2 mm (1 inch by 3 inches), such that the glue area fraction, A, for one glue spot can be given by

$$A = \frac{\text{Area of Glue Spot}}{\text{Area of Specimen}}.$$
 (1)

Thus,

$$A = \frac{(\pi \frac{1}{4}) (d + \Delta d)^{2}}{\text{Area of Specimen}}$$

$$= \frac{0.7854 \left[d^{2} + 2d\Delta d + (\Delta d)^{2}\right]}{\text{Area of Specimen}}$$

$$= \frac{0.7854 d^{2} + 0.7854 \left[2d\Delta d + (\Delta d)^{2}\right]}{\text{Area of Specimen}} (mm^{2}/mm^{2})$$

where d = actual diameter of the glue spot (mm)

Ad = error in determining the size of the glue spot ±0.5 mm for glue spots smaller than 12 mm in diameter or ±1 mm for glue spots greater than 12 mm in diameter

= uncertainty of measurement for the diameter of the glue spot

 $d + \Delta d = diameter$ of the glue spot determined using the template (mm) Area of Specimen = 76.2 x 25.4 (mm²).

From equation 2 the uncertainty in the calculation of the glue area fraction, u, can be given by

$$u = \frac{0.7854 \left[2d \Delta d + (\Delta d)^2\right]}{\text{Area of Specimen}} \tag{3}$$

The range of diameters of glue spots for which the template method could be applied was 1.5 mm to 26 mm, such that the determined glue area fraction had the uncertainty ranging from -0.0007 to 0.0005 for the smallest glue spot (A=0.0009) and from -0.0215 to 0.0207 for the largest glue spot (A=0.2704). Thus, the actual adhesion area fraction ranges from 0.0002 to 0.0014 for the smallest glue spot and from 0.2489 to 0.2911 for the largest glue spot.

As a result, the greater the size of glue spot is, the wider the range of the uncertainty becomes. But the deviation of a determined adhesion area fraction from corresponding actual adhesion area fraction is not too big to result in considerable error in analyzing experimental data.

Appendix B. Experimentally determined fundamental frequency and the corresponding Young's Modulus of each glass slide/glue composite specimen.

B-1. The experimental data for the glass slide/super glue composite specimens having one glue spot.

ADHESION AREA (%)	MASS (gram)	THICKNESS (mm)	GLUE BOND THICKNESS (mm)	FUNDAMENTAL FREQUENCY (Hz)	YOUNG'S MODULUS (GPa)
99.5	11.8340	2.550	0.018	2426.4	69.83
99.0	11.8530	2.552	0.018	2438.0	70.44
98.7	12.0782	2.664	0.017	2547.8	68.92
98.7	11.9316	2.568	0.019	2447.9	70.16
98.4	11.8806	2.556	0.017	2437.3	70.24
97.1	11.8478	2.555	0.011	2435.9	70.05
96.6	11.8429	2.545	0.007	2421.4	70.00
96.1	11.7362	2.533	0.020	2419.4	70.25
79.4	12.1187	2.628	0.029	2510.5	69.93
77.1	11.1979	2.408	0.011	2285.9	69.64
76.8	12.0768	2.618	0.029	2492.8	69.50
74.5	11.1738	2.410	0.030	2300.1	70.18
66.7	11.1479	2.404	0.019	2260.4	68.13
60.2	11.9513	2.590	0.029	2446.4	68.42
56.5	11.5123	2.481	0.020	2320.3	67.45
40.1	12.0192	2.609	0.028	2246.4	56.76
39.8	11.1239	2.398	0.019	1886.0	47.69
38.0	11.5939	2.504	0.021	1862.8	42.58
33.3	11.9545	2.589	0.019	1972.9	44.56
30.5	11.9365	2.589	0.028	2059.8	48.50
27.3	11.4676	2.471	0.012	1673.8	35.39

ADHESION AREA (%)	MASS (gram)	THICKNESS (mm)	GLUE BOND THICKNESS (mm)	FUNDAMENTAL FREQUENCY (Hz)	YOUNG'S MODULUS (GPa)
22.8	11.2542	2.432	0.020	1581.7	32.53
18.0	11.8410	2.564	0.019	1540.7	27.71
17.7	11.4585	2.472	0.019	1510.5	28.76
15.7	11.8571	2.570	0.020	1524.2	26.97
12.7	11.2383	2.422	0.015	1414.7	26.31
12.0	11.9966	2.595	0.020	1547.3	27.31
10.1	11.9458	2.590	0.019	1453.5	24.14
9.9	11.9288	2.582	0.019	1413.3	23.00
8.1	11.2479	2.424	0.012	1319.5	22.85
7.5	11.2340	2.425	0.012	1320.4	22.82
6.0	11.8819	2.572	0.018	1530.9	27.20
5.0	12.0471	2.601	0.011	1359.1	21.02
4.0	11.8227	2.551	0.010	1353.3	21.68
3.0	11.2232	2.422	0.014	1359.3	24.26
3.0	11.8420	2.556	0.012	1279.0	19.28
2.6	11.8760	2.580	0.018	1387.1	22.11

Average elastic modulus at 100% adhesion area, E_{100} = 69.99 GPa.

B-2. The experimental data for the glass slide/super glue composite specimens having two glue spot.

ADHESION AREA (%)	MASS (gram)	THICKNESS (mm)	GLUE BOND THICKNESS (mm)	Fundamental Frequency (Hz)	YOUNG'S MODULUS (GPa)
99.5	11.8340	2.550	0.018	2426.4	69.83
99.0	11.8530	2.552	0.018	2438.0	70.44
98.7	11.9316	2.568	0.019	2447.9	70.16
98.7	12.0782	2.664	0.017	2547.8	68.92
98.4	11.8806	2.556	0.017	2437.3	70.24
97.1	11.8478	2.555	0.011	2435.9	70.05
96.6	11.8429	2.545	0.007	2421.4	70.00
96.1	11.7362	2.533	0.020	2419.4	70.25
59.4	11.4795	2.478	0.020	2332.5	68.21
38.3	11.4576	2.486	0.019	2298.0	65.45
34.7	11.8428	2.565	0.019	2387.8	66.49
29.0	12.0438	2.599	0.011	2395.7	65.43
28.0	11.8429	2.567	0.019	2380.6	65.94
27.3	11.4510	2.478	0.020	2247.2	63.15
27.1	11.8697	2.571	0.020	2359.5	64.62
23.0	11.8910	2.575	0.017	2349.4	63.88
21.2	11.8746	2.575	0.020	2336.7	63.11
16.0	12.0086	2.591	0.012	2300.7	60.73
			0.011	2091.9	54.97
11.5	11.4885	2.477			
7.2	11.8774	2.562	0.017	2194.7 2105.0	56.53 51.50

Average elastic modulus at 100% adhesion area, E_{100} = 69.99 GPa.

B-3. The experimental data for the glass slide/super glue composite specimens having three glue spot.

ADHESION AREA (%)	MASS (gram)	THICKNESS (mm)	GLUE BOND THICKNESS (mm)	FUNDAMENTAL FREQUENCY (Hz)	YOUNG'S MODULUS (GPa)
99.5	11.8340	2.550	0.018	2426.4	69.83
99.0	11.8530	2.552	0.018	2438.0	70.44
98.7	12.0782	2.664	0.017	2547.8	68.92
98.7	11.9316	2.568	0.019	2447.9	70.16
98.4	11.8806	2.556	0.017	2437.3	70.24
97.1	11.8478	2.555	0.011	2435.9	70.05
96.6	11.8429	2.545	0.007	2421.4	70.00
96.1	11.7362	2.533	0.020	2419.4	70.25
89.0	11.8931	2.562	0.011	2446.4	70.34
87.0	11.9224	2.571	0.018	2455.3	70.28
86.7	11.9412	2.581	0.021	2467.8	70.29
76.0	12.0052	2.581	0.011	2470.5	70.82
74.5	11.6531	2.533	0.020	2419.9	69.78
72.0	11.9372	2.573	0.012	2434.0	68.99
64.0	11.9553	2.583	0.018	2441.4	68.72
60.0	12.0637	2.600	0.019	2461.9	69.13
44.0	12.0853	2.603	0.011	2430.2	67.25
42.3	11.8533	2.567	0.019	2411.2	67.70
31.0	12.0660	2.602	0.010	2350.5	62.89
30.7	11.8929	2.568	0.018	2325.7	63.13
14.3	11.8593	2.562	0.012	2216.1	57.55
13.8	11.2377	2.434	0.012	2061.6	55.04
10.6	11.2443	2.442	0.020	2087.6	55.92
8.9	11.2318	2.420	0.009	2001.0	52.73
6.5	11.2378	2.421	0.010	1982.2	51.71
6.1	11.2155	2.431	0.014	1936.3	48.64

ADHESION AREA (%)	MASS (gram)	THICKNESS (mm)	GLUE BOND THICKNESS (mm)	FUNDAMENTAL FREQUENCY (Hz)	YOUNG'S MODULUS (GPa)
6.0	12.0213	2.585	0.010	2043.0	48.27
3.6	11.1885	2.410	0.010	1881.4	47.02
3.0	11.1662	2.415	0.019	1949.8	50.09
2.9	11.1566	2.412	0.011	1871.0	46.31
2.4	11.1908	2.420	0.012	1840.6	44.16
0.35	11.1512	2.420	0.016	1635.0	34.95

Average elastic modulus at 100% adhesion area, E_{100} = 69.99 GPa.

B-4. The experimental data for the glass slide/super glue composite specimens having five glue spots.

ADHESION AREA (%)	MASS (gram)	THICKNESS (mm)	GLUE BOND THICKNESS (mm)	FUNDAMENTAL FREQUENCY (Hz)	YOUNG'S MODULUS (GPa)
99.5	11.8340	2.550	0.018	2426.4	69.83
99.0	11.8530	2.552	0.018	2438.0	70.44
98.7	12.0782	2.664	0.017	2547.8	68.92
98.7	11.9316	2.568	0.019	2447.9	70.16
98.4	11.8806	2.556	0.017	2437.3	70.24
97.1	11.8478	2.555	0.011	2435.9	70.05
96.6	11.8429	2.545	0.007	2421.4	70.00
96.1	11.7362	2.533	0.020	2419.4	70.25
16.9	11.2400	2.425	0.013	2175.0	61.96
13.7	11.2526	2.430	0.016	2100.8	57.52
11.4	11.2239	2.423	0.012	2084.8	56.99
10.2	11.2488	2.431	0.013	2102.1	57.50
7.0	11.2802	2.433	0.014	2035.2	53.91

Average elastic modulus at 100% adhesion area, E_{100} = 69.99 GPa.

B-5. The experimental data for the glass slide/epoxy cement composite specimens having one glue spot.

ADHESION AREA (%)	MASS (gram)	THICKNESS (mm)	GLUE BOND THICKNESS (mm)	FUNDAMENTAL FREQUENCY (Hz)	YOUNG'S MODULUS (GPa)
					
93.8	12.0099	2.629	0.111	2525.7	70.07
77.9	11.3689	2.568	0.179	2471.3	68.13
75.0	11.3028	2.518	0.130	2414.9	68.61
52.1	11.2273	2.533	0.142	2158.9	53.51
38.0	11.9162	2.699	0.167	2014.4	40.87
23.7	11.8574	2.631	0.092	1678.2	30.47
14.9	11.6075	2.587	0.106	1449.8	23.42
9.9	11.1338	2.456	0.056	1323.4	21.87
6.5	11.4778	2.511	0.051	1300.5	20.38
3.0	11.0725	2.404	0.010	1206.8	19.29
0.84	11.0951	2.432	0.031	1223.5	19.19

Average elastic modulus at 100% adhesion area, $E_{100} = 70.07$ GPa.

B-6. The experimental data for the glass slide/epoxy cement composite specimens having three glue spots.

ADHESION AREA (%)	MASS (gram)	THICKNESS (mm)	GLUE BOND THICKNESS (mm)	FUNDAMENTAL FREQUENCY (Hz)	YOUNG'S MODULUS (GPa)
93.8	12.0099	2.629	0.111	2525.7	70.07
78.1	11.3265	2.494	0.112	2392.6	69.46
48.9	11.2234	2.470	0.079	2308.9	65.98
33.2	11.2076	2.458	0.069	2249.9	63.86
22.0	11.1322	2.427	0.052	2173.9	61.15
19.5	11.1725	2.437	0.048	2123.4	57.84
12.9	11.1012	2.404	0.031	2060.5	56.38
8.4	11.1524	2.428	0.046	1975.5	50.53
4.9	11.1350	2.401	0.019	1917.5	49.15
1.0	11.8871	2.580	0.033	1843.9	39.11

Average elastic modulus at 100% adhesion area, $E_{100} = 70.07$ GPa.

B-7. The experimental data for the glass slide/epoxy resin composite specimen having three glue spots of 50% resin and 50% hardener.

ADHESION AREA (%)	MASS (gram)	THICKNESS (mm)	GLUE BOND THICKNESS (mm)	FUNDAMENTAL FREQUENCY (Hz)	YOUNG'S MODULUS (GPa)
100.0	12.2718	2.745	0.163	2613.8	67.36
100.0	11.8679	2.657	0.205	2554.7	68.62
100.0	12.4155	2.827	0.247	2693.3	66.24
100.0	11.4081	2.500	0.090	2394.0	69.54
100.0	11.8415	2.609	0.088	2502.6	69.40
100.0	11.7618	2.601	0.145	2492.7	69.02
100.0	12.1338	2.780	0.305	2673.7	67.09
100.0	12.0773	2.748	0.279	2647.6	67.80
100.0	11.7657	2.621	0.153	2518.4	68.87
100.0	12.4723	2.810	0.227	2694.4	67,82
100.0	11.4094	2.498	0.090	2391.1	69.55
100.0	12.1581	2.678	0.116	2570.6	69.52
100.0	11.7183	2.555	0.075	2440.5	69.54
97.9	12.2605	2.754	0.196	2613.9	66.65
91.9	12.4416	2.834	0.256	2679.1	65.20
88.3	11.6821	2.574	0.115	2463.8	69.10
87.8	12.1726	2.718	0.169	2607.9	68.52
86.7	12.2673	2.787	0.234	2660.9	66.68
84.4	11.6875	2.541	0.064	2430.0	69.91
80.2	12.3047	2.823	0.260	2666.6	64.63
75.8	12.1792	2.702	0.129	2574.8	68.02
73.3	12.5443	2.942	0.370	2837.9	65.93
69.5	11.6766	2.573	0.112	2454.8	68.65
64.7	11.5846	2.519	0.052	2386.9	68.62
63.3	12.1068	2.719	0.162	2554.1	65.29
57.3	12.1575	2.759	0.189	2563.6	63.22

ADHESION AREA	MASS	THICKNESS	GLUE BOND THICKNESS	Fundamental Frequency	YOUNG'S MODULUS
(%)	(gram)	(mm)	(mm)	(Hz)	(GPa)
54.7	11.6453	2.745	0.330	2629.3	64.68
52.1	11.6333	2.537	0.059	2375.5	66.81
49.7	11.7023	2.618	0.147	2442.2	64.64
48.9	11.8819	2.800	0.328	2636.5	62.52
48.9	11.6016	2.530	0.058	2358.6	66.23
48.8	12.0290	2.677	0.119	2490.6	64.64
46.7	11.7326	2.716	0.263	2523.8	61.99
43.4	11.7529	2.664	0.197	2565.1	67.97
38.8	11.6982	2.710	0.249	2532.9	62.66
38.7	12.0026	2.827	0.295	2652.5	62.11
31.1	11.5324	2.511	0.044	2274.5	62.62
30.5	11.6820	2.677	0.204	2347.3	55.76
30.1	12.1782	2.860	0.281	2600.4	58.50
29.4	12.0169	2.682	0.116	2437.3	61.49
28.0	11.6341	2.722	0.256	2459.0	57.96
27.3	12.0528	2.703	0.124	2391.0	57.98
26.7	11.6491	2.615	0.138	2351.8	59.88
26.1	12.6239	2.673	0.206	2341.7	60.23
25.6	11.5588	2.533	0.063	2277.3	61.30
22.7	11.9785	2.643	0.074	2330.7	58.57
21.9	11.9528	2.814	0.278	2425.6	52.44
21.8	11.6575	2.635	0.157	2324.3	57.20
21.5	11.2844	2.493	0.077	2208.7	59.04
21.4	11.5432	2.651	0.197	2346.5	56.69
18.1	11.9958	2.646	0.079	2293.8	56.62
15.6	11.2752	2.615	0.206	2213.2	51.32
14.3	11.2412	2.461	0.053	2099.1	55.22
14.2	11.5655	2.576	0.107	2182.7	53.57
13.3	11.9852	2.722	0.154	2237.0	48.88
11.6	11.2720	2.654	0.249	2079.8	43.34

ADHESION AREA (%)	MASS (gram)	THICKNESS (mm)	GLUE BOND THICKNESS (mm)	FUNDAMENTAL FREQUENCY (Hz)	YOUNG'S MODULUS (GPa)
9.7	11.9506	2.608	0.036	2156.4	52.06
8.7	11.3072	2.738	0.326	2143.1	42.04
7.3	11.4689	2.499	0.044	3036.0	50.78
5.8	11.9349	2.630	0.064	2055.9	46.08
5.6	11.9635	2.627	0.054	2074.6	47.20
5.4	11.5123	2.641	0.176	2036.7	43.08
5.1	11.5704	2.612	0.139	2015.9	43.85
5.0	11.2447	2.666	0.261	1950.0	37.50
4.5	11.5350	2.657	0.187	2010.9	41.32
3.8	11.5757	2.698	0.221	1918.2	36.04
2.9	11.5329	2.691	0.220	1946.9	37.28
2.5	11.5901	2.610	0.131	1808.5	35.43
2.2	11.8963	2.601	0.045	2350.8	40.33
2.2	11.9417	2.606	0.040	1949.2	42.60

Average elastic modulus at 100% adhesion area, E_{100} = 68.49 GPa.

B-8. The experimental data for the glass slide/epoxy resin composite specimens adhered by the epoxy resin of 35% resin and 65% hardener.

ADHESION AREA (%)	MASS (gram)	THICKNESS (mm)	GLUE BOND THICKNESS (mm)	FUNDAMENTAL FREQUENCY (Hz)	YOUNG'S MODULUS (GPa)
100.0	11.7782	2.605	0.134	2478.5	68.02
100.0	11.8840	2.645	0.175	2516.0	67.56
100.0	12.0646	2.740	0.272	2612.0	66.79
100.0	11.8365	2.625	0.159	2504.8	68.39
100.0	12.1636	2.770	0.301	2652.4	67.20
100.0	12.1220	2.781	0.312	2644.3	65.56
100.0	12.4970	2.884	0.347	2737.2	64.66
100.0	12.1103	2.756	0.285	2617.3	66.15
100.0	11.8631	2.731	0.323	2579.0	64.38
100.0	11.8093	2.691	0.276	2547.0	65.33

B-9. The experimental data for the glass slide/epoxy resin composite specimens adhered by the epoxy resin of 65% resin and 35% hardener.

ADHESION AREA (%)	MASS (gram)	THICKNESS (mm)	GLUE BOND THICKNESS (mm)	FUNDAMENTAL FREQUENCY (Hz)	YOUNG'S MODULUS (GPa)
100.0	11.3725	2.478	0.066	2380.4	70.38
100.0	11.5281	2.570	0.166	2465.7	68.62
100.0	11.7434	2.670	0.261	2572.3	67.84
100.0	11.8515	2.730	0.327	2644.7	67.71
100.0	11.8343	2.713	0.309	2647.6	69.04
100.0	11.6810	2.639	0.234	2555.8	68.99
100.0	11.8027	2.690	0.278	2611.7	68.73
100.0	11.7506	2.683	0.273	2579.0	67.25
100.0	11.7111	2.6380	0.221	2541.2	68.46
100.0	11.5302	2.571	0.160	2461.5	68.32

B-10. The experimental data for the glass slide/epoxy resin composite specimens adhered by the epoxy resin of 80% resin and 20% hardener.

ADHESION AREA (%)	MASS (gram)	THICKNESS (mm)	GLUE BOND THICKNESS (mm)	FUNDAMENTAL FREQUENCY (Hz)	YOUNG'S MODULUS (GPa)
100.0	11.4276	2.505	0.091	2411.4	70.25
100.0	11.5407	2.561	0.156	2480.1	70.31
100.0	11.4156	2.520	0.118	2430.7	70.21
100.0	11.7169	2.670	0.262	2569.8	67.71
100.0	11.7646	2.676	0.271	2591.8	68.61
100.0	11.8715	2.714	0.306	2641.6	69.09
100.0	11.5624	2.564	0.158	2473.0	69.80
100.0	11.6677	2.617	0.203	2522.0	68.81

LIST OF REFERENCES

- J. Kemeny and N. G. W. Cook, "Effective Moduli, Non-linear Deformation and Strength of a Cracked Elastic Solid", J. Rock Mech. Min. Sci. & Geomech. Abstr., 23[2]: 107-118, 1986.
- 2. Walsh J. B. "The effect of cracks on the uniaxial elastic compression of rock", J. Geophys. Res., 70: 399-411, 1965.
- 3. G. R. Irwin, "Analysis of stresses and strains near the ends of a crack traversing a plate", J. Appl. Mech., 24: 361-364, 1957.
- 4. G. C. Sih, <u>Handbook of Stress Intensity Factors</u>, Institute of Fracture and Solid Mechanics, Lehigh University, Bethlehem, 1973.
- 5. Eldon D. Case and Youngman Kim, "The Effect of Surface Limited Microcracks on The Effective Young's Modulus of Ceramics, I. Analysis", J. Mater. Sci., 28: 1885-1990, 1993.
- 6. B. D. Agarwal and L. J. Broutman, pp. 20-26 in Analysis and Performance of Fiber Composites, Wiley, New York, 1980.
- 7. E. Volterra and E. C. Zachmanoglou, pp. 321-322 in <u>Dynamics of Vibrations</u>, Charles E. Merrill Books, Inc., Columbus, OH, 1965.
- 8. S. K. Clark, pp. 75-87 in <u>Dynamics of Continuous Elements</u>, Prentice Hall, Inc., Englewood Cliffs, NJ, 1972.
- 9. C. C. Chiu and E. D. Case, "Elastic Modulus Determination of Coating Layers as Applied to Layered Ceramic Composite", Mat. Sci. and Eng., A132: 39-47, 1991.
- 10. S. P. Timoshenko and D. H. Young, pp. 113-115 in <u>Strength of Materials</u>, Fourth ed., Van Nostrand Reinhold Co., Princeton, NY, 1962.
- 11. F. Forster, "Ein neues Messverfahren zur Bestimmug des Elastiziatmoduls und der Dampfung" (A new Method for Determination of Modulus of Elasticity and Damping), Zeitschrift fur Metallkunde, 29[4]: 109-115, 1937.
- 12. E. Schreiber, O. L. Anderson, and N. Soga, Chapter 4 in <u>Elastic</u> <u>Constants and Their Measurements</u>, McGraw-Hill, New York, 1974.
- 13. S. Spinner and W. E. Tefft, "A Method for Determining Mechanical Resonance Frequencies and for Calculating Elastic Moduli from These Frequencies", ASTM Proc., 61: 1221-1238, 1961.

- 14. Won Jae Lee, "Thermal Fatigue in Ceramics and Ceramic Matrix Composites", A Dissertation Submitted to Michigan State University for the Degree of Doctor of Philosophy, Department of Metallurgy, Mechanics and Materials Science, 1991.
- 15. G. Pickett, "Equations for Computing Blastic Constants from Flexural and Torsional Resonant Frequencies of Vibration of Prism and Cylinder", ASTM Proc., 45: 846-865, 1945.
- 16. D. P. H. Hasselman, <u>Tables for the Computation of Shear Modulus and Young's Modulus of Elasticity from Resonant Frequencies of Rectangular Prisms</u>, Carborundum Co., Niagara Falls, NY, 1961.
- 17. Henry Lee, pp. 6-24 in <u>Handbook of Epoxy Resins</u>, McGraw-Hill, NY 1967.
- 18. Derek Hull, pp. 29 in <u>An Introduction to Composite Materials</u>, Cambridge Solid State Science Series, NY, 1981.
- 19. Prof. Averill, Assist. Professor, MSU, personal communication, March, 1993.
- 20. Javier De La Vega and Donald C. Bogue, "Mechanical Properties and Residual Stresses in Non-Equilibrium Glasses", Chem. Eng. Comm., 53: 23-31, 1987.
- 21. Orson L. Anderson and P. Andreatch, Jr., "Pressure Derivatives of Elastic Constants of Single-Crystal MgO at 23° and -195.8°C", J. Amer. Cer. Soc., 49[8]: 404-409, 1966.
- 22. R. A. Bartels and D. E. Schuele, "Pressure Derivatives of the Elastic Constants of NaCl and KCl at 295°K and 195°K", J. Phys. Chem. Solids, 26: 537-549, 1965.
- 23. H. J. McSkimin, P. Andreatch, Jr., and R. N. Thurston, "Elastic Moduli of Quartz versus Hydrostatic Pressure at 25° and -195.8°C", J. Appl. Phys., 36[5]: 1624-1632, 1965.
- 24. F. P. Mallinder and B. A. Proctor, "Elastic Constants of Fused Silica as a Function of Large Tensile Strain", Phys. and Chem. Glasses, 5[4]: 91-103, 1964.
- 25. C. C. Chiu, "Thermal Quench of Brittle Materials", A Dissertation Submitted to Michigan State University for the Degree of Doctor of Philosophy, Department of Metallurgy, Mechanics and Materials Science, 1991.